



*Design and optimization of an axial
compressor with use of Multi-Fidelity
approach*

by

Rafał Muchowski, M.S.

submitted in partial fulfillment of the requirements for the degree of

Doctor of Philosophy

at the Rzeszow University of Technology

Supervisor: Andrzej Majka, Ph.D, PRz Associate Professor

Advisor: Wojciech Bar, M.S.

Rzeszów, September 2023

The page intentionally left blank

Abstract

This thesis establishes a Multi-Fidelity concept that enables the prediction of performance parameters of state of the art 8 stage axial High Pressure Compressor for wide operational range utilizing Streamline Curvature Method as Low Fidelity cost effective sample, and High Fidelity 3D CFD computations for expensive sample. For the preparation of the concept validation run, several sensitivities studies have been performed.

In the beginning of CFD computation studies, simple representation of the compressor geometry was developed, containing only main gas path. For this configuration, studies on mesh resolution and turbulence model were performed to find best setup suitable for considered all three rotational speeds – High, Mid and Low Speed conditions. After establishing the setup which delivers satisfactory quality, studies on model detail complexity were conducted. As an outcome, sensitivities on different geometrical features being a representation of secondary-flow volumes, were defined. As the last sensitivity study, Streamline Curvature Method model was compared to the results of CFD solutions. Outcome of this studies had an impact on definition of Design of Experiment for further Multi-Fidelity concept validation.

With enhanced knowledge about sensitivities of 3D and 2D methods, Design of Experiment has been defined. To solve the optimization problem with Multi-Fidelity approach, concept containing Co-Kriging data aggregation has been proposed. With two step surrogate model improvement, it was possible to achieve positive correlation between two data sets for all discussed conditions. As the concept validation outcome, performance parameters, Isentropic Efficiency and Surge Margin have been improved for all three rotational speeds, showing a potential for wide operating range. Finally, conclusions and recommendations for further development have been defined.

Streszczenie pracy

Niniejsza praca zawiera opracowanie koncepcji wykorzystania metody Multi-Fidelity pozwalając na przewidywanie parametrów osiągowych ośmiostopniowej osiowej sprężarki wysokiego ciśnienia dla szerokiego zakresu warunków operacyjnych. W tym celu została wykorzystana metoda Streamline Curvature Method jako dane niskiej rozdzielczości oraz dane wysokiej rozdzielczości w formie wyników obliczeń numerycznych 3D CFD. W ramach przygotowań do walidacji konceptu, wymaganiem było wykonanie zbioru studium czułości.

Na początku studium czułości w obrębie obliczeń CFD, została przygotowana prosta reprezentacja sprężarki, zawierająca jedynie główny kanał przepływowy wraz z łopatkami. Dla tej konfiguracji zostało przeprowadzone studium wrażliwości rozdzielczości siatki obliczeniowej oraz dobór modelu turbulencji w celu zdefiniowania modelu referencyjnego odpowiedniego dla trzech prędkości obrotowych. Następnie, po dobraniu odpowiedniej konfiguracji, przystąpiono do zbadania wpływu zawierania detali modelu, takich jak np. geometrie struktur drugo-rzędnych przepływów (uszczelnienie labiryntowe pod rzędem statorów). Po zakończonych badaniach na podstawie obliczeń CFD, następnym krokiem było zbadanie trendów wynikających z porównania wyników CFD oraz wyników obliczeń modelu niskiej rozdzielczości Streamline Curvature Method. Jako wynik tych studiów możliwym było zdefiniowanie projektu eksperymentu na potrzeby walidacji metody Multi-Fidelity.

Wraz z wiedzą na temat czułości metod 3D oraz 2D, został zaplanowany eksperyment. By rozwiązać zagadnienie optymalizacyjne z użyciem podejścia Multi-Fidelity, zaproponowano koncept, zawierający metodę interpolacji przestrzennej Co-Kriging. Wynikające z konceptu dwu-stopniowe dopasowywanie modelu zastępczego pozwoliło na osiągnięcie pozytywnej korelacji pomiędzy wspomnianymi dwoma zbiorami danych dla wszystkich omawianych warunków pracy. Jako wynik walidacji konceptu, parametry takie jak sprawność izentropowa oraz zapas pracy statecznej uzyskały przyrost dla każdej z uwzględnianych prędkości obrotowych, wykazując potencjał dla całego zakresu pracy sprężarki. Na koniec zostały zdefiniowane wnioski oraz rekomendacje do rozwoju.

Acknowledgements

First and foremost I would like to express my sincerest thanks to my supervisor Professor Majka. After experience in Euroavia team having you as an advisor and later working with you during my M.S., I was encouraged, and convinced to pursue Ph.D. I would also like to express my gratitude to my advisor Wojciech Bar for supporting this thesis from the first, starting day. You both always have found time for me when it was needed. I deeply appreciate all your guidelines and discussions which always were valuable, also those less technical, helping me to grow as engineer and researcher.

I would also like to thank my colleagues, Giovanni Brignole, Markus Lenzen, Tobias Fröbel and Amadeusz Rękosiewicz for your insights and feedback on the results. Thank you for all the discussions we had and support I got.

With all my heart, I want to thank all of my family for their love and encouragement. To my Mom, Wiesława, and my Dad Władysław thank you for your endless love, for supporting my passion to aviation since very young age, and for believing in me. To Weronika, my love and wife. You know the best how many sacrifices it costed. Thank you for all your patience when I was spending nights and days working on the thesis, for a good word in a moment of doubt, and for your unconditional love. You are the reason that keeps me going, and I can't imagine it could be possible without you.

The thesis is carried under organized by Ministry of Education and Science, the 3rd edition of the Implementation Doctorate program. Research was performed in cooperation between the MTU Aero Engines Polska and Faculty of the Mechanical Engineering and Aviation at the Rzeszow University of Technology. Therefore I would like to express my gratitude to those institutions for enabling this dissertation.

Contents

1	Introduction	19
1.1	General information	19
1.2	Axial compressor design importance.....	20
2	Literature review	25
2.1	Turbomachinery modeling techniques.....	25
2.2	Optimization approaches	28
2.3	Multi-Fidelity approach	33
2.4	Conclusions from the current knowledge	39
3	Objectives and scope of work	41
3.1	Technical Gaps	41
3.2	Research objectives.....	41
3.3	Technical approach	41
3.4	Thesis Contributions	43
4	Numerical flow simulations	45
4.1	Test case description	45
4.2	3D CFD analysis.....	45
4.2.1	Methods used	46
4.2.2	Mesh study	48
4.2.3	Configuration study	57
4.2.4	Summary observations.....	69
4.3	2D analysis.....	70
4.3.1	Model description and study preparation.....	70
4.3.2	Performed calculations	73

4.3.3	Data comparison.....	82
4.4	Setup study conclusions	89
5	Multi Fidelity concept	91
5.1	Requirements for Multi-Fidelity	91
5.2	Design of Experiment.....	92
5.3	Methodology	94
5.3.1	The concept	94
5.3.2	Idea of variogram model	97
5.3.3	Prediction correlation and error.....	99
5.4	Multi-Fidelity prove of concept	99
5.4.1	High Speed	100
5.4.2	Mid Speed	112
5.4.3	Low Speed.....	123
5.4.4	Summary and statistics.....	133
6	Final conclusions	135
6.1	Summary	135
6.2	Conclusions	136
6.3	Recommendations for development.....	137
7	Bibliography	139

List of Figures

Figure 1.1 Compressor map.....	20
Figure 1.2 Locally collapsed flow	22
Figure 1.3 Fully developed stall with Surge Cycle.....	22
Figure 2.1 Example of through-flow model for axial compressor [9].....	25
Figure 2.2 Example of 3D CFD flow visualization [18]	27
Figure 2.3 Simplified visualization of the approach proposed by [20]	29
Figure 2.4 Flowpath parametrization [21]	30
Figure 2.5 Proposed procedure [23]	32
Figure 2.6 Approaches representation [30].....	33
Figure 2.7 Types of Lo-Fi models	34
Figure 2.8 Strategies of model management	34
Figure 2.9 Visual representation of Kriging/co-Kriging approximation [32]	35
Figure 2.10 Workflow of [37].....	37
Figure 4.1 Compressor cross-section.....	45
Figure 4.2 Domain representation.	47
Figure 4.3 Close look on a partial gap of S1	48
Figure 4.4 Comparison of the turbulence models (Low speed) [43].....	50
Figure 4.5 Comparison of the turbulence models (Mid speed) [43].....	51
Figure 4.6 Comparison of the turbulence models (High speed) [43].	51
Figure 4.7 Comparison of the mesh density (Low speed) [43]	53
Figure 4.8 Comparison of the mesh density (Mid speed) [43]	53
Figure 4.9 Comparison of the mesh density (High speed). [43].....	54
Figure 4.10 . Surge margin by pressure ratio definition. [43]	55
Figure 4.11 Surge margin percentage deviation in compare to the Measurements	56
Figure 4.12 Medium Grid and Measurements Surge Margin representation on a Compressor Map.....	57
Figure 4.13 Legend for wall conditions.....	58
Figure 4.14. “Full model” graphical representation [45].....	59
Figure 4.15. “Pure flow path” graphical representation [45].....	59
Figure 4.16 “Bleed only” graphical representation [45].....	60

Figure 4.17“Panels as cavities” graphical representation [45].....	60
Figure 4.18 Surge Margin delta – low speed [45].....	67
Figure 4.19 Surge Margin delta – medium speed [45].....	68
Figure 4.20 Surge Margin delta – high speed [45].....	68
Figure 4.21 CFD and SCM map comparison	72
Figure 4.22 Legend to the tables 13-18.....	74
Figure 4.23 High Speed delta efficiency assessment for IGV angle variation	83
Figure 4.24 High Speed delta efficiency assessment for S1 angle variation	83
Figure 4.25 High Speed delta efficiency assessment for S2 angle variation	84
Figure 4.26 Mid Speed delta efficiency assessment for IGV angle variation.....	85
Figure 4.27 Mid Speed delta efficiency assessment for S1 angle variation.....	85
Figure 4.28 Mid Speed delta efficiency assessment for S2 angle variation.....	86
Figure 4.29 Low Speed delta efficiency assessment for IGV angle variation	87
Figure 4.30 Low Speed delta efficiency assessment for S1 angle variation	87
Figure 4.31 Low Speed delta efficiency assessment for S2 angle variation	88
Figure 5.1 Multi-Fidelity concept flowchart	94
Figure 5.2 Sampling phase of the optimization task	95
Figure 5.3 Surrogate model definition phase of the optimization task	96
Figure 5.4 Best member detection phase of the optimization task.....	97
Figure 5.5 Semi-variogram and its parameters	98
Figure 5.6 Visualisation of spatial distribution of the samples for High Speed IGV/Stator 1 variant	101
Figure 5.7 Visualisation of spatial distribution of the samples for High Speed Stator 1/Stator 2 variant	101
Figure 5.8 Visualisation of prediction grid for High Speed IGV/Stator 1 spatial discretization	102
Figure 5.9 Semi-variance model for Multi-Fidelity IGV/Stator 1 efficiency variant ...	103
Figure 5.10 Semi-variance model for Multi-Fidelity IGV/Stator 1 Surge Margin variant	104
Figure 5.11 Semi-variance model for Multi-Fidelity Stator 1/Stator 2 efficiency variant	104
Figure 5.12 Visualisation of Efficiency delta prediction for High Speed IGV/Stator 1 variant.....	105

Figure 5.13 Visualisation of Surge Margin delta prediction for High Speed IGV/Stator 1 variant	106
Figure 5.14 Visualisation of Efficiency delta prediction for High Speed Stator 1/Stator 2 variant	107
Figure 5.15 Visualisation of improved Efficiency delta prediction for High Speed IGV/Stator 1 variant.....	108
Figure 5.16 Visualisation of improved Surge Margin delta prediction for High Speed IGV/Stator 1 variant.....	109
Figure 5.17 Visualisation of improved Efficiency delta prediction for High Speed Stator 1/Stator 2 variant	110
Figure 5.18 Speedlines comparison between reference model and Mu-Fi optimized – High Speed.....	111
Figure 5.19 Visualisation of spatial distribution of the samples for Mid Speed IGV/Stator 1 variant.....	112
Figure 5.20 Visualisation of spatial distribution of the samples for Mid Speed Stator 1/Stator 2 variant.....	113
Figure 5.21 Semi-variance model for Multi-Fidelity IGV/Stator 1 efficiency variant.	114
Figure 5.22 Semi-variance model for Multi-Fidelity IGV/Stator 1 Surge Margin variant	114
Figure 5.23 Semi-variance model for Multi-Fidelity Stator 1/Stator 2 efficiency variant	115
Figure 5.24 Visualisation of Efficiency delta prediction for Mid Speed IGV/Stator 1 variant	116
Figure 5.25 Visualisation of Surge Margin delta prediction for Mid Speed IGV/Stator 1 variant	117
Figure 5.26 Visualisation of Efficiency delta prediction for Mid Speed Stator 1/Stator 2 variant	118
Figure 5.27 Visualisation of improved Efficiency delta prediction for Mid Speed IGV/Stator 1 variant.....	119
Figure 5.28 Visualisation of improved Surge Margin delta prediction for Mid Speed IGV/Stator 1 variant	120
Figure 5.29 Visualisation of improved Efficiency delta prediction for Mid Speed Stator 1/Stator 2 variant.....	121
Figure 5.30 Speedlines comparison between reference model and Mu-Fi optimized – Mid Speed.....	122
Figure 5.31 Visualisation of spatial distribution of the samples for Low Speed IGV/Stator 1 variant.....	123

Figure 5.32 Visualisation of spatial distribution of the samples for Low Speed Stator 1 /Stator 2 variant	124
Figure 5.33 Semi-variance model for Multi-Fidelity IGV/Stator 1 efficiency variant .	125
Figure 5.34 Semi-variance model for Multi-Fidelity IGV/Stator 1 Surge Margin variant	125
Figure 5.35 Semi-variance models for Multi-Fidelity Stator 1/Stator 2 efficiency variant	126
Figure 5.36 Visualisation of Efficiency delta prediction for Low Speed IGV/Stator 1 variant.....	126
Figure 5.37 Visualisation of Surge Margin delta prediction for Low Speed IGV/Stator 1 variant.....	127
Figure 5.38 Visualisation of Efficiency delta prediction for Low Speed Stator 1/Stator 2 variant.....	128
Figure 5.39 Visualisation of improved Efficiency delta prediction for Low Speed IGV/Stator 1 variant	129
Figure 5.40 Visualisation of improved Surge Margin delta prediction for Low Speed IGV/Stator 1 variant	130
Figure 5.41 Visualisation of improved Efficiency delta prediction for Low Speed Stator 1/Stator 2 variant	131
Figure 5.42 Speedlines comparison between reference model and Mu-Fi optimized – Low Speed.....	132

List of Tables

Table 1 Mesh resolution.[43].....	49
Table 2 Mesh convergence.[43].....	49
Table 3 Numerical grid statistics. [43].....	52
Table 4 Surge margin delta [45]	62
Table 5 Computation time [45].....	62
Table 6 Design point parameters delta values for low speed [45].....	64
Table 7 Design point parameters delta values for medium speed [45].....	65
Table 8 Design point parameters delta values for high speed [45].....	66
Table 9 Surge Margin delta for all examined cases [45].	67
Table 10 Adjustment uncertainties at Working line	71
Table 11 Angle change matrix.....	73
Table 12 List of applied VGV setting – High Speed.....	74
Table 13 Pressure Ratio uncertainty	75
Table 14 List of applied VGV setting – Mid Speed	75
Table 15 Pressure Ratio uncertainty	76
Table 16 List of applied VGV setting – Low Speed.....	76
Table 17 Pressure Ratio uncertainty	77
Table 18 High speed variations – CFD.....	78
Table 19 High-Speed Mass Flow uncertainty – CFD.....	79
Table 20 Mid-speed variations – CFD.....	80
Table 21 Mid-Speed Mass Flow uncertainty – CFD	80
Table 22 Low-speed variations - CFD.....	81
Table 23 Low-Speed Mass Flow uncertainty – CFD	81
Table 24 Correlation coefficient for High Speed.....	84
Table 25 Correlation coefficient for Mid-Speed.....	86
Table 26 Correlation coefficient for Low-Speed	88
Table 27 List of optimization task parameters.....	93
Table 28 Mu-Fi process results compare – High Speed	111
Table 29 Mu-Fi process results compare – Mid Speed	122
Table 30 Mu-Fi process results compare – Low Speed.....	132
Table 31 Summary table of performed optimization processes	133

Nomenclature

Symbols:

\dot{m}	Mass flow rate [kg/s]
$P_{total\,in}$	Total pressure at inlet [Pa]
$P_{total\,out}$	Total pressure at outlet [Pa]
$\pi = \frac{P_{total\,out}}{P_{total\,in}}$	Pressure ratio
h	Specific enthalpy
$\eta = \frac{h_{out} - h_{in}}{h_{out,is} - h_{in}}$	Isentropic efficiency
Δ	Change in a variable
pp	Percentage point

Acronyms:

WET	Water Enhanced Turbofan
EASA	European Union Aviation Safety Agency
CFD	Computational Fluid Dynamics
SCM	Streamline Curvature Method
DLR	Deutsches Zentrum für Luft- und Raumfahrt (German Aerospace Center)
DP	Design Point
HPC	High Pressure Compressor
IGV	Inlet Guide Vane
OGV	Outlet Guide Vane

LE	Leading Edge
MP	Measurement Plane
N	Rotational speed
PR	Pressure Ratio
MF	Mass Flow
RANS	Reynolds-Averaged Navier-Stokes
R1	Rotor 1
SM	Surge Margin
SST	Shear Stress Transport
S1	Stator 1
TE	Trailing Edge
TRACE	Turbomachinery Research Aerodynamics Computational Environment
VGW	Variable Guide Vane
WL	Working Line
y+	Non-dimensional wall distance
2D	Two-dimensional
3D	Three-dimensional
CK	Co-Kriging
Mu-Fi	Multi Fidelity
Lo-Fi	Low Fidelity
Hi-Fi	High Fidelity

1 Introduction

1.1 General information

As in every field of engineering, the aviation industry continuously develops their products to still shifting technological boundaries toward market needs. In today's world, environmental knowledge in terms of aviation sector impact for the climate change and noise pollution has increased. As one of the steps towards making aviation a cleaner mode of transportation, EASA has published the report on this topic [1]. Such activities are pushing aviation industry to design more efficient components, with less environmental impact of the every aspect of the product life. Since the main source of pollution in the airplanes is located in engines due to process of combustion, manufacturers are trying to develop a component providing lower CO₂ emission and fuel savings. This may be achieved on different ways. One of it is usage of sustainable fuels together with highly efficient engine [2], where 20% of emission reduction is expected together with 75% smaller noise footprint. Another approach might be to rely on further developing of the technology, using state of the art materials and technics such as additive manufacturing [3]. By enhancing the performance, 25% fuel efficiency improvement is expected with further increase of bypass ratio development. To push environmental performance to the limits it's required to think out of the box, an excellent example of that is Water-Enhanced Turbofan (WET) concept [4]. This engineering challenge is containing benefits of using sustainable aviation fuels and Geared Turbofan but enhancing this with water injection of the vaporized water into combustion chamber to reduce fuel consumption, CO₂ emissions and contrail formation. In addition, vaporized water is collected by utilizing heat from exhaust gasses with use of heat exchanger. The reduction of general environmental impact is being expected to reach 80%, approaching climate neutrality. Each company has its vision of developing climate neutral product but in the end all ideas will face problems when they come to the design phase. Every aircraft engine is a sophisticated machine requiring thousands of engineering hours to design and manufacture the component.

To maintain operability of the engine, every module has to be optimized to reach the best possible performance in the wide operational range. As one of the most critical components in terms of the operability is a compressor. In the most state of art turbofan

aircraft engines, multistage axial compressor is the type of choice. The challenges behind designing of such module are being allocated into trade between efficiency, robustness and Surge Margin.

1.2 Axial compressor design importance

Axial compressor is the component of modern turbofan engines. The module itself is being considered as the critical part in the main gas path. In this type of turbomachinery, flow is travelling in axial direction through the Rotors, responsible for accelerating the fluid and Stators responsible for diffusing energized flow to reach the desired pressure rise. This principle indicates multistage way of designing the axial flow compressor.

Nowadays, the requirements set for compressors performance have been put on the high level due to requisition of lowering fuel consumption and environmental impact. It's necessary to achieve desired massflow, Pressure Ratio and the highest possible efficiency over wide operational range. Behind wide operational range, stability of the component is hid. Generally final design of the axial compressor is a trade-off between stability and efficiency, where gaining one of them, shows the fall of the other if talking about fine designed component.

To draw the complexity of axial compressor requirements the Compressor map is presented in the Figure 1.1.

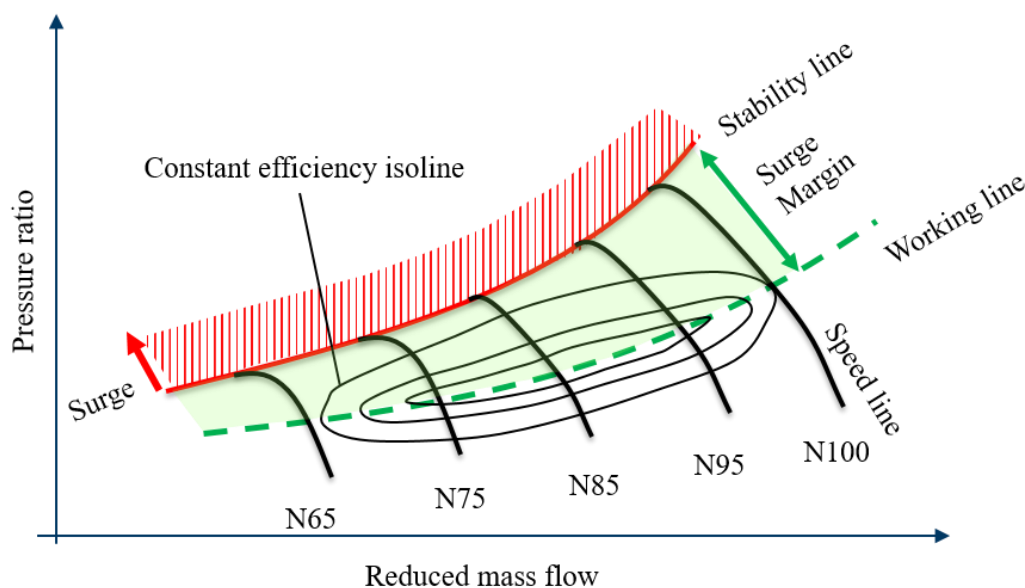


Figure 1.1 Compressor map

To describe compressor map the following individuals are being presented:

- Working line – a set of operational conditions for steady state work of a compressor defined by turbine operational range
- Speed line – operational range of a compressor at specific speed becoming an effect of compressor outlet choking
- Constant efficiency iso-lines – iso-lines representing efficiency within the operational range
- Stability line – a line representing set of last stable compressors working points. The area between the Working and Stability line is called Surge Margin expressing safe operational range for the compressor what is critical for transient behavior during regular operations. Above the Stability line, Surge has presence.

During the axial compressor design task except efficiency target which is considered via sophisticated aerodynamic design, it's important to keep valuable trade-off with Surge Margin which have to be taken into account as a primary parameter ensuring safety and operability of the final product from aerodynamics point of view.

Unfortunately for engineers, there are more than one type of compressor stall behavior needed to be consider and detection of this aspect is time consuming and unlikely possible to being approximated via simple empirical correlation on an early stage of design.

Two main groups of axial compressor instabilities are being observed:

- Rotating stall – the situation where only fraction of the flow is being stalled. As the effect, pressure rise, flow rate and efficiency is affected due to locally stagnated flow. At this point, general stability of compressor has not collapsed yet, but rotating stall cell may follow to completely developed surge.

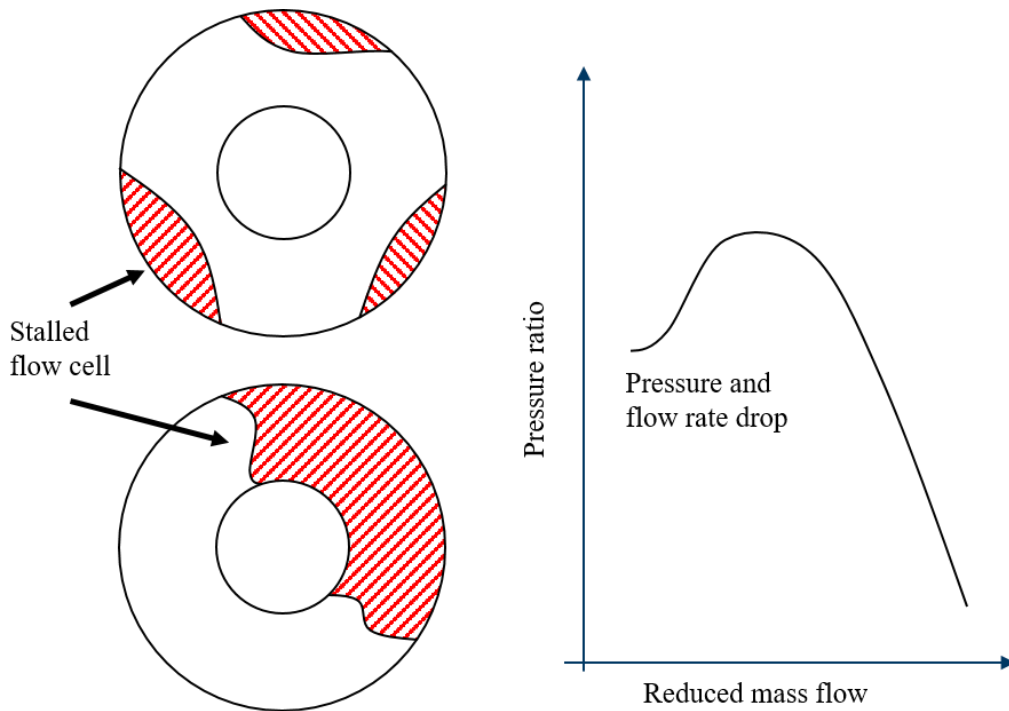


Figure 1.2 Locally collapsed flow

- Axial-symmetric stall (Surge) – this state of flow is critical for an axial compressor functionality. At this point, flow is collapsed for the entire cross-section of the module to the situation where flow is moving backwards following pressure potential. Mentioned event is repeatable, and usually [5] has a frequency in the range of 3-10 Hz and may be called Surge Cycle.

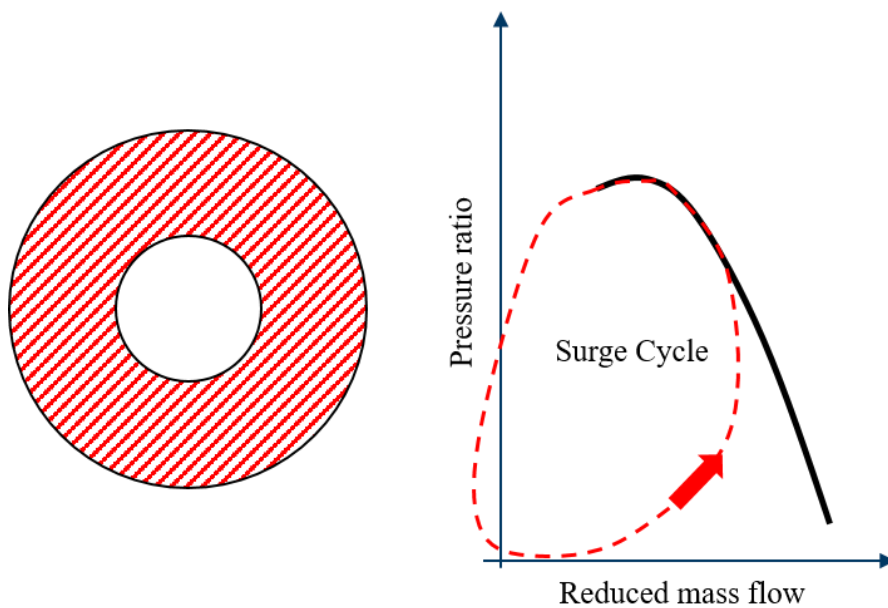


Figure 1.3 Fully developed stall with Surge Cycle

A surge event usually is terminal for the jet engine and it is providing to shut-down due to mechanical damage.

These reasons are standing behind importance of stability prediction during every design task of an axial compressor. Since it's a strongly three dimensional phenomenon, especially at its inception it's impossible to derive precise empirical assumptions. Wherefore expensive 3D CFD simulations have to be performed to take into account all the aspects of this phenomenon. And obviously CFD is not an oracle, to build confidence of the results, solver has to be validated to the tests of the specific conditions that are being considered.

In summary, axial compressor as a component of the jet engine is a critical module in terms of safety and achievable operational range. Therefore, stability aspects have to be considered during the design task with suitable confidence. To perform that, 3D CFD solutions needs to be provided to investigate three dimensional phenomena of stall inception what for the task of design optimization, would have excessive effect on computational cost to reproduce each of the sample with fully throttled speedline. Consequently, the methodology of reducing this effect is desired in order to increase level of quality and usability of the optimization for wide operational range, without expanding computational power.

2 Literature review

2.1 Turbomachinery modeling techniques

Design of an axial compressor is a complex task to perform, containing numerous boundary conditions and requirements to accomplish. As every turbomachinery project it starts with low-fidelity methods for introduction of key preliminary parameters as an input for subsequent steps and for time-efficient exploration of the design space. One of an early step in the gas turbine engines design is usage of 1D Mean-line method, which delivers conceptual sizing of the module (e.g. compressor [6]). The method can be fitted also to different tasks as e.g. being integrated to engine performance simulations as presented in the paper of Koliass et al. [7]. As the next step into flow detail level, another powerful low-fidelity method in the turbomachinery design is Streamline Curvature Method(SCM). SCM has its beginning in 1949 when was firstly described by Wu and Wolfenstein for axial flow application[8]. Since then method is being widely used for axisymmetric and blade to blade solvers for radial and axial turbomachinery [5]. SCM method matching is strongly dependent on the accuracy of empirical correlations that influences estimation of e.g. blade-row blockage and loss. This is revealing as a major inconsistency while computing off-design operational points where the flow is gaining in complexity. The example of SCM axial compressor model visualization is presented in Figure 2.1.

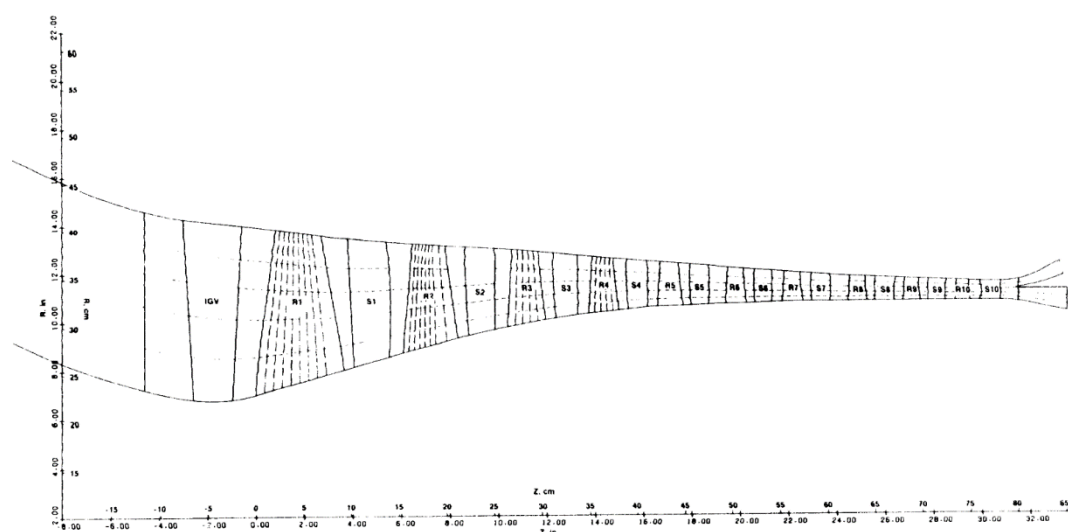


Figure 2.1 Example of through-flow model for axial compressor [9]

In order to close the gap of SCM correlation dependencies, numerous of studies have been performed. As the of on the solution, Jörger [10] proposed attention-grabbing approach of incorporating CFD resulting flow as an input for SCM, replacing empirical loss correlations, so avoiding case dependent 2D solver adjustment being usually made by engineer in posttest matching. Weakness of this approach may be located in need of gathering database of the High-Fidelity CFD calculation to feed the method what may increase computing-cost when new design task will arise.

Both described approaches for turbomachinery flow evaluation are based on empirical correlations which have to be adjusted to the specific conditions in advance to performed computations, what may introduce lack of performance estimation confidence during design space research especially when following setup will be far different then the starting point. The greatest advantage of 1D and 2D methods are unquestionably the computational cost which in compare to any CFD computations is negligible.

Already mentioned methodology as the expensive on is being widely used during gas turbine engine design for performing detailed 3D CFD calculations using RANS approach as good compromise between result accuracy and computational cost or URANS to enable the ability of realizing transient phenomenon with increased CPU demand [11, 12]. There are several works published on the usage of this High-Fidelity approach. Belamri et al. [13] presented methodology of preparing simulations of 15 stage axial compressor. In their work commercial CFX solver has been used, performing steady computations using stage interfaces and two turbulence models – SST and k-epsilon. Work shows approach of defining meshing strategy with sensitivity studies on discretization, tip gap modelling, simple IAS leakage model and turbulence model error. Entire studies were performed on extracted 5 stages. As the outcomes, fidelity levels were defined for various configurations which may be treated as a guideline for defining the approach for general turbomachinery problems modeling. To address specific problem Cornelius et al. focused in their work on increasing ability of predicting stall phenomenon for multistage axial compressor [14]. Their studies were performed on a single stage domain and incorporates geometrical details such as fillets. Steady and transient approach was utilized to find best practices for axial compressor performance prediction. Single stage studies are obviously cheaper to perform variety of setups but it would be worth to

perform such sensitivity on full multistage component to avoid missing stage balance effect.

Despite general compressor map calculations, CFD is used for detailed design as e.g. in work of Erler et al. [15] where tip clearance flow was taken into consideration as a driver for performance and stability desensitization or to enhance knowledge about particular phenomenon around improving Surge Margin where level of the flow detail requires usage of 3D flow solution [16, 17]. Visual example of the flow estimation presented in Figure 2.2 of the work in the field of compressor stability considerations.

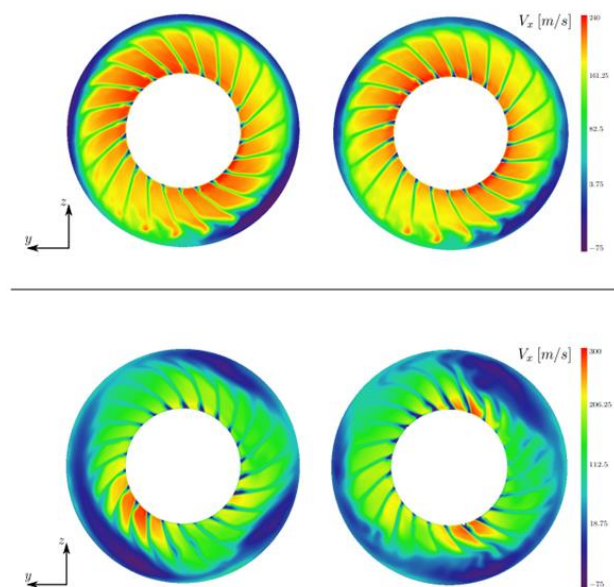


Figure 2.2 Example of 3D CFD flow visualization [18]

All these methods are being used and iterated over design process of turbomachinery systems. The general approach for the designing process has been formulated by Denton in [19] and may be paraphrased as the following:

1. Specification of overall parameters for sizing
2. Perform 1D mean-line calculation to obtain flowpath shape and mid-span blade angles
3. Running SCM calculations to obtain flow angles along the span
4. Continue with SCM calculations to predict initial row-wise performance
5. Blade design with blade-to-blade method (2D)

6. Initiate 3D simulations with simplified multistage grid
7. Perform detailed 3D calculations with High-Fidelity model to resolve all turbomachinery phenomena's as leakage flows, 3D features etc. to get final estimation of the performance.

All of these steps needs to be repeated in the iterative manner to find reliable, the most efficient, with sufficient Surge Margin and robust design.

As discussed above there is a variety of available methods for turbomachinery application where the significance lays in appropriate definition of the requirements which method should be used basing on the desired flow detail level estimation. Mean-line approach together with Streamline Curvature Method are capable to deliver good first estimation on the early stage of the design, where the target is to perform numerous number of simulations to establish initial parameters according to the requirements set. Results are obtained quickly but there is a necessity of having initially correlated loss models, what can be disadvantageous while trying to develop new machine. Moreover, those methods are rather of choice of design point considerations, since physically difficult to estimate the stability level and off design parameters with high confidence without correlation manipulation. For covering the gap of stability estimation and off design working points, 3D CFD computations are being used, which are capable of predicting the complexity of the phenomenon of non-design flow conditions. Nevertheless usage of such High-Fidelity computations at the phase of preliminary or early design would be way too expensive in terms of computational cost when considering number of needed variants to decide on promising configuration during the design task.

2.2 Optimization approaches

Optimization is an enormous area by itself in the engineering world. Turbomachinery can utilize many methods of predicting component performance obtaining different fidelity levels as discussed above. Due to that fact, number of possible approaches has a capability of improve. The general aim of the research in this field is to achieve the optimum with minimal computational cost or to provide multi-disciplinary design goal function.

The work of Joly, Verstraete and Paniagua [20] was focused on multi-objective optimization of highly loaded fan. Their idea was to reduce the iteration number between

disciplines during the design task – so then structural and aerodynamics optimization was performed. The strategy often is to utilize different fidelities and it's the approach utilized in their work (Figure 2.3).

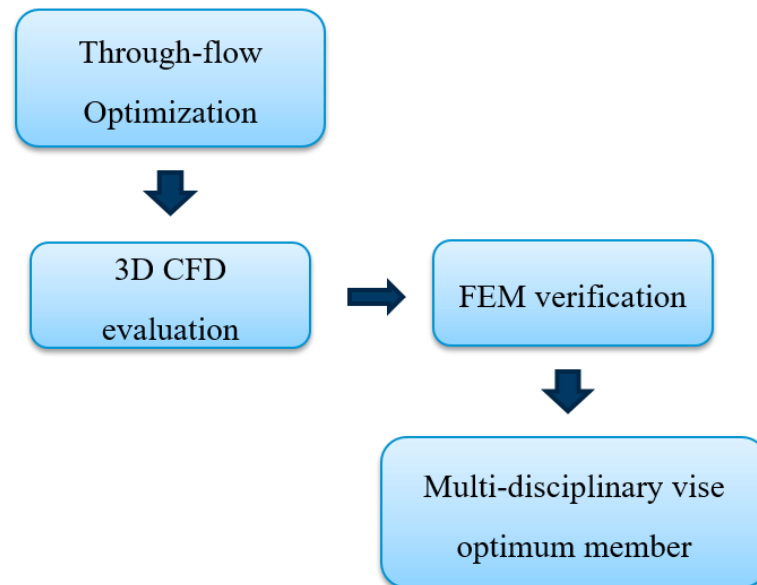


Figure 2.3 Simplified visualization of the approach proposed by [20]

Low fidelity part of the workflow was parametrized to vary the following:

- Flowpath
- Wheel speed
- Axial length
- Solidity
- PR distribution

As the objectives, the efficiency, minimum tip radius and Flow turning were set.

Based on this part, Pareto fronts were derived. This part was used as an input for high-fidelity solver to provide a baseline for further multidisciplinary requirements. In that part the authors performed simultaneous evaluation of fluid and structure performance.

As the constrains for the structural analysis centrifugal force, root faces freedom and flow pressure load were chosen. As the outcome of their study, two optimums were obtained, aerodynamic and aero-mechanical one.

The methodology proposed by the authors was based on progressively increasing fidelity of the solvers. This kind of approach is efficient, when 3D simulations doesn't require extensive domain with several rows included. Using multistage axial compressor for similar work flow would be extremely expensive in terms of computational cost. Also with more complex component, 2D method won't be precise enough to represent the design space as the only guide for optimization members.

Another interesting approach was proposed for intermediate compressor duct optimization in the work of Stürzebecher and others [21]. Contrary to the previous work authors decided to use only one fidelity of the solver - fully turbulent, 3D RANS simulations. As the domain, parametrized intermediate compressor duct was introduced (Figure 2.4). Mentioned approach with single fidelity usage was motivated by necessity of simulating 3D flow for loss assessment and OGV wakes influence.

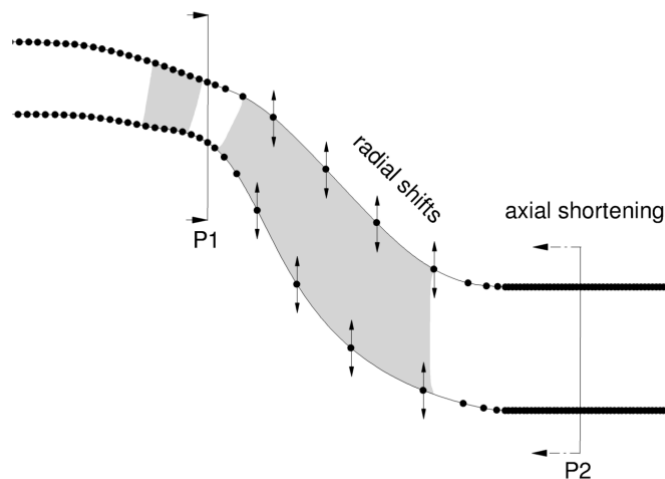


Figure 2.4 Flowpath parametrization [21]

To reduce possible rapid computational cost growth, authors divided optimization task into two separate processes. This approach is noticeably decreasing optimization parameters number for a single run what emphasizes task complexity diminishing.

In the first round the following objectives were defined:

- Axial shortening
- Entropy Rise Coefficient

In the second one more detailed containing OGV, feed with previous optimum member:

- Shear Stress Wall Area limitation
- Entropy Rise Coefficient

For each of optimization tasks, the metamodel of enhanced evolutionary algorithm AutoOpti [22] has been used, where “Kriging” was implemented for process acceleration purposes.

As the outcome, shortened, separation free duct has been developed with comment on future need incorporating complete upstream row for better flow behavior understanding in terms of wake interactions with separation tendency.

The work has presented detailed optimization of a single component - ICD. To reduce computational cost, authors divided the task into two steps but keeping the same High-fidelity solver. Usage of evolutionary algorithm allowed for efficient design space exploration. In the ideal world, the best solution would be to check every combination of the parameters, but this is always limited by computational cost, particularly with use of 3D RANS simulations together with large number of parameters. Question arises whether would be possible to cover some of the design space with lower fidelity method e.g. with coarser meshing.

As a half-way solution for fidelity level decision is an introduction of a correlation of flow parameters, to be able to predict desired behavior without obtaining explicit solution. Such an approach was presented by Ratz et al. [23]. The aim of the work was to determine objective function, available at design point to indicate Surge Margin potentials, flowchart of the procedure is presented in Figure 2.5.

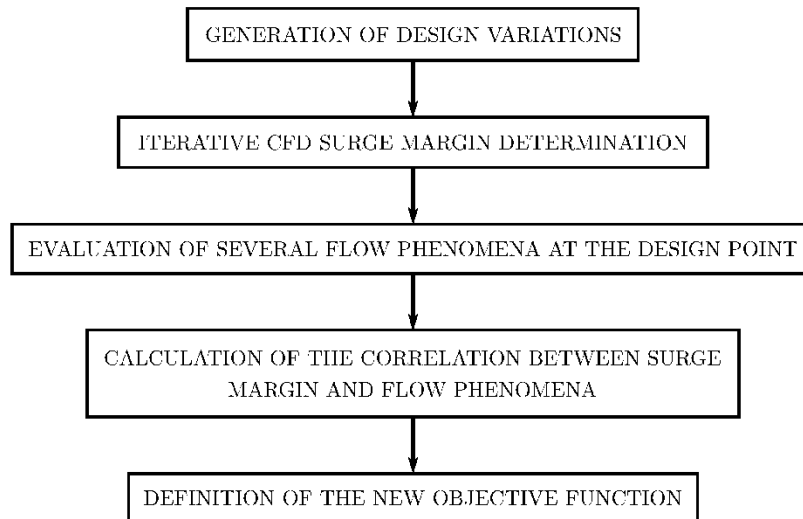


Figure 2.5 Proposed procedure [23]

As a first step, authors determined standard approach CFD simulations with use of High-Fidelity RANS simulations to obtain “computed” Surge Margin basing on last converged point component numerical stability. To determine correlation, 73 designs were generated as a full speedline representation for design point of SM indicator seeking. As an outcome, new throat deceleration ratio function was determined. Authors validated new parameter with optimizations which confirmed improved impeller and diffuser design.

Despite using of High-Fidelity solver, computational cost has been reduced to design point computations. Definitely it is an advantage when it’s not required to iteratively obtaining full speedline until divergency appear. Unfortunately due to complexity of multistage axial compressor component, it is impossible to obtain such a flow parameter possible to read at design operational point. In the case of presented centrifugal compressor, there are only two interacting components – impeller and diffuser. In multistage machines, there are several Rotor and Stators, mutually interacting and balancing what causes impossibility of application of this approach. Studies on stall and surge, especially for axial compressor have progress since Second World War [24] and are still continuing [e.g. 25, 26, 27, 28] what emphasize the importance and complexity of the mentioned subject. Probably the most popular in axial compressors world indicator for stability margin prediction is Koch criterion [29] formulated in 1981 by C.C. Koch. It’s an empirical correlation based on the experimental data giving well estimated stalling pressure rise capability for an early design phase. Due to empirical roots, method has limits and often with, particularly modern solutions of axial compressors criterion is not qualitatively applicable anymore.

As shown, definition of an optimization task of an axial compressor may be complicated dependent on chosen design parameters and goal function. The compromise between computational cost and results accuracy will differ, when computing design point and when considering off-design conditions for predicting efficiency and Surge Margin. In the circumstances of having multiple methods to describe the system i.e. axial compressor performance in the mentioned case, Multi-Fidelity approach is rising as a promising field to explore joining multiple levels of accuracy of using solvers.

2.3 Multi-Fidelity approach

As the complexity of design tasks increases, the need of efficient method for design space exploration arises. Previously presented examples of optimization tasks were based on multi-level cascade approach, where fidelity increases without aggregating the data. Multi-fidelity approach assumes usage of Low and High fidelity data for prediction of consolidated input for the subsequent loop of the optimizer.

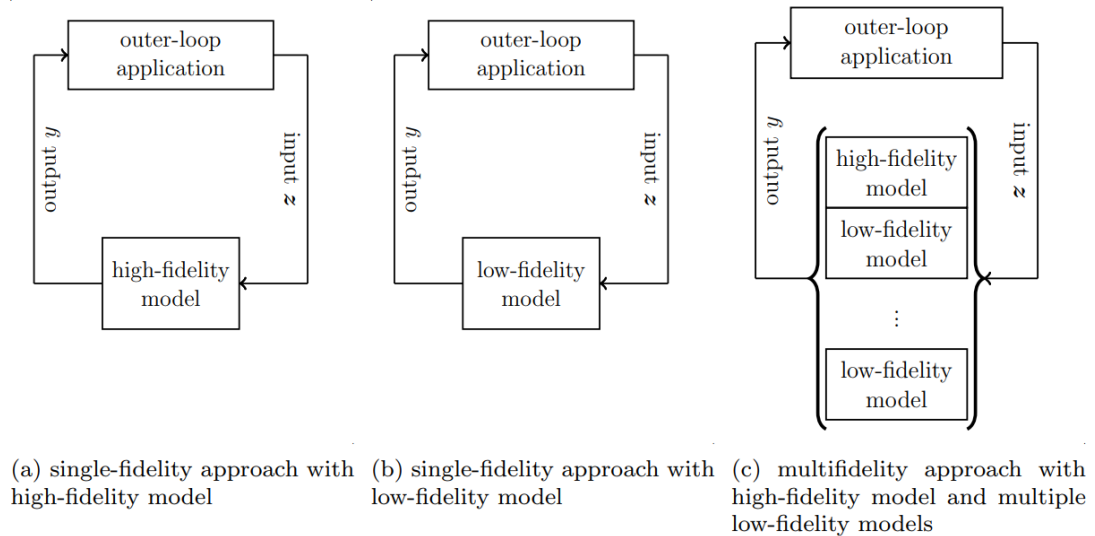


Figure 2.6 Approaches representation [30]

As presented in Figure 2.6, from the work of Peherstorfer, Willcox and Gunzburger, three main approaches may be defined: Single-Fidelity approach with use of high or low fidelity model and Multi-Fidelity approach which is involving high and low fidelity models at once. Form of the methodology can vary relying on low-fidelity model definition and model management strategy.

As collected in [30] it is possible to categorize three types of Lo-Fi models, presented in Figure 2.7.

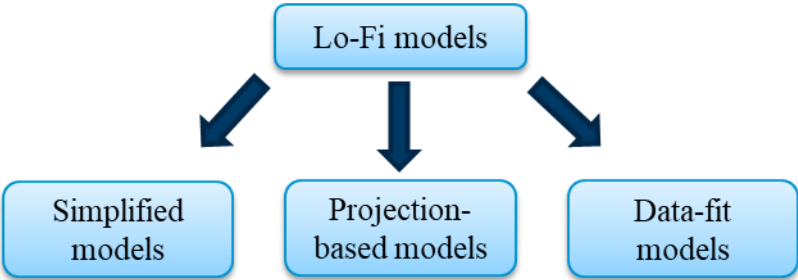


Figure 2.7 Types of Lo-Fi models

Simplified models, represents approach of using less accurate version of Hi-Fi model, e.g. using LES simulations as Hi-Fi and RANS simulation as lower quality response. Within this group, reducing of mesh resolution for Lo-Fi model is located as well. Projection-based models are created by mathematically exploiting the problem structure of Hi-Fi model. Data-fit models considers derivation of the Lo-Fi data directly from Hi-Fi with use of approximation. An example may be a Kriging approximation build on a single Hi-Fi results. [30]

For model management strategy, also 3 types were pointed out by the authors listed in Figure 2.8.

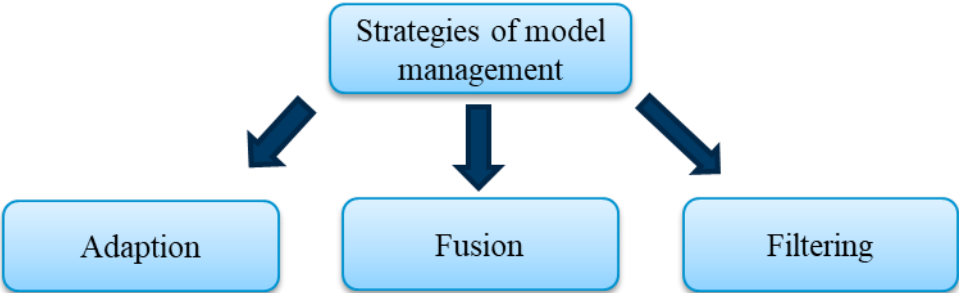


Figure 2.8 Strategies of model management

For adaption, Mu-Fi process corrects the model during the sampling with new data. Fusion strategy has to allow the process to aggregate different fidelities to predict new response. And filtering, stands for sampling strategy based e.g. on importance of specific parameter. [30]

As seen, Mu-Fi approach as novel methodology is structured in the matter of defining Low-fidelity leveled model, and in terms of prescribing strategies of compiling Low and

High Fidelity data. The application in the computer science have wide range of potentials and may be a good approach for complex design/optimization task to reduce computational cost without resigning from the accuracy of Hi-Fi solver.

According to the approach listed in Figure 2.7, simplified model may be used for exploring the design space with use of reduced mesh resolution for lowering the fidelity and decreasing computational cost. Good example of this approach is presented by Shahpar and others [31]. Authors presented optimization concept of transonic compressor rotor using multi-fidelity methodology with fine and coarse grid RANS simulations. Their Low-Fidelity variant of Rotor domain was including reduced grid resolution (from 740000 of fine mesh to 240000 nodes), no fillet at the hub. Cheap configurations showed discrepancy in prediction of efficiency by 2-3%.

Optimization strategy was based on geostatistical methods Kriging/Co-Kriging (Figure 2.9), responsible for aggregating Low and High database. For the design space sampling, Latin Hypercube sampling has been used.

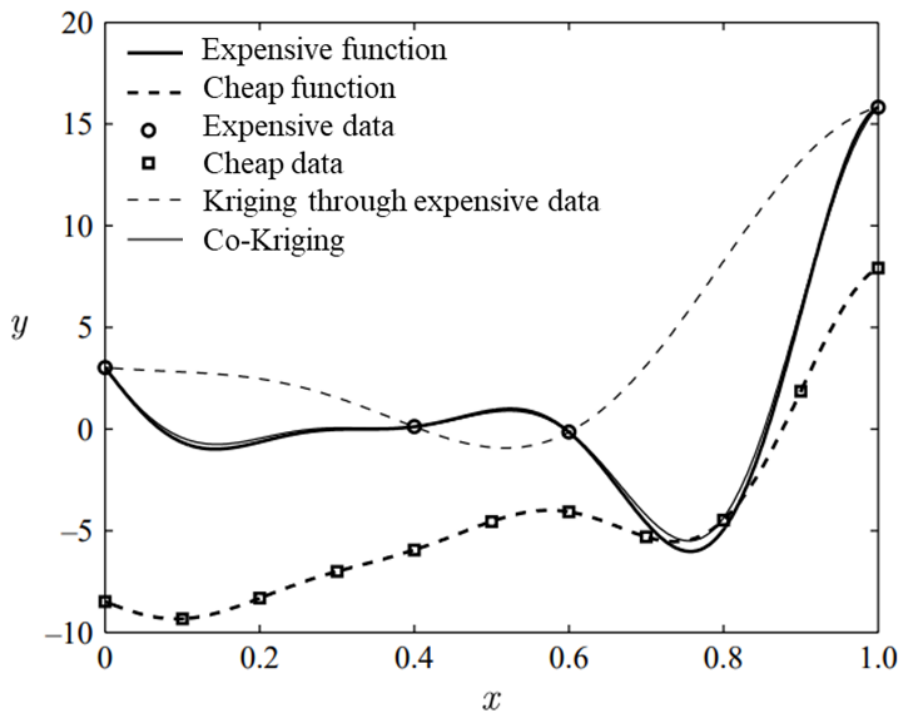


Figure 2.9 Visual representation of Kriging/co-Kriging approximation [32]

The work, has been executed in two manners. First with Kriging, where Hi-Fi sampling was being interpolated on the design space to achieve the optimum. This single Fidelity

part may be efficient, but due to computational budget cap, there is a risk of insufficient space exploration in optimum seeking. Second strategy was introducing multi-fidelity strategy with use of Co-Kriging. Budget has been divided for High and Low Fidelity data. The strategy for reducing an error of co-Kriging was to cover findings of expensive data with the cheap on for each update iteration. For both strategies, efficiency improvement of optimization has been found. For Kriging approach optimization: +1.79%, and co-Kriging: +2.34%. Mu-Fi strategy outperformed Kriging enhanced single fidelity optimization. Here the role has been played by space exploring resolution.

The methodology shows benefits for simple, isolated Rotor optimization case. Efficiency improvements were major, what may indicate, initial geometry wasn't well designed. The optimization was also conducted for a single operating point, what possibly will affect performance in wide operational range within multistage component.

The Multi-Fidelity methodology is not only being used for Turbomachinery application. High computational cost and complexity of the nature was also met in super-cavitating hydrofoils in naval engineering presented in the following papers [33, 34, 35]. In those works, 2D and 3D RANS and 3D URANS simulations were utilized for variate fidelity. In contrary to previous example, for multi-fidelity modelling Bayesian nonparametric approach based on Gaussian process was being chosen. Approach covers construction of accurate multi-fidelity surrogates based on three levels of fidelity. High, medium and low. Medium fidelity models were introduced for minimizing number of High fidelity runs. In the [35] optimization was enhanced with multi-disciplinary approach for penalizing optimized member with structural limitation of FEM simulations. As the outcome, computational cost has been reduced and optimized members with extended variety of parameters were predicted.

Another approach was proposed by Joly and others [36]. In their work, counter-rotating compressors were the object of optimization. Multi-fidelity and multidisciplinary methodology has been developed. Basing on aerodynamics assessment, authors used two fidelities containing Lo-Fi 2D SCM for flowpath and axial cords design and Hi-Fi 3D CFD. Here no direct Fidelity connection has been used. Two methods are working in consecutive manner where SCM is providing preliminary designs for further implementation in CFD simulations. Joly et al. pointed out the risk of using surrogate models due to relatively high number of non-converged flow solutions explaining by that

resigning from metamodeling. For design space exploring, Differential Evolution algorithm is used. Despite of used Mu-Fi approach, work has shown usage of SCM method for preliminary design space exploration, but no correlation level between Hi and Low fidelity has been shown.

As axial compressors are a sophisticated machines equipped with complex aerodynamics, the centrifugal compressors are also dealing with 3D flow phenomenon's being difficult to assess with two-dimensional methods. Due to that, designing of such component also requires amplified computational resources so Mu-Fi approach may be applicable. Use of the approach is shown by Schemmann et al. [37]. Work proposes a multi-fidelity method of "Filtered Sampling" for aerodynamic and structural optimization (Figure 2.10). Methodology assumes use of Latin Hypercube Sampling of the whole parameter space, for which each of proposed member in the first step has to be evaluated by low-fidelity method – 1D loss models for aerodynamics prediction and metamodel for structural assessment. For the Hi-Fi assessment, CFD computations were carried out with use of Ansys CFX – no more details were included.

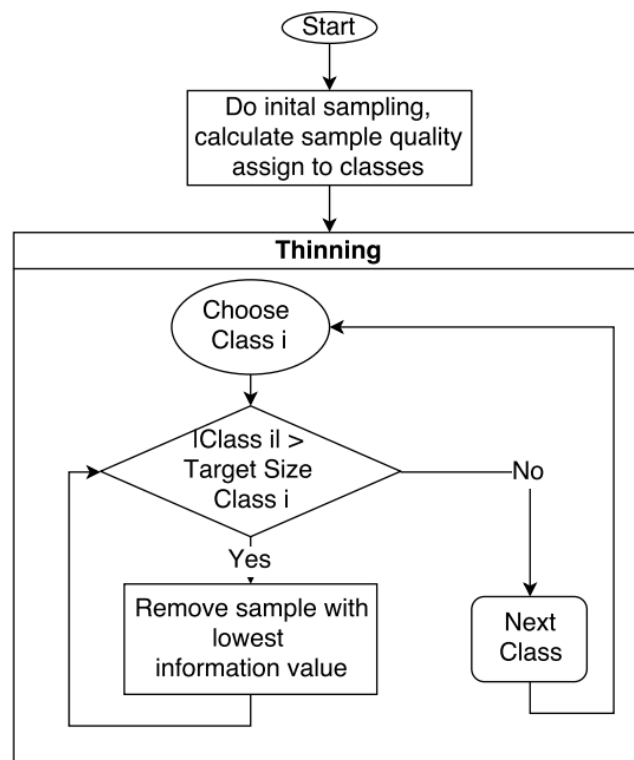


Figure 2.10 Workflow of [37]

The optimization like in many examples was conducted for the design point without lower speeds assessment. The authors stated, that proposed methodology with metamodel based

on filtered sampling showed the same prediction quality as metamodel based on conventionally created sampling. Outcomes of the work are currently applicable only for this particular example of centrifugal compressor.

Despite system component optimization, Multi-Fidelity may be also useful for detailed design. As one of the example, optimization of film cooling hole used in turbine blades as presented in [38]. Zhang et al. proposed as Low fidelity method an empirical correlation for efficiency prediction based on geometrical and coolant properties. As a High Fidelity method, RANS simulation were performed. In this work, again LHS design space exploration together with co-kriging metamodel has been used. The work has shown that Mu-Fi co-kriging outperforms single fidelity kriging for efficiency prediction.

A different application of Mu-Fi is presented in the work of Schnoes et al. [39]. Authors based their studies on four stage compressor with two first transonic rotors. Once more, as a Mu-Fi data aggregation, Co-Kriging has been used. The work strongly relates to axial compressors and preliminary design tools that are being used in this field. As Low Fidelity method, SCM was the tool of choice. Since the optimization has to cover Surge Margin on certain level, Koch stability criterion was applied. For the High Fidelity method, 3D CFD RANS simulations were introduced, covering simple geometry with flowpath and the blades, without any auxiliary features as Bleeds, Leaks of cavities of IAS. As stability criterion, convergence over the speedline throttling was the limiter. It's commonly used approach for steady state simulations. The optimization was carried out for two rotational speeds – 95% and 100%, so both close to the design point. For the objective, maximum efficiency at both speeds at the Working Line and no stability loss was defined. For design parameters, flowpath and blade contours were set as well as staggering for all the airfoils beside IGV is allowed to be changed in the specific range. As the outcome, efficiency gain of more than 1% has been achieved with computational cost reduction. Authors, were complaining on usage of Koch criterion as stability indicator, although off-design rotational speeds weren't taken into account but only close to design point conditions. Due to simple 3D geometry, there is no data on how Mu-Fi would correspond with complex model, and with wide operating range. If thinking about off-design optimization, assessment of stability margin needs to be reviewed. Nevertheless, work of Schnoes et al. shows potential in further developing of this method.

2.4 Conclusions from the current knowledge

The review of available literature within the spectrum of turbomachinery flow solving methods and optimization approaches has been conducted. Design and optimization of a turbomachinery component or specifically axial compressor is an interesting topic of research in the context of computational cost reduction without sacrifice of the results accuracy. The common method used as a reference in optimization task is 3D model with use of CFD RANS simulations in the phase of the design. Found approach was to use the model, representing only flowpath and blades geometry without addition of secondary flow volumes such as IAS. Such simplification, should results in good prediction of efficiency trend representation but in some cases such approach may not be fully suitable, due to interaction with outflows of Inner Air Seal leakage, what despite efficiency influence, may have an impact on Surge Margin estimation but no detailed studies on this topic have been found but only simplified leak interface application. Obviously increasing the details of the model has direct impact on the computational cost what can reduce the capability of optimizer to cover the design space in the efficient way. The solution on the increasing cost is allocated into Multi Fidelity methodology which allows for creating metamodel based on more than single fidelity solution. This approach is opening the opportunities to exchange the cost of creating hundreds of highly expense models to thousands of cheap, low fidelity solutions corrected with use of metamodel with a few expense results. Reviewed works utilized such an approach but in most of applications simple 3D model has been used and optimization took a place only for the design point omitting the operability of lower speeds. Basing on the literature and own experience, Streamline Curvature Method may be a fidelity of choice for cheap solution but there is a requirement of model adaptation. The better adjustment will be performed before use, the better correlation between fidelities is expected. For the data aggregation the common way is to use co-kriging method. The method originally designed for geostatistics for spatial approximations of minerals has found its usage in engineering application.

Basing on the literature, method of Multi-fidelity approach has found its application for turbomachinery, since low and high fidelity models are expected to have initial correlation. Following the preceding, research gap has been found in this field. Literature shows lack of research on CFD sensitivity for axial compressor models incorporating

secondary flow volumes e.g. Inner Air Seal cavity or bleed. It is expected to reveal an influence on stability prediction and efficiency. Another observed gap is located in the field of Multi-Fidelity approach. Since the first usage in axial compressor has been presented, then from the perspective of axial compressor operability it is necessary to extend the usability of the method to off-design conditions. For this reason, concept of methodology has to be introduced. As a result of conducted literature review, and drawn conclusions, the thesis can be formulated.

3 Objectives and scope of work

3.1 Technical Gaps

As the outcome of the literature review, the following technical gaps can be formulated and will be addressed in this thesis:

1. Unknown sensitivity of high and low fidelity models for CFD computations and their advantages in terms of computational effort for axial compressors.
2. Limited application of Multi-Fidelity methodology for off-design optimization for axial compressors.
3. Limited capabilities of Multi-Fidelity Surge Margin predictions at design/optimization task for axial compressors.

3.2 Research objectives

This thesis addresses the following objectives:

1. Develop limitations in prediction of efficiency and stability estimations for various model complexity, and fidelity of flow solution methods for wide range of operational conditions.
2. Establish applicable Multi-Fidelity concept for exploring the design space for extended operational range including efficiency and Surge Margin prediction for an axial compressor.

To demonstrate capabilities of the method, modern 8 stage axial High Pressure Compressor representation have been chosen where Variable Guide Vane schedule will be optimized with Mu-Fi approach and later validated with High-Fidelity representation of the optimized member.

3.3 Technical approach

To discourse described technical gaps and research objectives it was necessary to conduct studies on multiple fidelity models and approaches. Based on literature review, methods

for Multi-Fidelity concept definition have been chosen. As common approaches of available literature, CFD Reynolds Average Navier Stokes and Streamline Curvature Method simulations have been chosen as methods for addressing thesis objectives.

Sensitivity studies have been divided into three stages:

- Studies on mesh sensitivity for model of compressor main gas flow path
- Sensitivity studies on model representation complexity
- Streamline Curvature Method sensitivity in compare to reference 3D CFD representation of the HPC being a result of previous steps

Within first part of sensitivity studies, mesh resolution sensitivity was addressed to be considered. Works were performed basing on 3 rotational speeds to understand how response of the model is changing. During the studies, two turbulence models have been tested in order to find good experiment representation. Aim of this part was to test, if reducing grid resolution may be a model of choice for reduced fidelity solution. To assess that, qualitative and quantitative evaluation has been performed.

Second part, the studies on model representation complexity were the continuation of the first part as an extension for finding good Hi-Fi model and to evaluate sensitivity of fidelity restriction with use of different modeling approaches. Works have been performed with use of 3 rotational speeds, and in addition, different Vane settings were introduced. The intention was to evaluate sensitivity of different model fidelities response on the change of vane angles, where values of pressure ratio, mass flow, and Surge Margin were compared. As summary qualitative and quantitative assessment has been done.

In the third mentioned part of the model sensitivity studies, Streamline Curvature Method was employed. Purpose of the studies, was to detect trends between SCM and RANS solutions. In order to perform that, VGV studies were introduced. In contrary to previous studies, here changes were isolated to each Vane, what has to introduce non-optimal flow field to find limitations of SCM prediction. Tests were focused on trend comparisons, and beside qualitative, visual check, quantitative R correlation coefficient has been used.

Accomplishing mentioned sensitivity studies, constrains for Multi-Fidelity concept definition were available to extract. Consequently choose of Low-Fidelity and High-Fidelity model representation was achievable with known level of correlation between methods, what is the primary condition for Multi-Fidelity application.

The final considerations to address research objectives were focused on application of Multi-Fidelity methodology concept and test of the functionality in order to evaluate the results and draw the conclusions. Method has been tested on 3 rotational speeds, Low Speed, Mid Speed and High Speed to demonstrate the usability for wide operational range. For the optimization example, Variable Guide Vanes setting was evaluated, since the sensitivities were known for these variables. To address quality of the prediction, coefficient of determination R^2 and Root Mean Square Error was introduced as quantitative parameters. For quantitative examination, comparison of the reference and final design was prepared.

3.4 Thesis Contributions

The motivation of this thesis is to increase capabilities of the optimization task for a wide range of the operations by proposing a methodology which can be practical from the point of view of Aerodynamics Engineer and covers primary objectives of axial compressor design. For this reason there is a necessity to cover pointed out technical gaps.

As the main contribution of the following thesis is a methodology containing Multi-Fidelity optimization capabilities for wide operational range of axial compressors based on a multi-stage example, providing:

1. Increased capability for performance estimation using multi-fidelity approach covering design point and off-design conditions containing prediction at Working Line, and for Stability requirements.
2. Reduction of computational cost in terms of exploring assumed design space with decreased number of High-Fidelity members for wide operating range.

A secondary input of the thesis is the definition of the boundaries for involving Streamline Curvature Method into Mu-Fi approach for off-design and finding the sensitivities for reducing the fidelities of CFD model using different model representations.

4 Numerical flow simulations

4.1 Test case description

As mentioned in the chapter of technical approach investigations were based on a axial compressor module. For this reason modern high pressure compressor rig has been chosen. The rig has been developed by MTU Aero Engines AG.

This 8 stage high pressure compressor is designed with shrouded stators i.e. each of them is equipped with labyrinth sealing underneath. For the flow control under different conditions Variable Guide Vanes are introduced for the first 3 vanes starting from Inlet Guide Vane. Machine is equipped in a single bleed port.

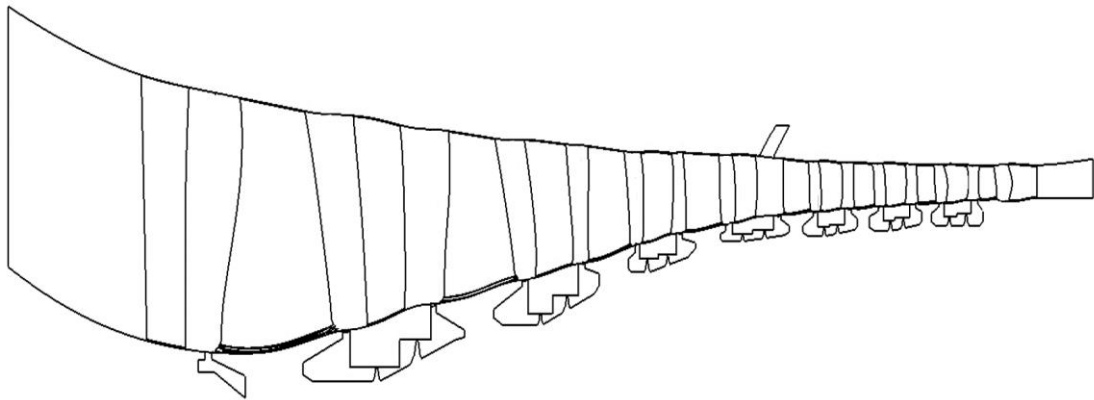


Figure 4.1 Compressor cross-section

Presented compressor has taken part in test runs so the experimental measurements are available. For the work purposes the operational range will be covered with low, medium and high rotational speed which represents compressor characteristics for three rotational speeds. All the following studies are prepared with respect to the experiment based boundary conditions specific to the chosen operational point.

4.2 3D CFD analysis

In this chapter 3D CFD studies are presented. The work has been divided for 2 phases – mesh study and separate configuration study. The aim of studies conducted in this chapter was to find the best low fidelity setup for 3D model which can bring results adequate to the high fidelity reference with reduced computation cost. Results will be used for multi-fidelity concept validation.

4.2.1 Methods used

CFD calculations has wide usage in nowadays design process in any application that requires flow prediction. In the case of this thesis where different fidelities are being mixed out the 3D CFD model has been chosen to represent High-Fidelity database. For this reason it was necessary to choose computational approach and provide sensitivity studies to maintain high quality of the results.

All the computations presented in this work, containing three-dimensional flow simulation were solved with use of TRACE (Turbomachinery Research Aerodynamics Computational Environment), CFD code being developed by DLR Institute of Propulsion Technology and MTU Aero Engines AG. TRACE is a software system for solving three-dimensional internal flow in turbomachinery problems. It is capable to solve multi-stage compressors and turbine components. For this specific work, steady state Reynolds-Averaged Navier-Stokes approach has been used.

3D domain is a single passage representation of described high pressure compressor with inlet and outlet position extracted from the measurement planes where pressure and temperature profiles measures have taken place. According to the measures, inlet conditions of the compressor domain have been prescribed. Outlet conditions have been defined with static pressure value specific to the throttling level of the operational point.

The specificity of compressor modeling i.e. Rotor-Stator domains, requires an interface to connect two frames of reference. To fulfill this requirement, Rotating and Stationary frame are being connected using Mixing Plane condition for the interface. Mixing Plane interface allows to exchange the information of the flow field between two frames of reference in averaged condition [40].

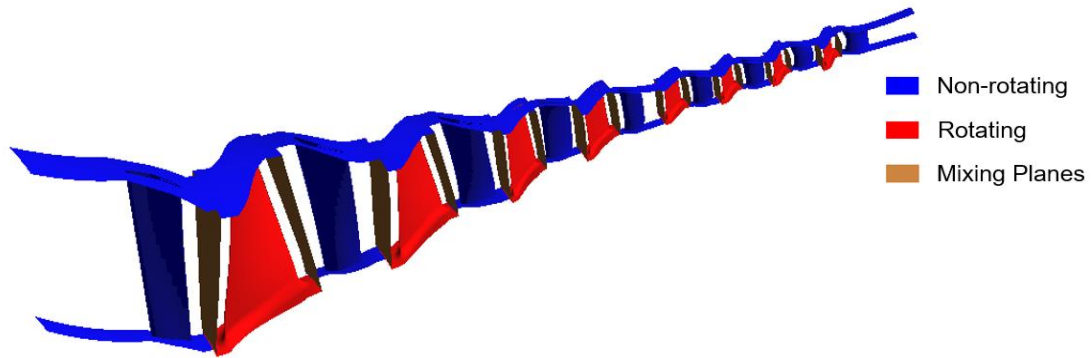


Figure 4.2 Domain representation.

The modelling of the boundary layer have been established to use Low-Reynolds approach, in order to actually resolve more accurate near wall velocity gradient. For this specific study, two two-equation turbulence models were tested to decide on the method to model boundary layer – Wilcox 1988 $k-\omega$ described in [41], and Menter’s SST 2003 $k-\omega$ described in [42].

For all the simulations that have been conducted, initial flow conditions were provided. As a source, flow field computed with use of Streamline Curvature Method was used. Boundary conditions for those simulations were adjusted to the exact Rig operational conditions. Benefit of this approach is to reduce computational time of the flowfield solving especially during the first few starting iterations.

The following study contains only main gas path geometry, so all the features, like bleeds, Inner Air Seals and other are omitted. To maintain secondary flow phenomena, fillets of the blades were reproduced according to real geometry. Clearances over the rotors were reproduced with agreement to the rotational speed that was investigated. In addition, with known importance of all the clearances in compressor, partial gaps appearing in VGV’s have been taken into account also according to specific angle and with respect to curvature of the flowpath (Figure 4.3).



Figure 4.3 Close look on a partial gap of S1

4.2.2 Mesh study

The Finite Volume discretization of the model was made with use of commercial software AutoGrid developed by Numeca which is a powerful meshing tool, providing high-quality multi block meshes specifically for turbomachinery applications.

Usage of this tool allows to manipulate the mesh in a fluent way what helps with conducting studies like the following. Mesh has been prepared according to the general CFD best practices and available block schemes, and this was a starting point for further manipulations. Because of treating boundary level with Low-Reynolds approach, it was intended to obtain non dimensional close to wall cell height parameter $y^+=1[-]$. It has been a requirement for all three rotational speeds, and their mesh variations. In order to control mesh resolution, cell growth ratio was manipulated in the reason of minimizing discretization error at boundary layer during mesh coarsening.

One of the main point was to handle quality of airfoil curvature discretization with respect to coarsen mesh quality. Due to that fact, passage meshing, o-block strategy was used with attention to Leading Edge (LE) and Trailing Edge (TE). To reduce possible negative influence of mesh coarsening, similar node number and distribution at LE and TE was introduced to follow the quality [43].

Since the initial mesh resolution (“Fine”), was created with attention to the suitable geometry discretization with use of automated grid generator for turbomachines AutoGrid software [60], and further studies have taken into considerations only coarser meshes, it

was decided to verify the mesh convergence with only one, increased resolution refinement. The resolution change has been achieved by minor cell growth ratio increase for each rotational speed that was taken into account for mentioned sensitivity studies. Mesh statistics are presented below (Table 1).

Table 1 Mesh resolution.[43]

Rotational speed	Nodes (fine)	Nodes (Extra fine)
Low speed	11 390 860	16 315 334
Mid speed	10 719 632	15 277 574
High speed	10 662 928	15 292 726

Having meshes presented above, CFD models have been prepared and run. Mesh dependency studies considered only close to Working Line (WL) operational points, and Wilcox $k-\omega$ turbulence model. Received results revealed no requirement for further grid refinement what also confirmed the quality of initial mesh setup.

Table 2 Mesh convergence.[43]

Rotational speed [%]	PR deviation (Fine-Extra Fine) [%]	Mass Flow deviation (Fine to Extra Fine) [%]
Low speed	0.00	0.032
Mid speed	0.00	0.033
High speed	0.00	0.013

Table 2 shows the deviations of Pressure Ratio and Mass Flow at Working Line conditions for specific rotational speed for different grid resolutions. Values above shows that current “Fine” mesh configuration is actually resolution independent for all rotational speeds and can be used for further investigations. Observable Mass Flow deviations are negligible and may be a result of convergence phenomena.

The second part of preliminary studies was to investigate which turbulence model is better suited for described task. As previously mentioned, two turbulence models are being taken into account – Wilcox 1988 $k-\omega$ and Menter’s SST 2003 $k-\omega$ – both commonly used in the literature (e.g. [13], [14], [61]).

Basing on the mesh dependency studies “Fine” grid resolution has been used for this purpose for three rotational speeds. This time, not only the WL operation point was considered but entire speedline, throttled up to stability limit. Here, the stability limit was defined as last numerically converged simulation where outlet static pressure was being increased with specified increment.

For results representation, Mass Flow and Pressure Ratio have been normalized according to the following formula.

$$x_{norm.} = \frac{x_i}{x_{ref.}} \quad (\text{Eq. 1})$$

, where:

- $x_{norm.}$ – normalized parameter value, presented on plot
- x_i – variable parameter value, dependent on considered point
- $x_{ref.}$ – reference parameter value for current data set

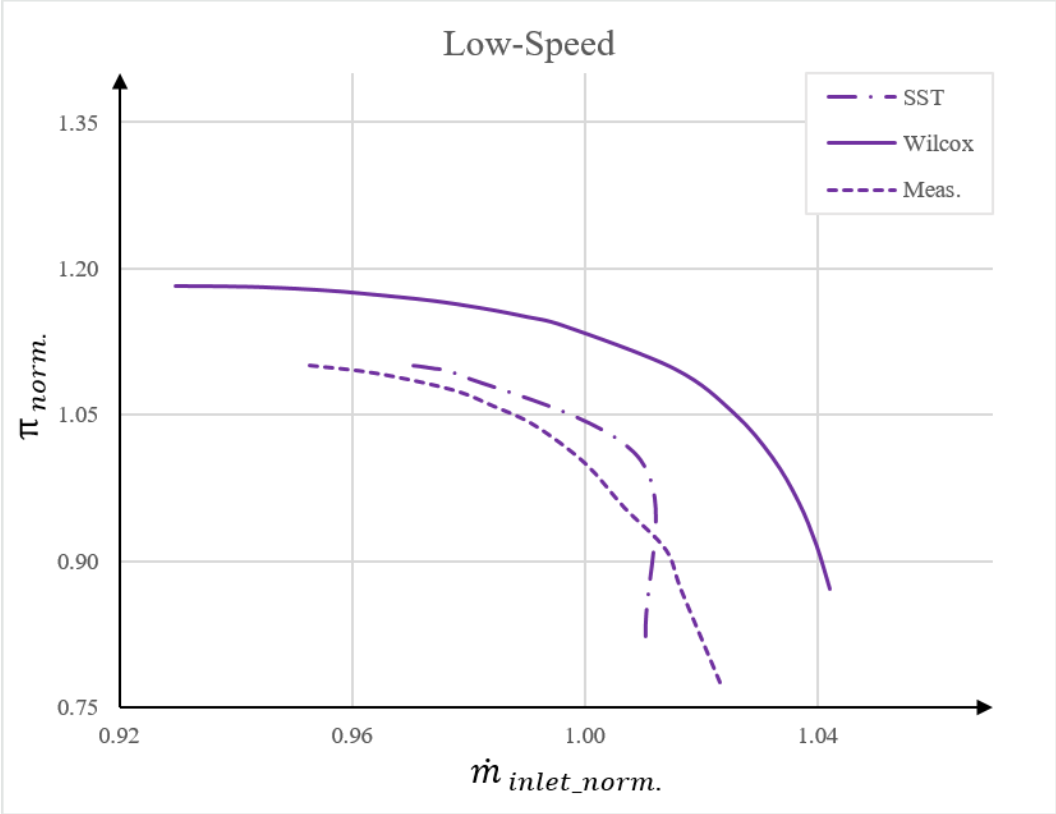


Figure 4.4 Comparison of the turbulence models (Low speed) [43]

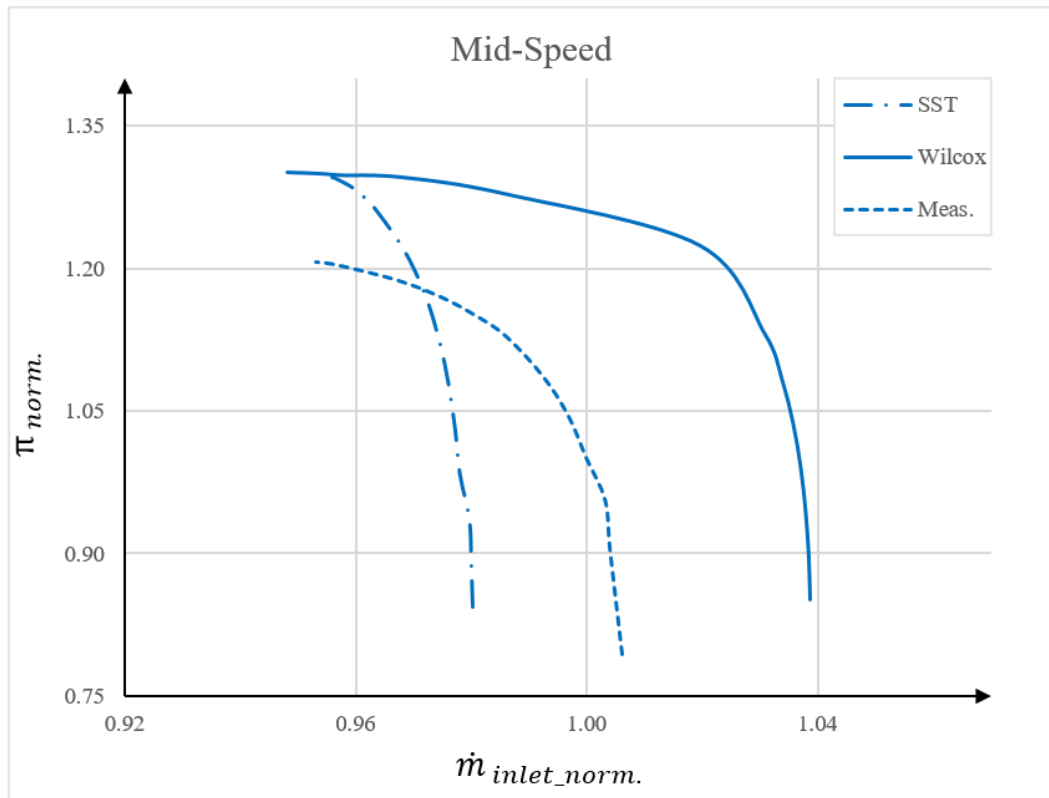


Figure 4.5 Comparison of the turbulence models (Mid speed) [43]

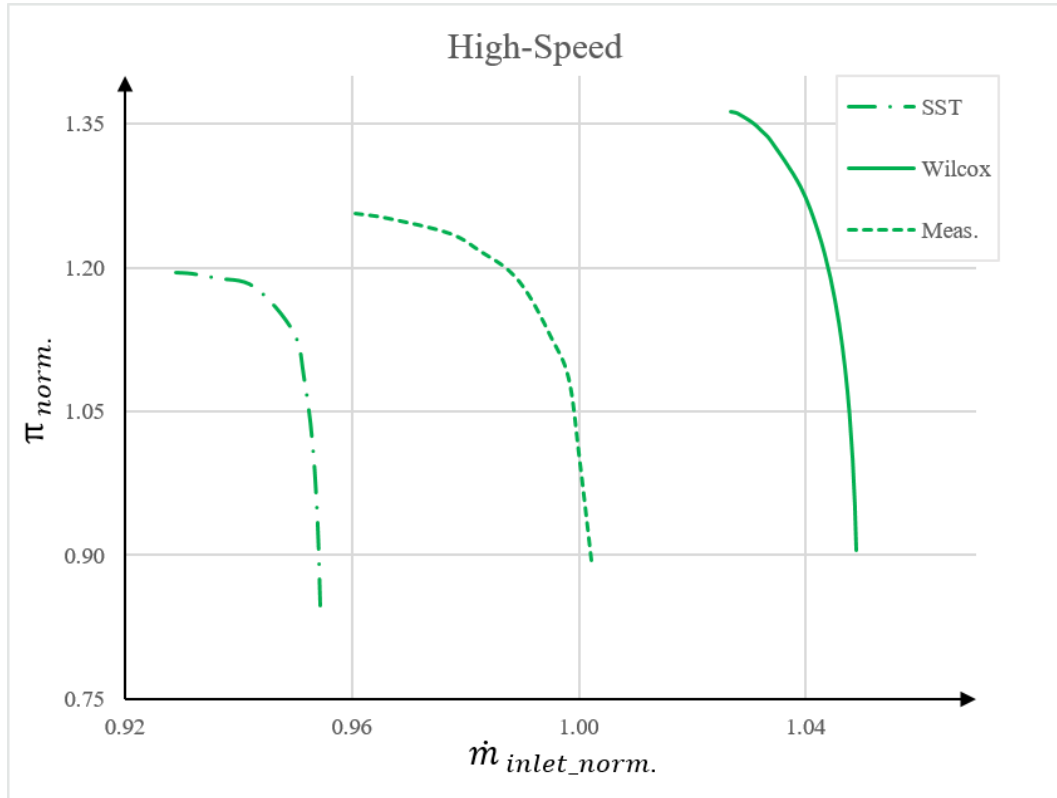


Figure 4.6 Comparison of the turbulence models (High speed) [43].

For all three rotational speeds – Low, Medium and High – both turbulence models have been compared to the experimental data. Figures Figure 4.4 -Figure 4.6 reveals that Menter’s SST model is not predicting constant distribution through the speed in contrary to Wilcox k- ω turbulence model. Low speed and Medium speed shows the strongest mismatch in terms of characteristics shape reproduction. Pressure Ratio and Mass Flow shift is observable for all the configurations. The difference is arising from the modeling approach, where no IAS or bleed have been modeled but different turbulence models are showing discrepancy in boundary layer blockage estimation. Due to the background of the following studies, which was to find reference setup for further considerations it was necessary to focus on predictable bias and reproducibility of characteristics shape for defined rotational speeds. The final decision was to use Wilcox k- ω turbulence model for further analyses as a more trustful choice for this specific usage. Menter’s SST model, wasn’t capable to correctly predict characteristics for the lowest rotational speed in compare to the experiment. Since the turbulence model decision has been made, it was possible to begin the studies of fidelity reduction of the CFD model.

The studies presented below were the first part of 3D CFD model fidelity level sensitivity to obtain promising low-fidelity option for further usage. For this purpose 3 different meshes have been prepared. The coarse, medium and the fine one (mesh statistics shown in Table 3). As mentioned previously, mesh was controlled with use of cell growth ratio with taking care of airfoil curvature discretization. To isolate boundary level influence, y^+ target value have been kept constant for all configurations.

Table 3 Numerical grid statistics. [43]

Rotational speed	Nodes (Coarse)	Nodes (Medium)	Nodes (Fine)	Target y^+
Low speed	3 302 589	5 616 126	11 390 860	1
Mid speed	3 282 963	5 376 538	10 719 632	1
High speed	3 172 653	5 273 786	10 662 928	1

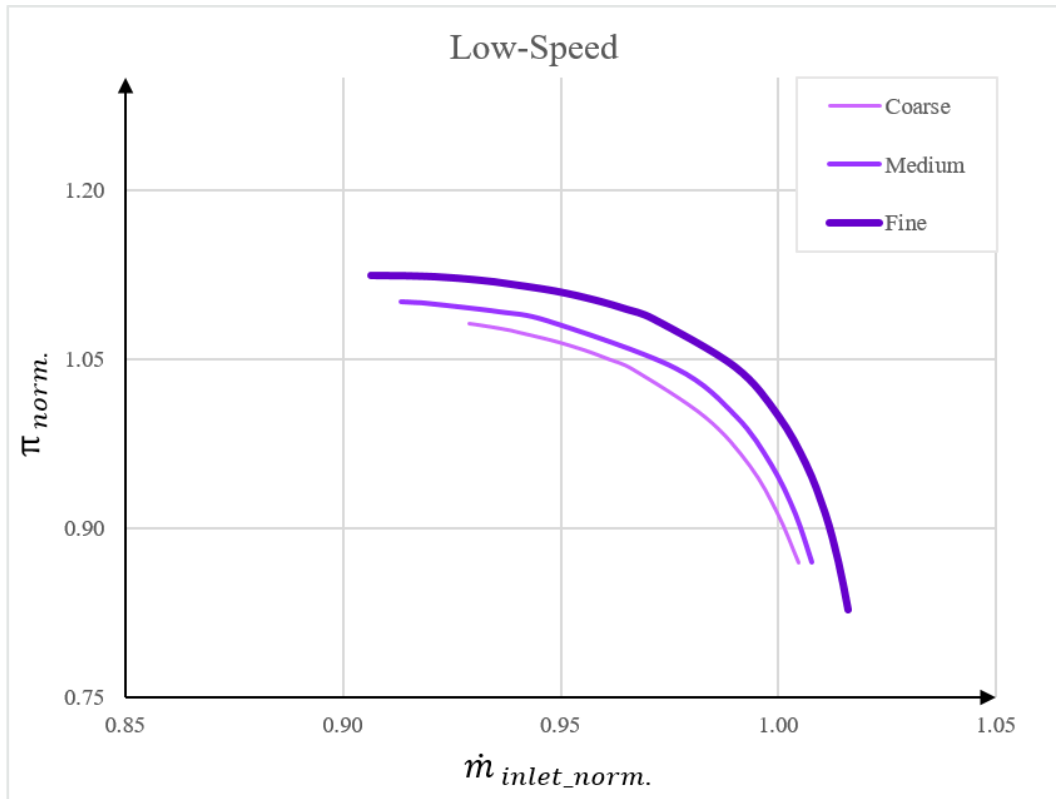


Figure 4.7 Comparison of the mesh density (Low speed) [43]

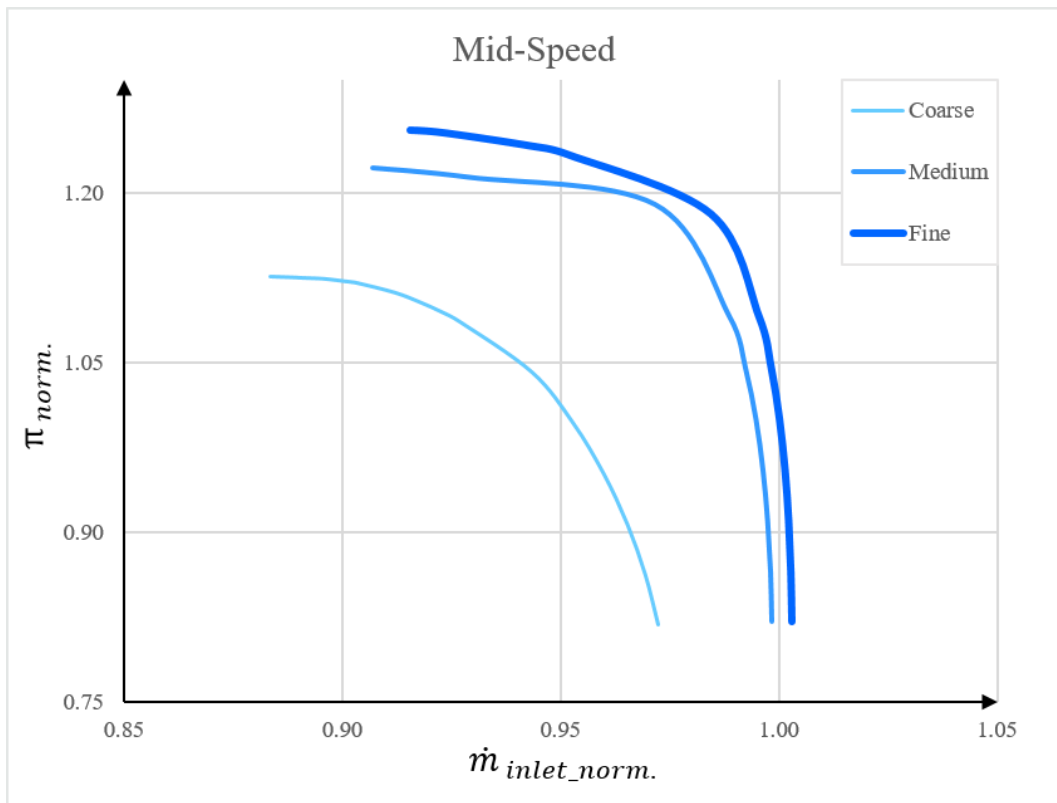


Figure 4.8 Comparison of the mesh density (Mid speed) [43]

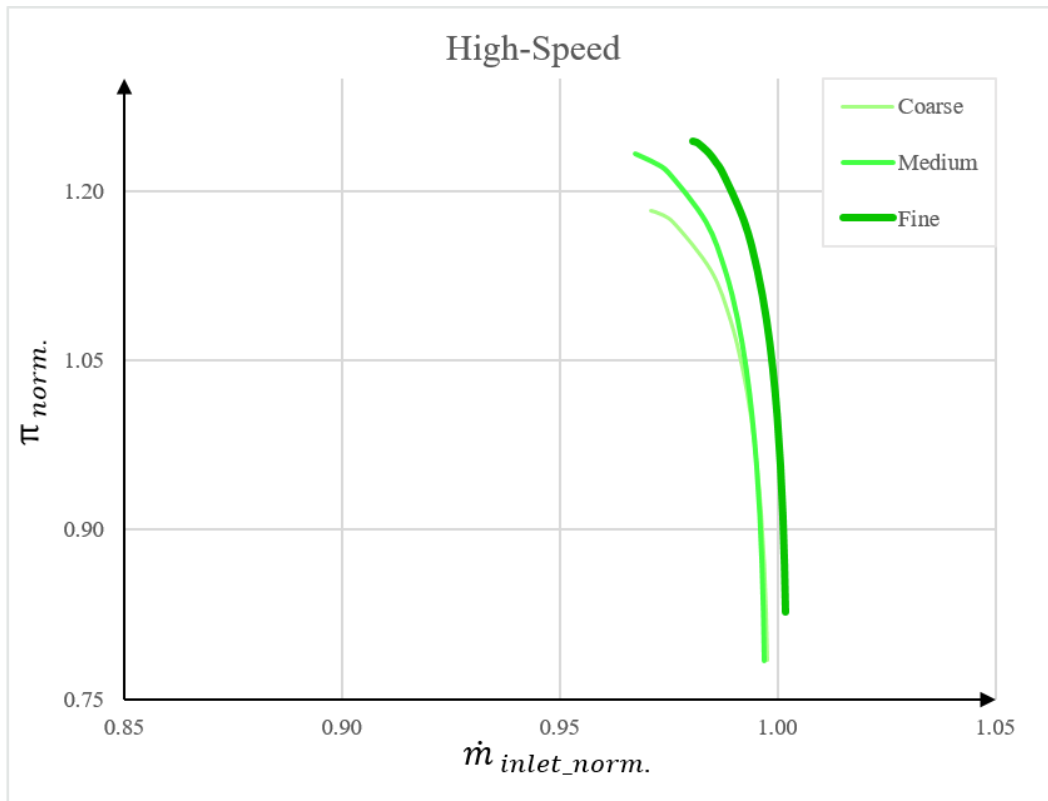


Figure 4.9 Comparison of the mesh density (High speed). [43]

Figures above are presenting sets of speedlines for 3 rotational speeds and 3 mesh variants. On a first glance for all rotational speeds, grids with lower resolution shows shift for Mass Flow and for Pressure Ratio as expected. Results showed that the sensitivity is not constant through the operational speed. Inconsistency with the highest deviation has been observed for Medium speed (Figure 4.8). Due to the shift on a characteristics map obviously Pressure Ratio and Mass Flow has changed but beside that, also the shape has been changed especially for the lowest grid resolution “Coarse”. For the rest speeds, major effect is visible as characteristics shift that the general compressor throttling behavior.

Because resolution change was the same for all speed variants, the question has raised: what is the source of such the discrepancy for this single “Coarse” mesh at Medium speed? Because aim of this work is not to dive into deep flow analysis it was decided to verify quantitatively how endwall blockage is changing[44] due to discretization quality. The argumentation behind this idea was the suspicion that increased cells size can tend to unphysical flow stagnation rise. Details of the performed measure are available in the article of the thesis author [43].

To conclude, it was decided to exclude Coarse Grid from further studies. Results of this variation are unpredictable and may cause problems during next assessments.

As the last part of current investigation, Surge Margin evaluation was conducted. Many definitions of Surge Margin are available in the literature. For this comparison the one prescribed by Cumpsty has been used[5]. His definition contains constant inlet mass flow of WL operational point and PR's rise over the speedline (1).

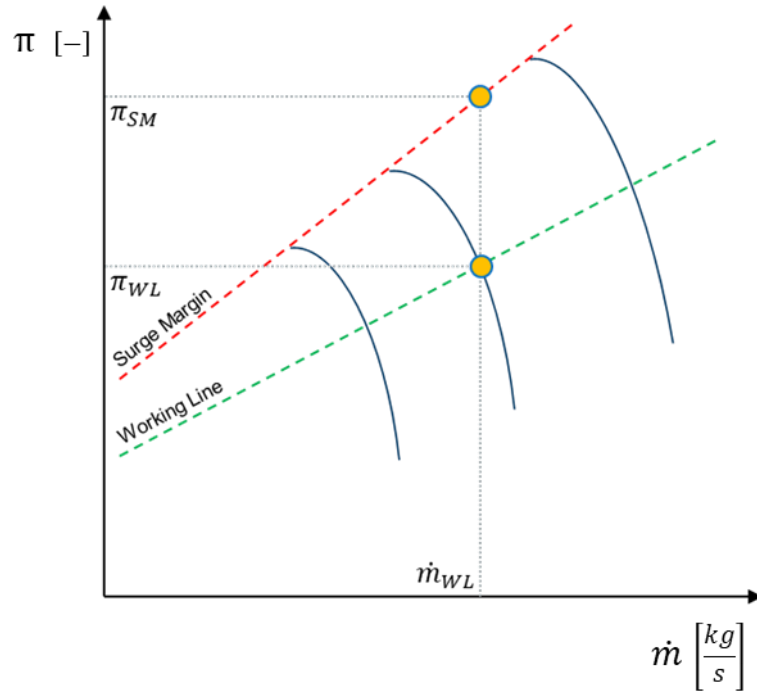


Figure 4.10 . Surge margin by pressure ratio definition. [43]

$$SM = \frac{\pi_{SM} - \pi_{WL}}{\pi_{WL}} \quad (\text{Eq. 2})$$

Using the equation (Eq. 2), Surge Margin for all speedlines has been derived. Basing on those values, the deviation bars were plotted. Figure 4.11 shows how the deviation in compare to measurement is changing for specific grid variation over the speed.

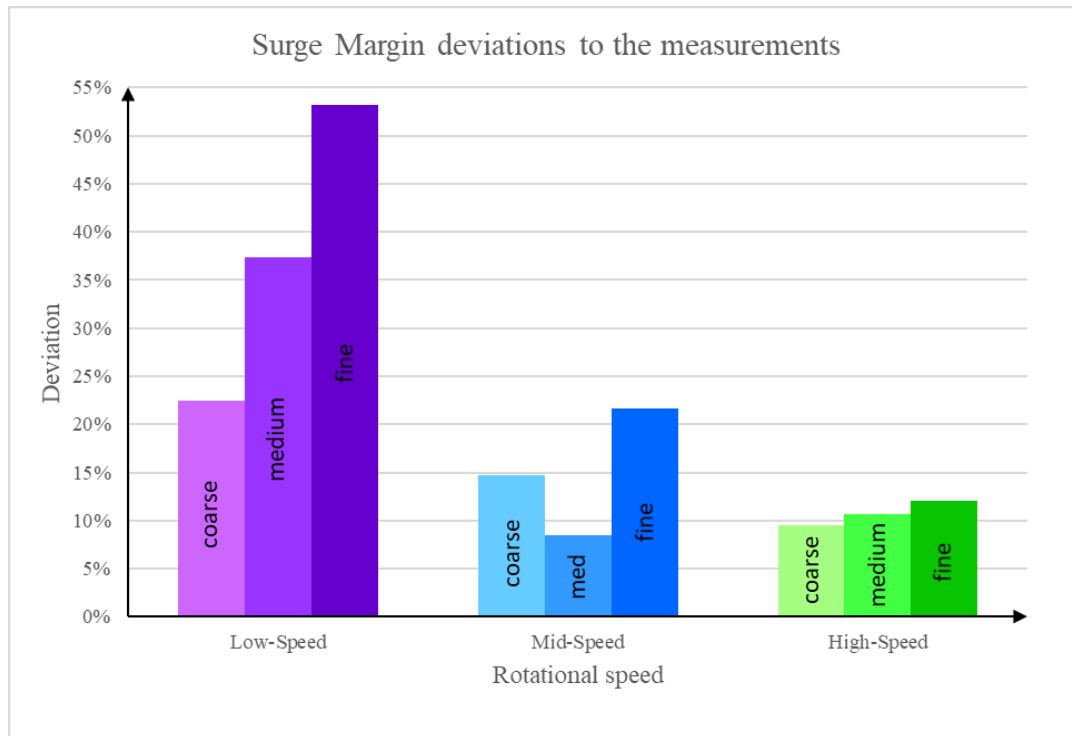


Figure 4.11 Surge margin percentage deviation in compare to the Measurements

Figure above explicitly shows how Surge Margin prediction is sensitive on Grid resolution manipulations. Only High speed variant is showing negligible effect but two other, especially Low speed configuration revealed major sensitivity. In this example, deviation compared to measurement data is not so important. Here a huge influence has an approach to derive the Surge Margin. The definition used here has some disadvantages e.g. massflow drift over the throttling is not taken into account but it is relevant to evaluate influence of isolated variable like presented grid resolution sensitivity study. As the most important outcome of this part is the fact, that SM discrepancy was rising with moving rotational conditions towards off-design regime. This may be a show-stopper when it comes to stability estimation with lower fidelity model discretization.

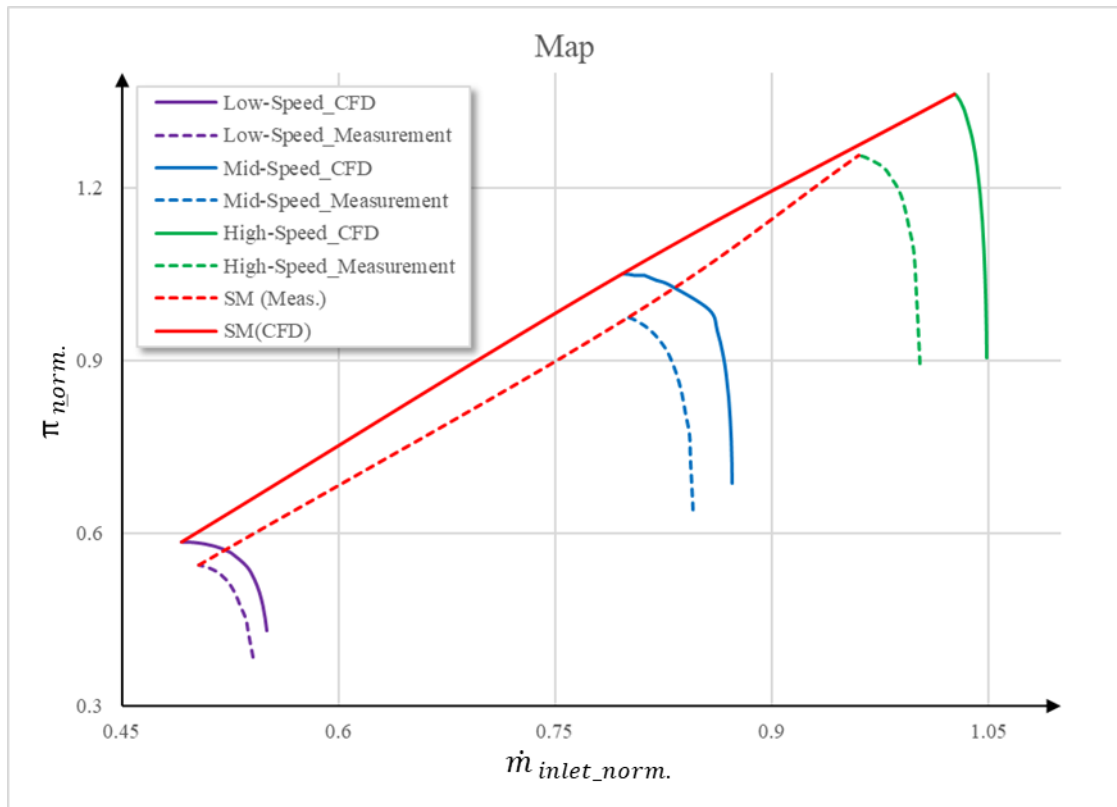


Figure 4.12 Medium Grid and Measurements Surge Margin representation on a Compressor Map

Summarizing, intention of the work presented above was to find low resolution grid configuration which will be applicable for design or optimization strategy providing time reduction with low quality loss. Finally, time reduction of Medium grid has been reached – by about 30% to get numerically converged results. Mentioned configuration has shown acceptable fitting in the qualitative meaning of characteristics distribution for all rotational speeds. Quantitative evaluation showed discrepancy, especially for stability prediction, being an important parameter for axial compressor design. Nevertheless, medium grid resolution has been chosen to be tested in the next phase of the studies, as one of available case for elaboration to be compared with reference models containing detailed representation of the compressor.

4.2.3 Configuration study

The following studies were performed by Wojciech Tulik as a part of his Master Thesis [45] during internship at MTU Aero Engines Polska Sp. z o.o. under company supervision of the author of current PhD thesis. Studies are the continuation of mesh sensitivity evaluation from the previous chapter and are based on the same 8 stage high pressure

axial compressor. The outcome of this work has been used for further Multi-Fidelity concept evaluation.

Author has proposed 2 phase evaluation containing different level of complexity of the model, and different grid resolution.

- Phase I – configuration study for defined operational conditions
 - Geometry representation complexity variations
 - Grid resolution variations (Fine, and Medium mesh from previous study)
 - All above, performed for 3 rotational speeds – Low, Medium and High
- Phase II – VGV manipulation response sensitivity
 - Configurations determined by previous phase
 - 3 rotational speeds
 - 4 variants of Vane Scheduling performed for dedicated configurations

The CFD setup used in these studies has been the same as presented in the previous chapter. Currently the reference model role is overtaken by configuration with cavities, bleeds and leak so called “Full model” – close representation of actual HPC.

To describe each of configuration, short description is presented below together with colors which are representing the condition of specific wall in CFD model.







	Rotating domain
	Stationary domain
	Mixing-plane interface
	Zonal interface
	Leak in panel
	Leak out panel

Figure 4.13 Legend for wall conditions

- Full model.

Configuration where all geometrical features are reproduced. It is the closest representation of real HPC geometry in the following study. Beside the flowpath it's equipped with Labyrinth Sealing cavities and bleed valve chimney (Figure 4.14).

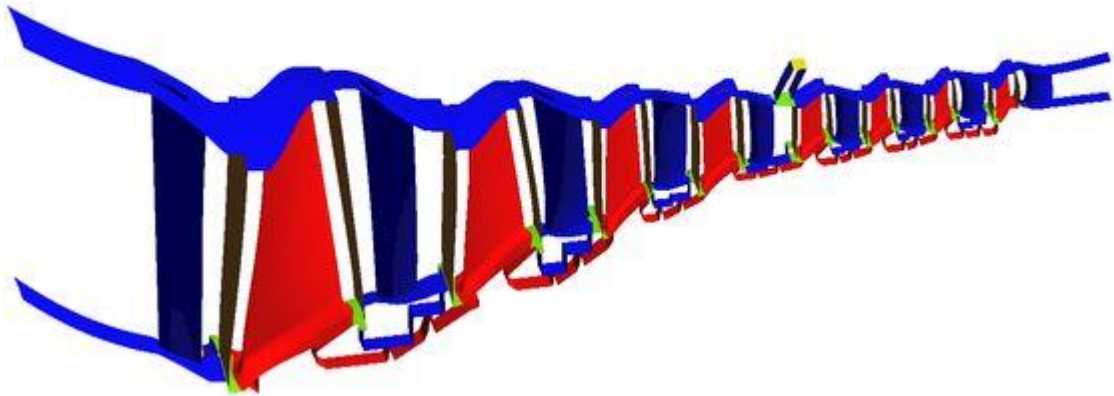


Figure 4.14. “Full model” graphical representation [45]

- Pure flow-path.

The simplest representation of real HPC – model without any feature, just an annulus and blades – this configuration has been used in previously presented investigations (Figure 4.15).

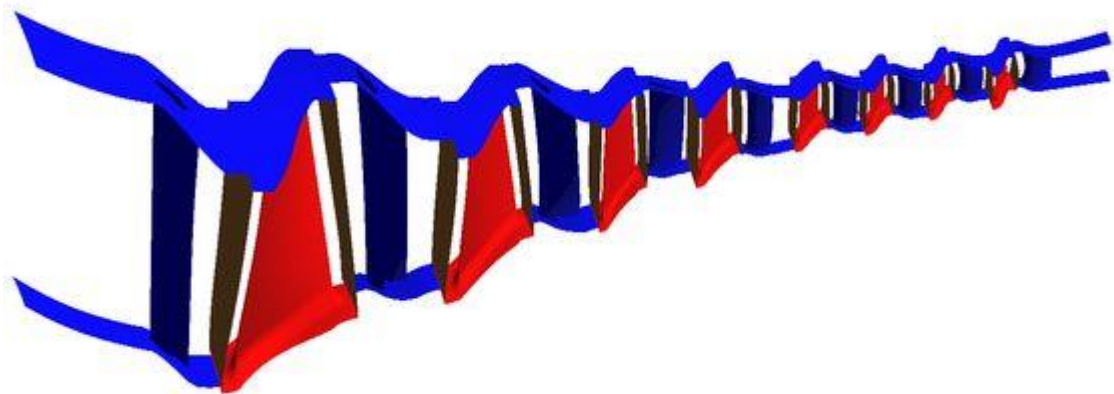


Figure 4.15. “Pure flow path” graphical representation [45]

- Bleed only.

Configuration, geometrically containing only annulus geometry and bleed geometry. Idea behind this variant is dictated by the fact that bleed port is the compressor specific feature (Figure 4.16).

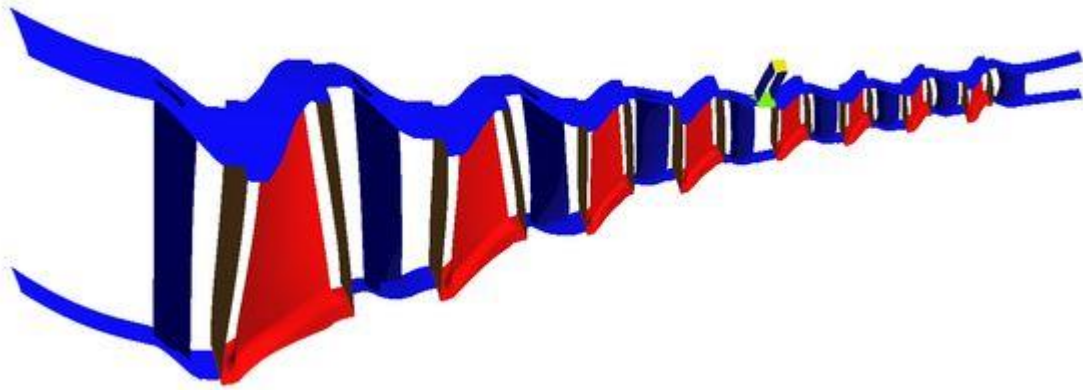


Figure 4.16 “Bleed only” graphical representation [45]

- Panels as cavities.

Configuration, where labyrinth sealing are modeled via leak in and leak outlet boundary condition panels. Presented approach from the mass balance point of view should be capable to reproduce the reference model (Figure 4.17).

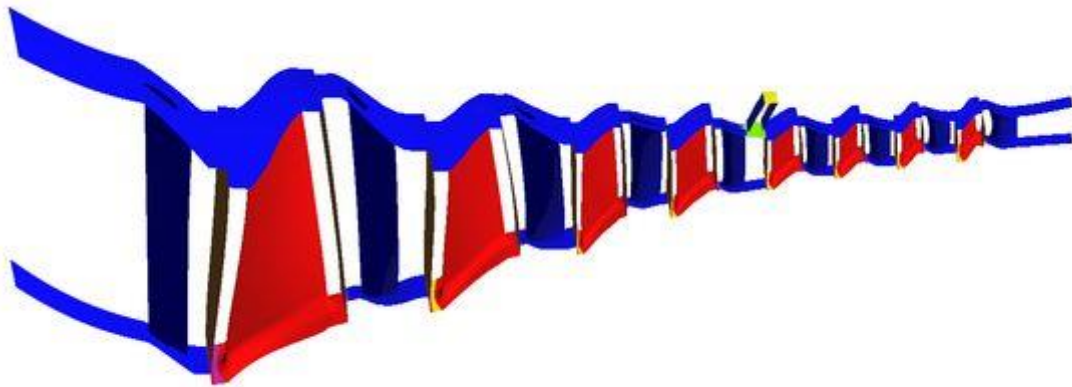


Figure 4.17 “Panels as cavities” graphical representation [45]

- Coarsen mesh.

Configuration, with the same geometry setup as in variant 1 (see Figure 4.14). The difference is hidden in grid resolution of the main flow. Here, the outcome of previous studies has been applied.

Within Phase I evaluation of different model complexity has been performed. The purpose of this part was to establish which of presented configurations has best prediction

in compare to the reference case. For each of variation, full speedline has been computed, including resolving of Surge Margin. The work of Tulik described the behavior of each configuration for all considered rotational speeds i.e. High Speed, Mid Speed and Low Speed.

As an intermediate summary, author observed that the higher rotational speed the greater deviation of Mass Flow and Pressure Ratio for all presented configurations. Most cases presented comparable to the reference data. Only “Panels as cavities” configuration has tendency to predict unphysical solution due to not realistic flow definition [45].

Closer look on particular geometrical variations:

- “Pure flow path” configuration comparability, despite of major simplifications has been confirmed.
- “Bleed only” case is characterized with major mass flow deviation. That effect can be explained by the mass which was being leaking what cause increase of compressor capacity i.e. increased mass flow rate capability. Furthermore, flow was not limited by blockage becoming from secondary air systems flows, entering and recirculating within the main flow and influencing its conditions.
- In “Panels as cavities” case, the most unstructured data. When the rotational speed and PR increases, the characteristics were becoming more and more disparate and it may be an artefact of simulations, related directly with averaging parameters at panel interfaces, poorly reproducing the actual flow conditions, resulting in numerical instability and obtaining not constant, unreliable data.

Mix of “Coarsen mesh” and “Full model” configuration resulted in reaching comparable data, most corresponding to experiment records for all configurations. For better data evaluation, Surge Margin assessment was required. All deltas has been derived in compare to the test data but as mentioned before, “Full model” configuration is the reference CFD model representation due to independent mesh resolution and being equipped in all additional features.

Table 4 Surge margin delta [45]

Speed	Full model			Pure flowpath			Bleeds only			Panels as cavities			Coarse mesh		
	Low	Mid	High	Low	Mid	High	Low	Mid	High	Low	Mid	High	Low	Mid	High
SM Δ [%]	8.71	1.50	1.01	11.64	9.79	0.54	7.36	2.75	0.67	9.48	13.37	13.12	7.71	0.55	1.06

“Panels as cavities” configuration again exposed significant deviations, what was expected basing on qualitative examination. Other cases were constantly showing increased aberration for Low Speed variant. “Pure flowpath” has shown the greatest delta SM at Medium speed. At High speed the best test data value was reproduced by “Bleeds only” configuration.

Table 5 Computation time [45].

Speed	Full model			Pure flow path			Bleeds only			Panels as cavities			Coarse mesh		
	Low	Mid	High	Low	Mid	High	Low	Mid	High	Low	Mid	High	Low	Mid	High
Time [%]	100.0	100.0	100.0	15.2	53.9	49.2	46.5	17.5	67.6	17.1	79.2	153.1	44.8	48.1	109.4
Average [%]	100.0			39.41			43.83			83.14			67.39		

In view of time cost of described cases, statistics have been presented in Table 5. As a reference for evaluation “Full model” configuration was used. Values used for this assessment were taken from the last numerically stable point for each of the speed. These conditions are usually the most expensive in the meaning of computational cost. In comparison to reference model, taking average time expense, “Pure flowpath” and “Bleeds only” configurations were achieved the greatest reduction by about 60%.

Having in consideration all presented insights and conclusions, configuration “Panels as cavities” has been rejected from further investigation. Decision was made basing on unphysical results and doubtful time reduction. “Pure flowpath” and “Bleeds only” were similarly economical but the second case was more reliable in terms of Surge Margin prediction.

Finally as a tradeoff between time reduction and prediction consistency, three configurations were chosen for further sensitivity evaluation [45].

- “Full model” – as a reference
- “Bleeds only” – as a best tradeoff configuration

- “Coarse mesh” – due to promising consistency and time reduction by about 33%. Additionally it is closest to the reference model in terms of geometrical representation and has previously approved coarse grid resolution.

The Phase II a second part of sensitivity studies, have been performed to asses validity of configuration determined by Phase I considerations and it is more decisive from the perspective of this PhD dissertation. Three chosen by Tulik setups have provided equivalent performance data and as a next step of validation, there was a necessity to evaluate model response on a change in aerodynamics to define performance prediction sensitivity in order to future potential use in optimization [45].

Continuing applicability in a wide operational range, this part of the study was also conducted for three rotational speeds – Low, Mid and High one. As variable parameter Variable Guide Vanes scheduling has been chosen. To explain colloquial terms used in the description, for an angles with negative sign, so to say below 0 degree, axial compressor is called “closed” – with this conditions, velocity triangles moves into direction, where less Mass-Flow can be realized. While sign is positive, so all variants above 0 degree, the reference one, machine will be called opened due to increase in Mass-Flow capacity. To manipulate VGV setting, relative, function has been introduced driven by IGV angle. Due to fragility of the MTU data, no function is presented.

In the thesis of Tulik [45], all maps were described to the detail. Below only summary tables are referenced with overall conclusions of the author.

Table 6 Design point parameters delta values for low speed [45].

Mass flow Δ [%]					
Angle	-2	-1	0	1	2
Full model	-4.98	-2.44	-	2.27	4.53
Bleed only	-5.31	-2.58	-	2.49	4.9
Coarse mesh	-4.87	-2.4	-	2.19	4.33
Pressure ratio Δ [%]					
Angle	-2	-1	0	1	2
Full model	-0.19	-0.09	-	0.09	0.18
Bleed only	-0.2	-0.09	-	0.1	0.19
Coarse mesh	-0.18	-0.09	-	0.09	0.17
Isentropic efficiency Δ [pp]					
Angle	-2	-1	0	1	2
Full model	-1.96	-0.95	-	0.78	1.57
Bleed only	-2.06	-0.96	-	0.89	1.71
Coarse mesh	-1.89	-0.93	-	0.75	1.49

Analyzing Table 6 performance deltas for Working Line point are presented. As previously observed out of presented maps, Mass Flow and Pressure Ratio deviation is present. “Full model” and “Coarse mesh” are comparable in these terms along all variants of Variable Guide Vanes settings. Discrepancy arises for “Bleed only” configurations. This is the result of blockage introduced with Inner Air Seal cavities, which are not present within model with only Bleed applied. From the perspective of isentropic efficiency, only +1 and +2 degree configurations reveals increased sensitivity.

Next considered conditions was Mid Speed. Again presented in quantitative manner showed in the table.

Table 7 Design point parameters delta values for medium speed [45].

Mass flow Δ [%]					
Angle	-2	-1	0	1	2
Full model	-7.91	-3.77	-	3.43	6.72
Bleed only	-7.79	-3.69	-	3.49	6.83
Coarse mesh	-7.64	-3.64	-	3.32	6.49
Pressure ratio Δ [%]					
Angle	-2	-1	0	1	2
Full model	-0.36	-0.17	-	0.16	0.31
Bleed only	-0.35	-0.17	-	0.16	0.32
Coarse mesh	-0.35	-0.16	-	0.16	0.3
Isentropic efficiency Δ [pp]					
Angle	-2	-1	0	1	2
Full model	-1.64	-0.76	-	0.63	1.27
Bleed only	-1.6	-0.74	-	0.66	1.26
Coarse mesh	-1.6	-0.75	-	0.61	1.2

Analyzing Table 7 no outlined prediction is available. All parameters which are considered at Working Line showed similar deltas for described parameters revealing low sensitivity on the modeling from the perspective of Mid Speed conditions.

Mid Speed findings shows how CFD sensitivity varies between deeply off-design Low Speed conditions and slightly higher, but still far of design conditions middle speed. Therefore, the closest to design conditions – High Speed – is expected to reveal low sensitivity for VGV variants over different modeling approach.

Table 8 Design point parameters delta values for high speed [45].

Mass flow Δ [%]					
Angle	-2	-1	0	1	2
Full model	-9.44	-3.76	-	3.35	7.06
Bleed only	-9.03	-3.77	-	3.64	7.16
Coarse mesh	-7.49	-3.65	-	3.52	6.92
Pressure ratio Δ [%]					
Angle	-2	-1	0	1	2
Full model	-0.48	-0.19	-	0.17	0.36
Bleed only	-0.45	-0.19	-	0.19	0.37
Coarse mesh	-0.38	-0.19	-	0.18	0.35
Isentropic efficiency Δ [pp]					
Angle	-2	-1	0	1	2
Full model	-1.75	-0.63	-	0.31	1.1
Bleed only	-1.65	-0.62	-	0.56	1.08
Coarse mesh	-1.28	-0.61	-	0.53	1.03

Data available in the table above shows deltas for High Speed parameters. Throughout all modelling approaches, “Coarse mesh” revealed enhanced discrepancy for extreme VGV variants for Mass Flow and efficiency prediction for maximally closed setting. Within first variant of VGV setting, i.e. -1 and +1 degree, all parameters shows analogous shift despite efficiency of opened case where delta have increased. None of the parameters achieved wrong trend i.e. from the perspective of predicting potential response of the system, both simplified models are sufficient.

To supplement studies, Surge Margin has been taken into account as a parameter to evaluate. Since derivation of stability limit strongly depends on used approach, results are treated more in qualitative manner and main focus was put to estimate trend of change rather than absolute value. Deltas gained from all configurations are presented in below Table 9.

Table 9 Surge Margin delta for all examined cases [45].

		Surge Margin Δ [pp]				
Speed	Angle	-2	-1	0	1	2
Low	Full model	1.43	0.55	-	-0.22	-1.37
	Bleed only	0.39	0.41	-	-3.35	-0.88
	Coarse mesh	0.90	1.13	-	-0.36	-1.96
Mid	Full model	2.62	1.91	-	-6.18	-5.67
	Bleed only	9.31	7.98	-	5.02	5.15
	Coarse mesh	2.43	1.26	-	-6.77	-6.34
High	Full model	-1.64	0.19	-	-2.32	3.67
	Bleed only	2.11	3.28	-	5.26	5.12
	Coarse mesh	2.98	-4.30	-	0.66	-0.41

Assessing data from the table, it was difficult to determine any functioning trend. Level of the deltas is spread and unfollowable. To help to understand the data, more quantitative representation of the Surge Margin were presented in the following figures presenting bar charts to observe direction of considered deviation neglecting absolute value.

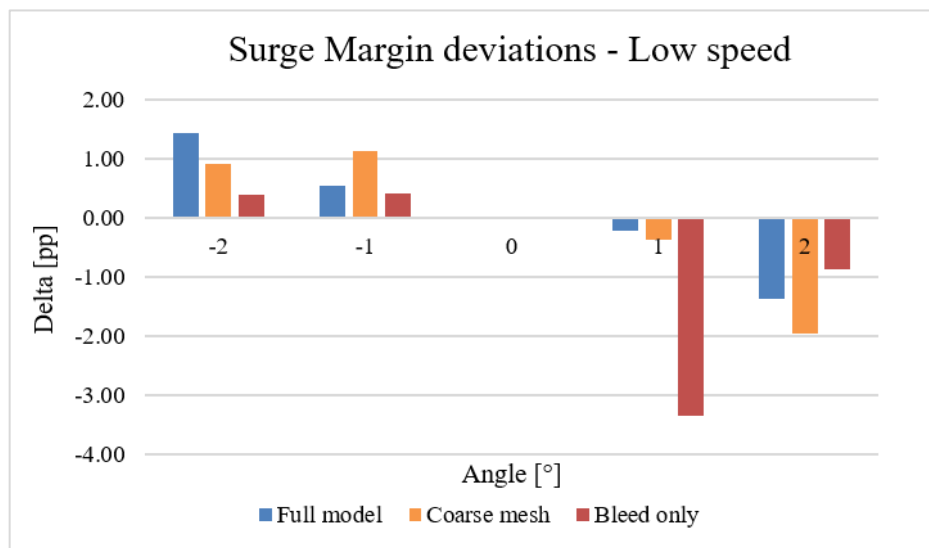


Figure 4.18 Surge Margin delta – low speed [45]

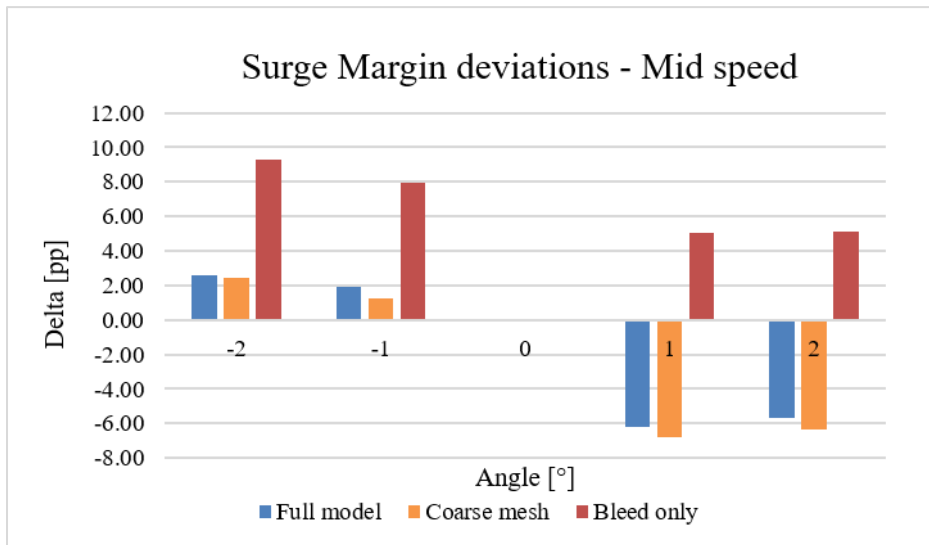


Figure 4.19 Surge Margin delta – medium speed [45]

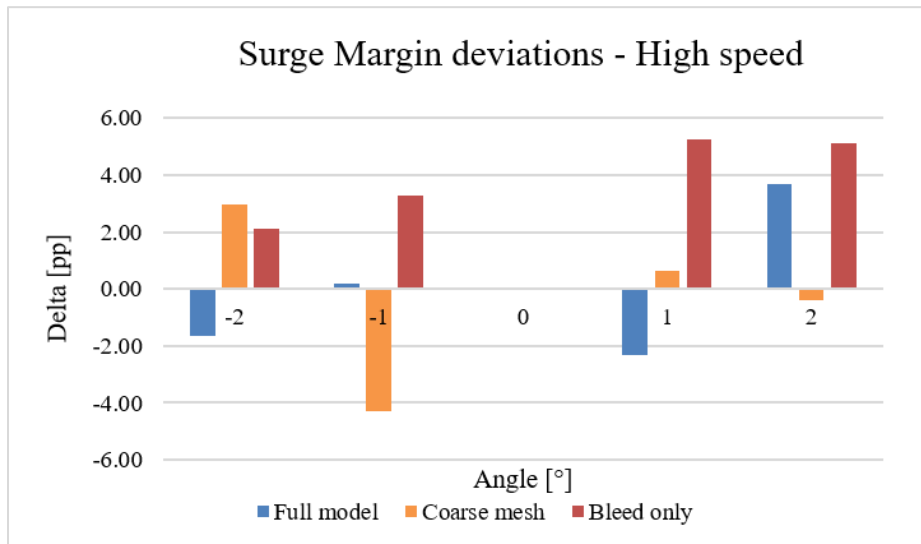


Figure 4.20 Surge Margin delta – high speed [45]

Examining figures above, it's clear that there are no possibility to evaluate Surge Margin in the way of specific delta between different detail models. Low speed conditions showed in Figure 4.18 presents discrepancy between configurations in the manner of delta SM prediction. For the reference model – “Full model”, delta Surge Margin has shown constant increase together with closing the machine and decreasing with opening. This tendency was not recovered for any of proposed configuration. Trend has been estimated for all cases in the same manner. The greatest deviation was exposed by “Bleed only” configuration for -1 degree VGV setting. For Mid Speed conditions (see Figure 4.19), prediction of SM delta was also revealed to be insufficient. In the case of “Bleed only” also predicting of the trend is untruthful. Despite showing enhanced response on VGV setting change, for opening variants, delta SM has opposite reaction. “Coarse mesh” case

reproduced the trend of changes in the reference following manner. In the last comparison of High Speed conditions, no correlation can be found. All 3 types of modelling, were behaving in unpredictable way. The most likely reasoning of this response were the flow conditions acting at this rotational speed.

4.2.4 Summary observations

Presented studies have revealed sensitivity of simplified models for estimating performance conditions at different Variable Guide Vanes setting. Cases chose for Phase 2 i.e. reference “Full model”, model with all geometry features but reduced resolution of the mesh – “Coarse mesh” and geometrically simplified case “Bleed only” where mesh stayed untouched, but Inner Air Seal cavities have been extracted from the model. Assessment showed weakness of reproduction for specific delta of any of the parameter examined in the studies. The influence of the geometry simplification or mesh coarsening has revealed to be recognizable. For the performance parameters, both propositions were representing correct trend over the changes showing capability of design space search for desired gradient. In the field of Surge Margin tendencies, “Bleed only” model has failed to correctly represent stability behavior. For “Coarse mesh”, Low and Mid rotational speed conditions were accessible in trend prediction. For High Speed conditions, both simplified cases failed to correctly represent response of the system in terms of VGV setting chance and its influence on stability performance. As the conclusion, necessity of all geometry features has been recognized. Therefore, reducing of the numerical grid resolution showed less impact into performance parameters prediction. The difficulties found for SM estimation have underlined the complexity of stall phenomenon and how sensitive in terms of model creation it is. Basing on that, for exact prediction of compressor operability range it’s suggested to apply only validated setups at least for the final design case assessment. Comparing computational cost reduction and results discrepancy for reduced fidelity CFD model, it is not efficient to build Mu-Fi model based only on high and low fidelity RANS simulations from the perspective of Surge Margin estimation.

4.3 2D analysis

4.3.1 Model description and study preparation

Since the CFD reduced fidelity models didn't show satisfying computational cost reduction, it was decided to perform sensitivity study on Streamline Curvature Method for estimating axial compressor characteristics within wide operational range to establish level of confidence for the design space exploration purposes. Worth to point out is that only trends will be checked – this work is not aiming for 1 to 1 representation of CFD by SCM but to obtain comparable trends for both methods since it is a crucial requirement for successful design space exploration. Exact representation of efficiency and Surge Margin might require enhanced correlation adjustment what might have an impact for SCM model variations. Therefore Pressure Ratio, Mass flow and outflow angles at the Working Line are the parameters of interest.

SCM is widely known method for resolving 2D meridional flow with use of radial equilibrium equations [8, 46, 5, 47]. The code used in the following work is owned and developed by MTU Aero Engines AG, due to that, no detailed description will be provided since the basics of the method are presented in mentioned works.

The study was planned in the following order:

- Use 3 mechanical speeds – low, mid and high as in the previous studies
- Adapt SCM model in terms of outflow angles, losses and blockage to fit CFD conditions at the Working Line
- Run compressor map for validation of the adaption
- Define a matrix of VGV variations for sensitivity study
- For SCM calculations:
 - Introduce new VGV setting
 - Introduce correction of RPM to obtain mass flow within 0.5% deviation compared to reference
 - Run full speed line for each rotational speed and each variation

- Run CFD simulations of “Full model” using boundary conditions of each SCM variation
- Compare the results

All the configurations have been adjusted in terms of boundary conditions, losses and blockage to fit operational point at the Working Line for specific speed. As the reference for the adjustments, CFD computations of full model derived in the previous chapter were used (see Figure 4.14).

Table 10 Adjustment uncertainties at Working line

Adjustment uncertainty comparing SCM to CFD			
Speed	High	Mid	Low
Pressure Ratio	-0.299%	0.484%	-0.211%
Reduced Mass Flow	-0.004%	0.011%	-0.425%
Isentropic Efficiency	-6.011%	-4.715%	-0.632%

As presented in the Table 10, SCM has become adjusted to the specific conditions at the working line with fine quality. For all cases, Pressure Ratio and Mass Flow is adjusted with accuracy under 0.5%. Efficiency shows enhanced deviation but the reason behind is the way of model settings. The target was to achieve specified flow conditions and efficiency is the resulting parameter. For all speeds, SCM is overestimating efficiency what is signifying the approach of model adjustment. Manipulating for exact value representation in that manner, could cause interruption for loss correlation models when it comes to model specification change (e.g. change of Vane schedule) and lead to wrong deltas for design space exploration.

Since SCM model is adjusted at the Working Line operational point, speedline characteristics can be computed. Computations are performed for all three considered speeds – Low, Mid and High and compared to CFD results of “Full model” configuration (see Figure 4.14). Figure below presents qualitative comparison of the two methods.

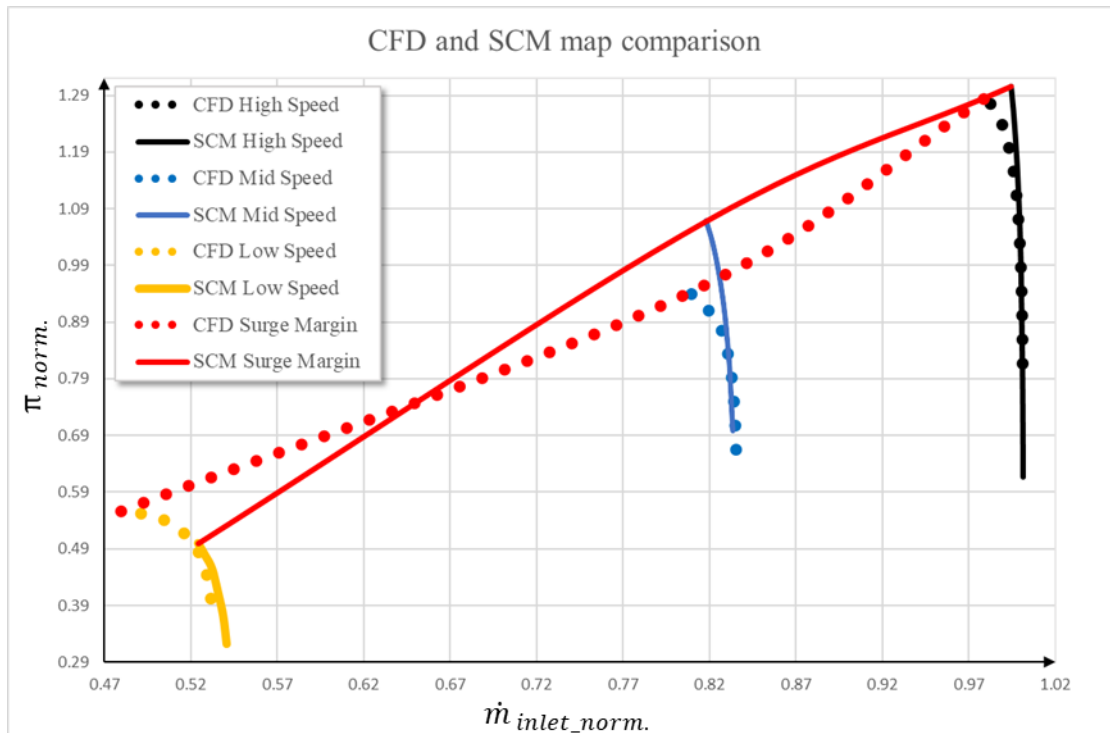


Figure 4.21 CFD and SCM map comparison

To begin with, off-design deviation of the SCM method prediction has been observed. Both Mid and Low speed shows observable difference in maximum Pressure Ratio prediction – the limiting one. For Mid Speed overestimation of Surge Margin is observed. Perhaps in the reality, rotating stall event has taken place in the frontal part of the machine which cannot be detected with use of SCM method or steady state CFD. For the Low Speed conditions, Streamline Curvature Method could just throttle the compressor over a small part of the CFD speedline. This demonstrates how strongly loss and blockage correlations are modified to reach specific conditions and how three dimensional flow is for such off-design speed. For High Speed which is close to the design one, showed close fit to the CFD characteristic for the shape as well as for Surge Margin prediction. In all three cases, characteristics are steeper and not showing boundary layer increase towards stability limit as was expected – blockage of SCM model was fitted to WL operational point.

Nevertheless despite of uncertainty of off-design results, the sensitivity studies have to be performed. The aim is to validate what is the response of SCM in compare to CFD over model modification. As the outcome of the studies, scope of method applicability has to be defined.

For the studies parameter, Variable Guide Vanes variation has been chosen as planned application is to optimize VGV schedule for variate conditions. Positive values means opening the machine, negative, closing. Planned deviations are presented in Table 11.

Table 11 Angle change matrix

IGV sensitivity			Stator 1 sensitivity			Stator 2 sensitivity		
IGV Δ [°]	S1 Δ [°]	S2 Δ [°]	IGV Δ [°]	S1 Δ [°]	S2 Δ [°]	IGV Δ [°]	S1 Δ [°]	S2 Δ [°]
-8	-	-	-	-8	-	-	-	-8
-2	-	-	-	-2	-	-	-	-2
-0.5	-	-	-	-0.5	-	-	-	-0.5
+0.5	-	-	-	+0.5	-	-	-	+0.5
+2	-	-	-	+2	-	-	-	+2
+8	-	-	-	+8	-	-	-	+8

The idea was to isolate each variable parameter to analyze whether sensitivity is constant. Proposed scope had to cover wide deviation range to force applicable limit detection.

4.3.2 Performed calculations

4.3.2.1 SCM adjustment to new VGV settings

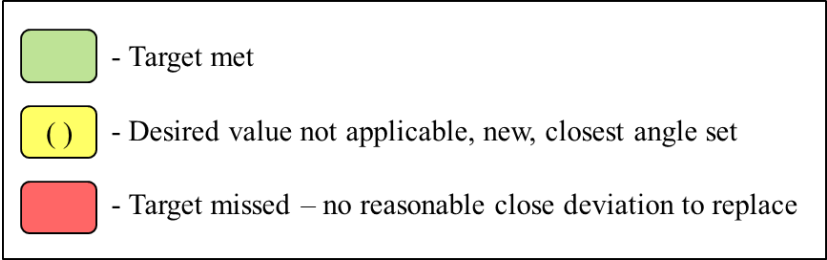
As a very first step into performing the sensitivity study, proposed matrix of deviations has to be introduced into the Streamline Curvature Method model and be adapted to realize Working Line conditions within required uncertainty level.

The procedure is the following:

- Introduce angle changes to VGV setting
- Keep the Mass flow at desired level (in this type of run, Mass Flow rate is an input)
- Iterate Rotational speed to meet Pressure Ratio within uncertainty of 0.5%

Works have been performed for all considered speeds – Low Speed, Mid Speed, and High Speed – separately to find right outcomes. In total, 54 configurations will be held.

To read out included tables, legend is presented in Figure 4.22.



As a first case, High Speed variant. This is the one with boundary conditions closest to the design working point. In the table below, table with applied Vane angle change can be found.

Table 12 List of applied VGV setting – High Speed

Modified row – High Speed			
	IGV Δ [°]	S1 Δ [°]	S2 Δ [°]
Vane angle change	-8 (-4)	-8 (-6)	-8
	-2	-2	-2
	-0.5	-0.5	-0.5
	+0.5	+0.5	+0.5
	+2	+2	+2
	+8	+8	+8

As noticeable, most of the variations are completed with success. All extreme (-8 degree) variants for closing the compressor have failed. This setting was limited by aerodynamics of this performance point at specific required conditions. For Stator 2 variant further attempts got abandon. For IGV and Stator 1 it was decided to decrease the change and find the closest possible Vane closure. Therefore -4 and -6 degree angle change has been introduced respectively.

In terms of Pressure Ratio adjustment the following uncertainty is observed (see Table 13)

Table 13 Pressure Ratio uncertainty

		Modified row		
		IGV [%]	S1[%]	S2[%]
Vane angle change [°]	-4/-6	0.19	0.19	-
	-2	0.01	0.08	0.02
	-0.5	0	0.03	0.06
	+0.5	0.03	0.05	0.08
	+2	0.03	0.07	0.02
	+8	0.01	0.08	0.01

As presented above, all introduced variants are adjusted to the desired Pressure Ratio within 0.2%. The next considered condition is Mid-Speed. Modifications introduced for this configuration are the same as in the previous case and were manageable as presented below.

Table 14 List of applied VGV setting – Mid Speed

		Modified row – Mid Speed		
		IGV Δ [°]	S1 Δ [°]	S2 Δ [°]
Vane angle change	-8 (-6)	-8	-8	-8
	-2	-2	-2	-2
	-0,5	-0,5	-0,5	-0,5
	+0,5	+0,5	+0,5	+0,5
	+2	+2	+2	+2
	+8	+8	+8	+8 (+4)

For a second time, further closing the compressor for extreme proposed setting failed. Stator 1 was unachievable even for reasonable offset to the original attempt. For IGV the neighbor angle was found. For the middle range speed for the first time, opening procedure has failed for second variable stator. Instead of +8 angle change, +4 is used as the closest accessible setting.

Table 15 Pressure Ratio uncertainty

		Modified row		
		IGV [%]	S1[%]	S2[%]
Vane angle change [°]	-8/-6	0.19	-	0
	-2	0.08	0.01	0.02
	-0.5	0.03	0.01	0
	+0.5	0.05	0.03	0
	+2	0.07	0.03	0.2
	+8/+4	0.08	0.01	0.2

Again, Pressure Ratio is being kept with uncertainty below 0.2% of deviation to the starting point.

The last used condition – Low Speed – is the most off-design case within presented studies. Compressor here has heavily closed Vane setting to compensate reduced axial velocity and set the angles at optimum level to prepare flow for downstream rows. Before start of the studies, it has been expected to meet geometrical and aerodynamic limitations for proposed wide range of deviations. As a result, the following is achieved:

Table 16 List of applied VGV setting – Low Speed

Modified row – Low Speed			
Vane angle change	IGV Δ[°]	S1 Δ[°]	S2 Δ[°]
	-8	-8	-8 (-6)
	-2	-2	-2
	-0.5	-0.5	-0.5
	+0.5	+0.5	+0.5
	+2(+1)	+2	+2
	+8	+8	+8

Geometrical limitation are met for IGV extreme closure. The same problem is actual for Stator 2 for the closure setting – -6 degree was used instead. For the opening variations

of second stator, none of angles were possible to set. Further changes might require readjustment of the correlations what is not a part of this work.

For every successfully executed modification, Pressure Ratio uncertainty requirement of 0.5% is met. See Table 17.

Table 17 Pressure Ratio uncertainty

		Modified row		
		IGV [%]	S1[%]	S2[%]
Vane angle change [°]	-8/-6	-	0.06	0.02
	-2	0.02	0.01	0.02
	-0.5	0.06	0	0
	+0.5	0.08	0	-
	+2/+1	0.02	0	-
	+8	0.01	0	-

4.3.2.2 CFD representation of VGV variations

In view of the fact that SCM model shows capability of modifying the VGV setting and compensate the effect to reach desired performance conditions the next step was to perform comparison of SCM and CFD data to derive functionality limits for potential Multi-Fidelity utilization.

As a representation of 3D CFD model, configuration of “Full model” has been chosen (see Figure 4.14). Beside assessment of the delta behavior over VGV variations, the same boundary conditions as for SCM, were used so rotational speed adjustment uncertainty will be examined.

To bring compressor specification as close as possible between SCM and CFD model, the following conditions were updated:

- VGV setting (according to the Table 11)
- Rotational speed (with SCM correction for specific Pressure Ratio and Mass Flow)

- Initialization from SCM solution accordingly to variation (no impact for results, but supporting computational convergence speed)

The remaining conditions such inlet boundary conditions, bleed valve leakage level stayed the same for both models so no update was required.

For the reason of using SCM results as a boundary conditions input, it's necessary to obtain satisfactory representation within CFD model when considering utilization of those methods for automated optimization where no fine tuning is available. Due to that, summary of the successful and failed runs and their uncertainty to WL performance conditions are presented in the following tables.

Starting with High-Speed configuration, list of successful cases is presented in the table below.

Table 18 High speed variations – CFD

Modified row – High Speed			
	IGV Δ[°]	S1 Δ[°]	S2 Δ[°]
Vane angle change	-8(-4)	-8(-6)	-
	-2	-2	-2
	-0.5	-0.5	-0.5
	+0.5	+0.5	+0.5
	+2	+2	+2
	+8	+8	+8

- Converged result
 - Simulations failed

Summary shows that not all configurations were possible to compute redoing SCM variations. For this conditions, setup of Stator 1 closed by 2 degrees was showing numerical instability. Due to the aspect of potential usage in optimization process no further investigation was performed in this manner, since all other variations have been successfully computed with converged result.

Availability of High-Fidelity representation is not the only requirement for successful studies. The most important is how CFD model behaves while using SCM conditions in

terms of performance point shift. Table 19 is presenting Mass Flow deviations in compare to reference case. Because SCM model was adjusted with 0.5% of PR uncertainty to the starting point, it was decided to increase this requirement while computing CFD representation to 1%. Since way of modeling is forcing particular Pressure Ratio (see chapter 3D CFD analysis), Mass Flow has been the parameter of the crosscheck.

Table 19 High-Speed Mass Flow uncertainty – CFD

		Modified row		
		IGV [%]	S1[%]	S2[%]
Vane angle change [°]	-4/-6	-0.56	-19.06	-
	-2	-0.042	-	-0.22
	-0.5	-0.056	-0.17	-0.033
	+0.5	0.028	0.15	-0.018
	+2	0.099	0.48	-0.11
	+8	-10.94	-0.66	-0.78

- MF under 1% of deviation
 - MF out of 1% of deviation

As can be read from Table 19 most variations were successfully representing assumed performance point. Beside further sensitivity studies of efficiency and stability limit trends, it's exceedingly important that Streamline Curvature Method can bring satisfying boundary conditions for CFD solution. Uncertainty outside required quality is observed for two extreme VGV angle change of IGV opening and Stator 1 closing – those configurations have been excluded from further studies. This indicates limitations of Low Fidelity estimation.

Table 20 shows successfully performed calculations of Mid-Speed configuration. All simulations reached numerical convergence.

Table 20 Mid-speed variations – CFD

Modified row – Mid Speed			
Vane angle change	IGV Δ [°]	S1 Δ [°]	S2 Δ [°]
	-8 (-6)	-	-8
	-2	-2	-2
	-0,5	-0,5	-0,5
	+0,5	+0,5	+0,5
	+2	+2	+2
	+8	+8	+8 (+4)

- Converged result
 - Simulations failed

Considering Mass Flow representation, Table 21 shows the level of SCM estimation confidence. Mid-Speed has revealed tight limitations for isolated Variable Guide Vane variation. 9 of 17 available variants were above assumed Mass Flow discrepancy. These results showed how different prediction can be considering different fidelity methods. It is worth to mention, that this study has to initiate this kind of discrepancy, where axial compressor is being pushed to unusual conditions out of optimum setting solution.

Table 21 Mid-Speed Mass Flow uncertainty – CFD

		Modified row		
		IGV [%]	S1[%]	S2[%]
Vane angle change [°]	-8/-6	-3.19	-	-4.178
	-2	-0.24	-8.07	0.07
	-0.5	-0.13	-1.33	-0.14
	+0.5	-0.37	0.45	-0.29
	+2	-2.48	1.27	-0.54
	+8/+4	-8.56	-2.49	-1.41

- MF under 1% of deviation
 - MF out of 1% of deviation

Last considered case has been Low-Speed. It was expected to observe there enhanced discrepancy due to level of boundary layer influence to the flow.

Table 22 shows executed setups. 3 of 14 available SCM predictions have failed during CFD simulations. All three were singled as extreme variations.

Table 22 Low-speed variations - CFD

Modified row – Low Speed			
Vane angle change	IGV Δ [°]	S1 Δ [°]	S2 Δ [°]
	-	-8	-8 (-6)
	-2	-2	-2
	-0.5	-0.5	-0.5
	+0.5	+0.5	-
	+2(+1)	+2	-
	+8	+8	-

- Converged result
 - Simulations failed

Closer look into the results has discover expected limitations (see Table 23). 7 of 12 available deviations reached higher Mass Flow deviation than assumed 1%. As observed, some of eliminated cases have shown discrepancy slightly higher then assumed value what might be a sign of hidden potential for further development. Therefore, variants exceeding the limit have been excluded from further evaluation.

Table 23 Low-Speed Mass Flow uncertainty – CFD

		Modified row		
		IGV [%]	S1[%]	S2[%]
Vane angle change [°]	-8/-6	-0.43	-	-4.46
	-2	-0.41	-6.02	-1.3
	-0.5	-0.79	-1.885	-0.98
	+0.5	-1.08	-0.66	-
	+2/+1	-1.18	2.6	-
	+8	-	-	-

- MF under 1% of deviation
 - MF out of 1% of deviation

Performed crosscheck has exposed limitations for boundary conditions delivery from SCM computations. Presented studies were designed in the manner to expose all misalignments with isolating changes and inducing misbalance between stages to discover both solvers response.

4.3.3 Data comparison

CFD variants representation have discovered limitations of SCM model predictions in terms of working line performance point recovery with use of rotational speed. Therefore all successful cases are required to be assessed in regard to efficiency gradient prediction as a primary indicator for optimization potential.

The following analyses are presented with respect to Vane angle variant and Isentropic Efficiency delta separately for each rotational speed and to simplify qualitative assessment regression line is available. For quantitative evaluation, correlation coefficient R has been calculated described by the equation)

$$R = \frac{\sum(x_i - \bar{x})(y_i - \bar{y})}{\sqrt{\sum(x_i - \bar{x})^2 \sum(y_i - \bar{y})^2}} \quad (\text{Eq. 3})$$

,where

- x_i – values of the variable x in a sample
- \bar{x} – mean of the values of x variable
- y_i – values of the variable y in a sample
- \bar{y} – mean of the values of y variable

Available High Speed variants of Variable Guide Vane are presented in Table 19 where only two cases were unsuccessful for performance point adjustment. Efficiency correlation is the following.

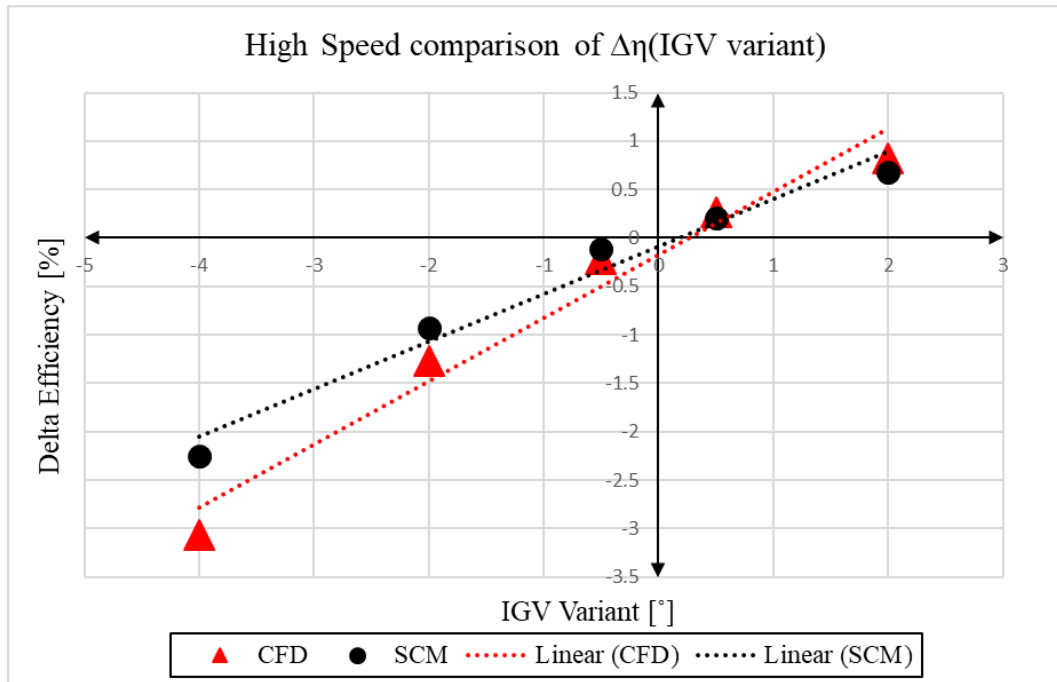


Figure 4.23 High Speed delta efficiency assessment for IGV angle variation

In the Figure 4.23 IGV variation for High Speed is presented. Qualitatively speaking both solvers showed mutual trend over angle changes.

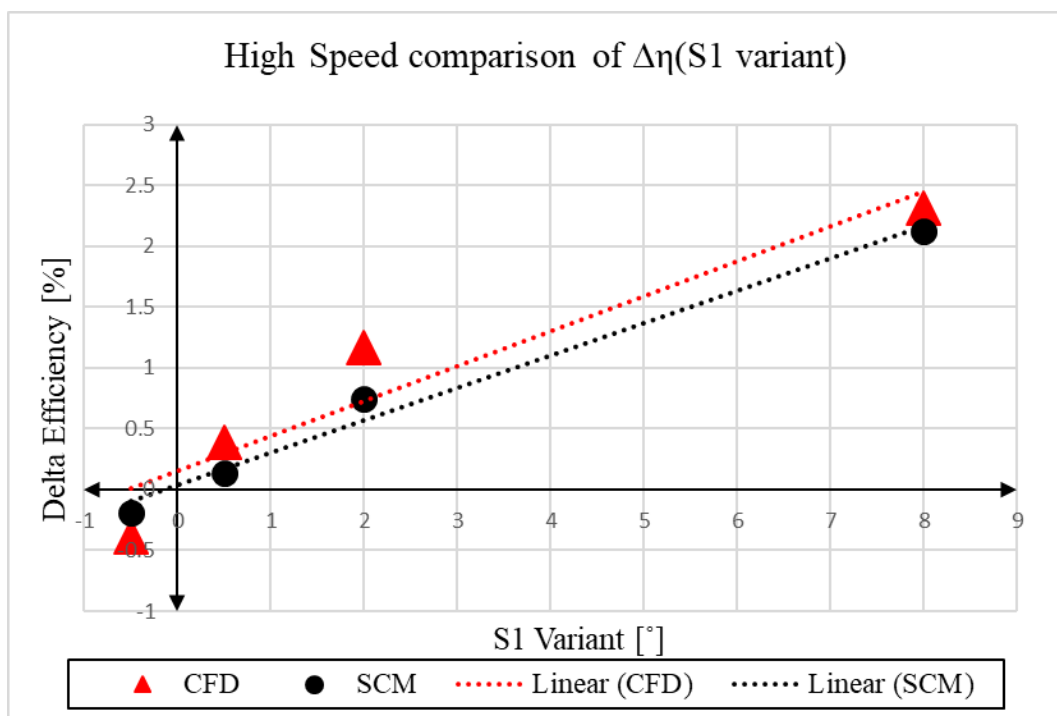


Figure 4.24 High Speed delta efficiency assessment for S1 angle variation

Similarly to IGV variation, Stator 1 shows very good gradient coverage between High and Low fidelity solver. Due to performance point adjustment mismatch, for closing the Vane, only -0.5 degree variant is available.

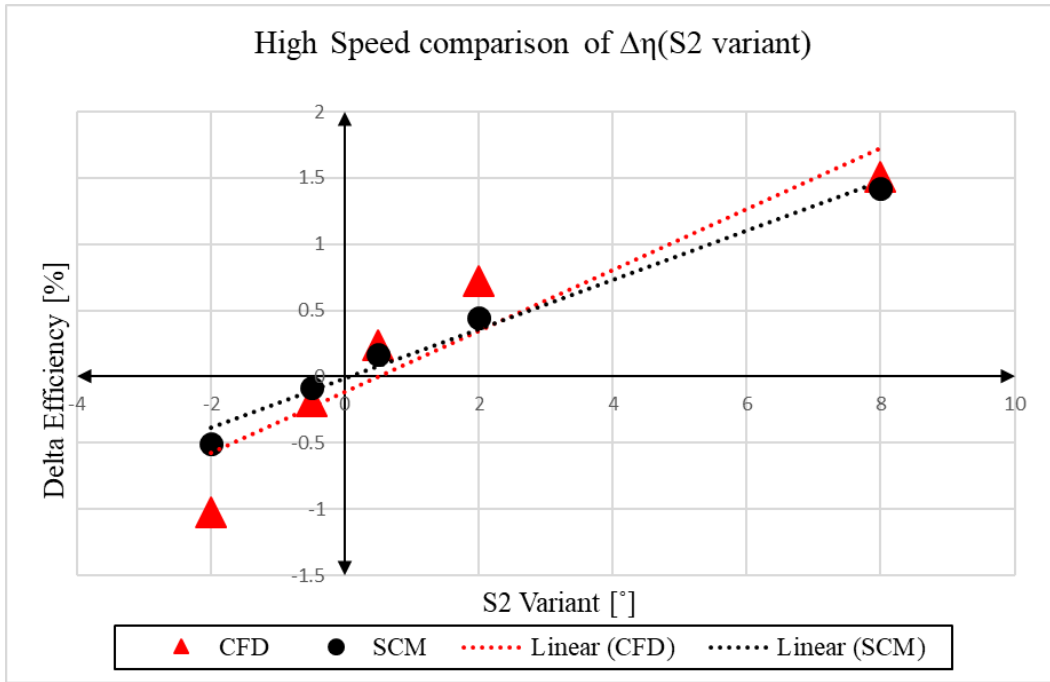


Figure 4.25 High Speed delta efficiency assessment for S2 angle variation

Last variable parameter, Stator 2, despite unavailable extreme closing variant, also showed good agreement between two fidelity methods.

High rotational speed showed high potential in terms of efficiency prediction. All three VGV variants exposed excellent delta efficiency gradient coverage. To quantitatively summarize level of correlation, Table 24 shows table of Correlation Coefficient for the presented data.

Table 24 Correlation coefficient for High Speed

	IGV	S1	S2
High speed	0.9998	0.9771	0.9727

All three variants satisfied correlation coefficient close to 1. This confirms qualitatively data coverage predictions between two solvers.

The following condition is Mid-speed. As previous assessment presented in Table 21 showed most of assumed configurations, were unsuccessful for CFD representation.

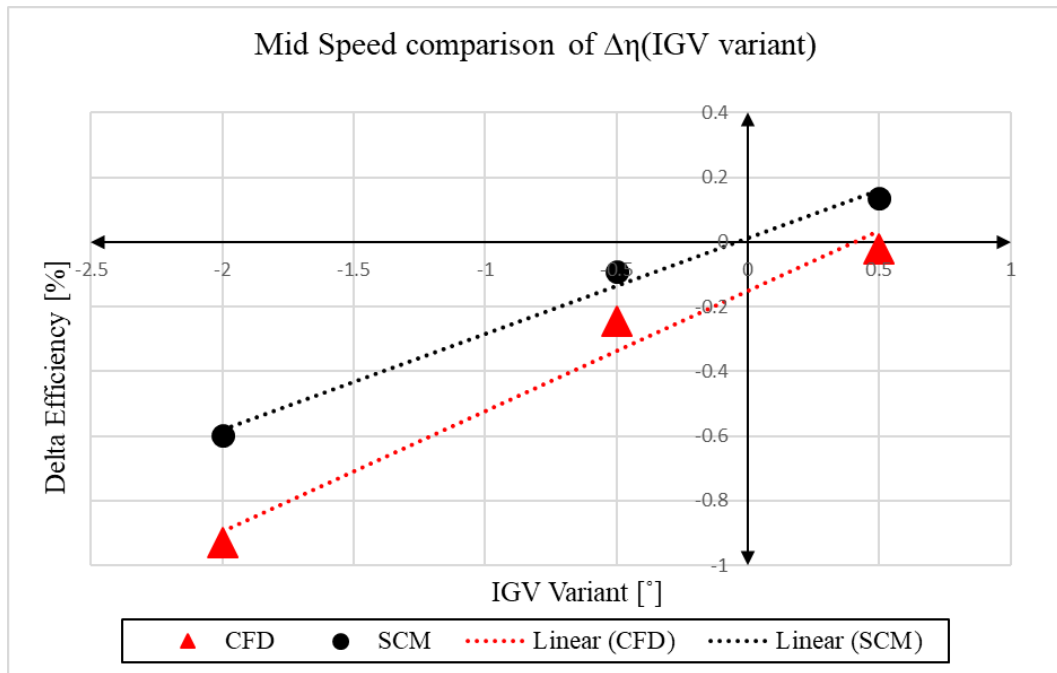


Figure 4.26 Mid Speed delta efficiency assessment for IGV angle variation

For available IGV variants (Figure 4.26), both solvers showed similar trend. From the optimization point of view, opening variant, +0.5 degree showed inconsistency in efficiency change prediction. For this particular setting, CFD has presented loss in efficiency level in contrast to SCM prediction, which revealed positive delta.

Unfortunately, for Stator 1 only one variant was available (Figure 4.27). Trend derivation wasn't possible for the limited data.

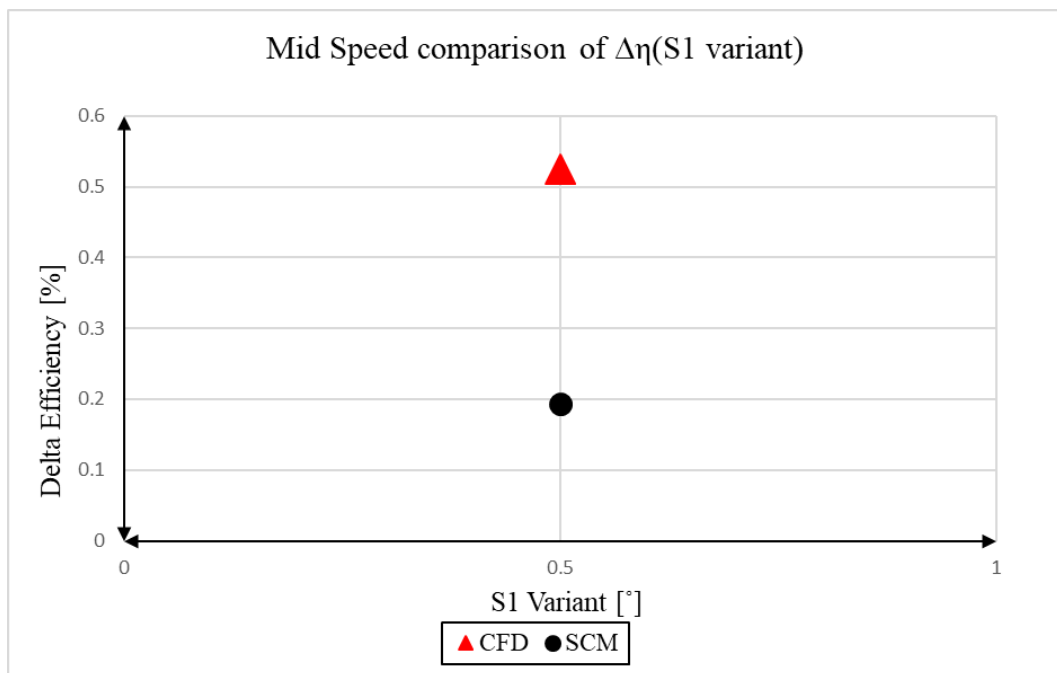


Figure 4.27 Mid Speed delta efficiency assessment for S1 angle variation

This single variant, showed the same trend, so it indicates potential to not decline middle range of the rotational speed for optimization.

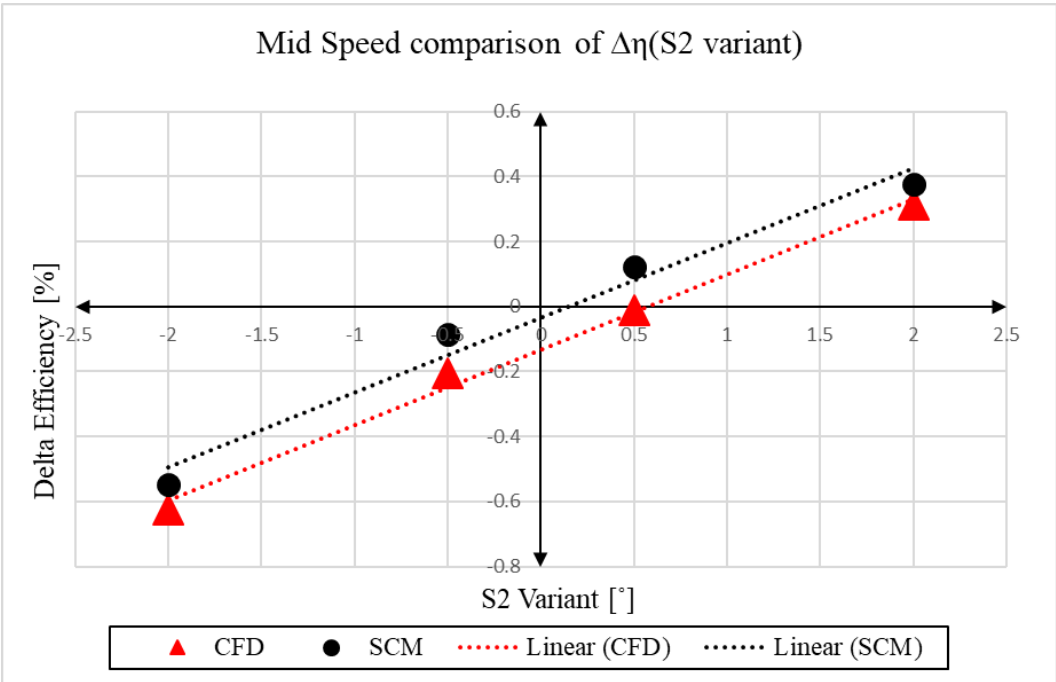


Figure 4.28 Mid Speed delta efficiency assessment for S2 angle variation

As it has been observed for IGV variant, the opening of Stator 2 angle by 0.5 degree also revealed different delta, but general trend of the variations has been kept between solvers (Figure 4.28). To quantify the quality of the two data sets correlation coefficient is presented in Table 25.

Table 25 Correlation coefficient for Mid-Speed

	IGV	S1	S2
Mid Speed	0.9975	-	0.9962

For available cases correlation factor is close to 1. This estimates good forecast for high fidelity method of efficiency change.

Last considered rotational speed is Low Speed. As presented in the Table 23 off-design conditions has difficulties to be recomputed with use of CFD method. Only IGV variations were achieved for more than one case as presented in Figure 4.29.

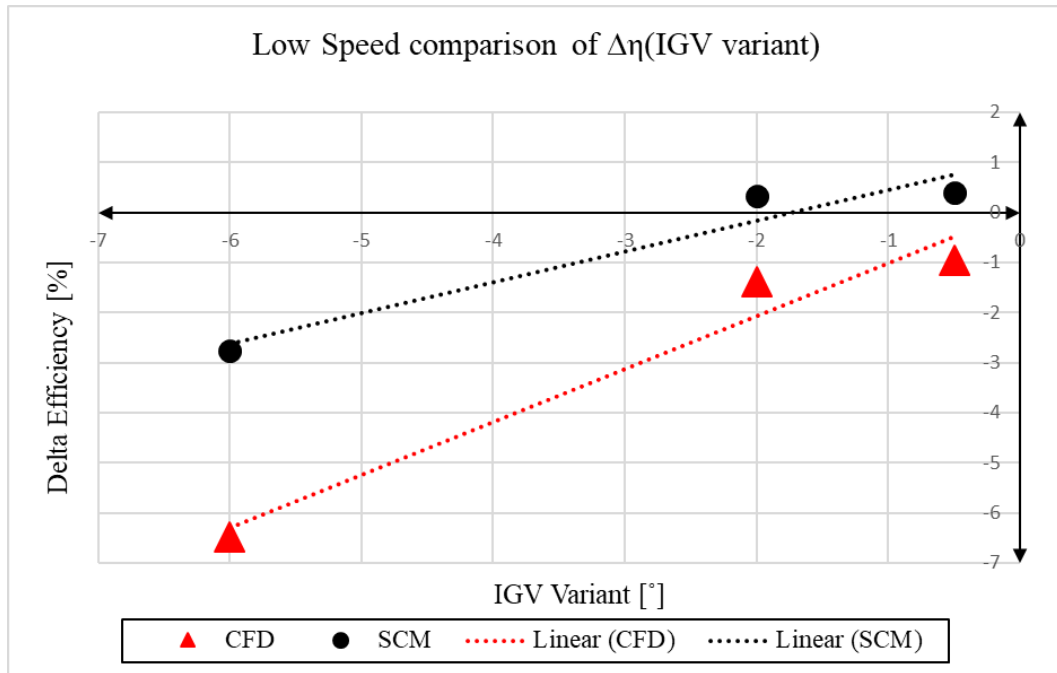


Figure 4.29 Low Speed delta efficiency assessment for IGV angle variation

Trend has been observed to be similar for both solvers, but for variant -0.5 and -2 degree there is a mismatch in prediction between CFD and SCM method.

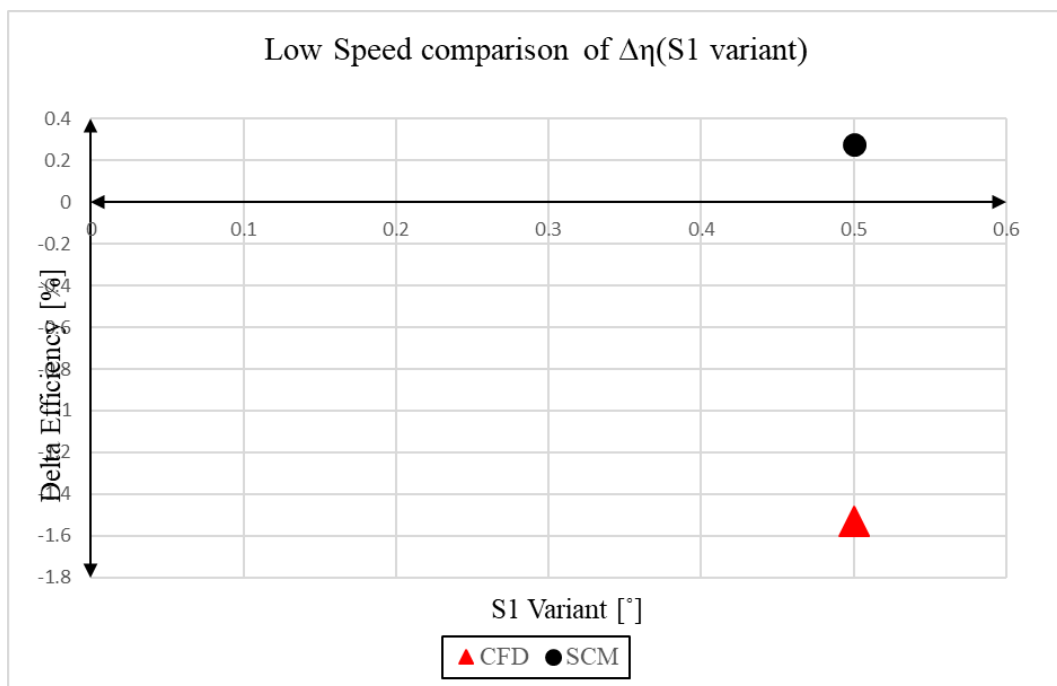


Figure 4.30 Low Speed delta efficiency assessment for S1 angle variation

For Stator 1, only one case has been achieved, and showed the difference in efficiency prediction. Again in contrary to CFD, SCM solution has indicated gain of the efficiency as presented in Figure 4.30.

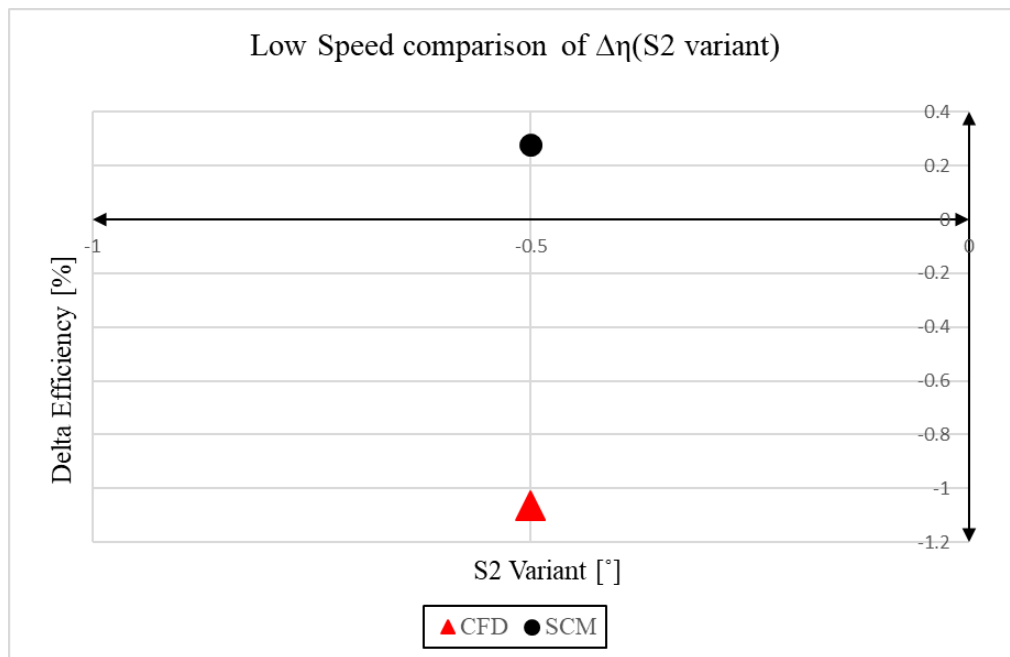


Figure 4.31 Low Speed delta efficiency assessment for S2 angle variation

Stator 2 variant solutions, were also available only for a single angle change. As pointed previously, again for this configuration SCM shows optimistic efficiency prediction in contrary to CFD (Figure 4.31).

Table 26 Correlation coefficient for Low-Speed

	IGV	S1	S2
Low Speed	0.9988	-	-

Despite leak of Stator 1 and Stator 2 coefficient, IGV variation shows high level of coefficient but according to Figure 4.29, 2 of 3 variants showed negative gradient. In the range of efficiency estimation, SCM model predictions have showed to be available to estimate efficiency increase over the design space for wide operational range. Low-Speed conditions for available variant also revealed poor correlation between solvers, but it's necessary to point out the specification of performed study. Isolated changes had enhanced influence of misbalancing throughout stages and had influence on flow prediction with 2 dimensional, Streamline Curvature Method flow prediction.

To summarize performed studies, High Speed and Mid Speed revealed satisfactory level of prediction correlation for future use in Multi-Fidelity optimization. Low-speed conditions exposed weakness of results quality in compare to CFD. As was mentioned in the beginning of this chapter, it was expected to observe increased discrepancy for the

conditions, where boundary layer had greater encouragement into flow characteristics, for which SCM have no detailed estimation capability.

4.4 Setup study conclusions

Studies of different fidelity models have been performed. Investigations were split for 3D CFD model simplifications with variants of numerical grid and geometrical representation of the real geometry. Second part of the studies were based on sensitivities of 2D Streamline Curvature Method, which brings the best computational cost reduction.

To the final comparison of 3D method, “Bleed only” and “Coarse mesh” configurations were taken showing ~57% and ~33% of time reduction respectively. Studies have shown that both variants are capable of efficiency prediction for Variable Guide Vane setting variation over wide operational range. In terms of Surge Margin prediction configuration without modelled Inner Air Seal cavities has showed increased discrepancy for trend prediction for Mid and High Speed conditions. Low and Mid speed conditions were well reflected for tendency estimation across changes in VGV setting.

In the second part, 2D SCM model sensitivities, have been found. For this part, approach of deviate VGV setting changed. It was decided, in the reason of fully extract potential out of efficiency prediction, to isolate changes to separate Variable Guide Vane. Another field was to evaluate whether Streamline Curvature Method is capable of rotational speed adjustment to adapt the configuration with changed VGV setting back to the starting conditions in terms of pressure ratio and mass flow. Studies were conducted for three rotational speed – Low, Mid, and High Speed conditions as it was performed in the studies of CFD modeling. Limitations of the method have been found. SCM was capable to estimate efficiency and performance point adjustment mainly for low range of deviation. For conditions adaption, uncertainty level has been increased to 1% between CFD and SCM since 2D method itself was adjusted within 0.5% deviation limit with respect to Pressure Ratio and Mass Flow. The most limited condition was Low Speed – this off-design point estimation has failed due to potential strong separations of the flow which cannot be considered with Streamline Curvature Method. As main observation, limits in VGV modification are found and shouldn't exceed +/-2 degrees for isolated Vane. This requirement probably can be extended in the case of full rescheduling with stage-to-stage balancing kept on reasonable level with respect to flow conditions.

5 Multi Fidelity concept

Throughout the following chapter, Multi Fidelity concept is being introduced. As a proposal of Mu-Fi strategy, attempt of researching design space with use of High-Fidelity 3D CFD model and Low-Fidelity 2D SCM calculations have been taken. The reason of choosing 2D model instead of CFD lowered fidelity is hidden in computational cost reduction observed out of conducted studies, which is not satisfying for this particular usage. As was discussed in literature review, there were approaches of using CFD and SCM methods for Mu-Fi considerations, but only for high speed, close to the design one. The concept here has to extend this application to off-design conditions with introduced Surge Margin evaluation based on High-Fidelity trends.

5.1 Requirements for Multi-Fidelity

Basing on the conclusions from literature review, the data aggregation method of choice has become Co-Kriging method. Surrogate models have been based on two data sets, High Fidelity CFD “Full model” representation and Low Fidelity Streamline Curvature Method simulations.

The method of Co-Kriging is an extension to primary ordinary Kriging where in contrary to OK to improve the quality of the interpolation includes additional observation (variable), known as co-variate. Kriging was developed to extend the knowledge for spatial exploration via sampling [48]. During sampling, the information about the considered parameters are available only at the position of this sample. Kriging allows for estimation of the information between those samples, performing weighted interpolation based on the distance to the neighbor available data to the newly estimated position [49]. Co-Kriging as the extension provides possibility of use another set of the data which usually is a more expense to sample but increases the quality of the prediction.

The following studies with application of the Co-Kriging have been performed with use of R – free software for statistical computing providing environment and being a programming language by itself [50]. The software finds its use in geostatistics where Kriging and Co-Kriging have had a wide application range together with gstat package [51, 52].

The usage of Co-Kriging Multi-Fidelity estimation is not unlimited and has requirements to be fulfilled. Also the strategy of application is important since the method has restrictions. Therefore to successfully use Co-Kriging the following aspects have to be taken into account [30, 32]:

- Low and High fidelity data have to had correlated quantity of interest – the better correlation of two datasets, the better outcome of the interpolation will be possible to achieve
- Minimize variable count – good practice is to define dominant variables to keep efficiency of different fidelities usage. With increase of variables, having low importance for gradient prediction, Multi-Fidelity speed-up impact will be reduced.
- Definition of sampling strategy – the most common approach for sampling approach is providing High fidelity data in the promising area, to enhance the prediction quality but often creation of initial surrogate model is required.

5.2 Design of Experiment

The aim of this work is to demonstrate the concept of Multi-Fidelity process which is capable to work for wide operational range and to support stability criterion fulfilment during optimization task with use of 3D CFD and 2D SCM solvers. To validate this approach it was necessary to design an experiment which will be capable of discovering strengths and weaknesses of the method and not to concentrate on complex optimization task with hundreds of variables.

Since most of modern high pressure axial compressors are equipped with Variable Guide Vanes, and presented in previous chapters sensitivity studies were based on such Vanes variations, it was decided to perform an optimization of VGV setting as a demonstrator of proposed methodology.

Table 27 List of optimization task parameters

Variables	Relative lower bound	Relative higher bound	Tolerance
IGV angle	-3°	+3°	0.1%
Stator 1 angle	-3°	+3°	0.1%
Stator 2 angle	-3°	+3°	0.1%
Rotational speed	-0.5%	+0.5%	0.1%
Constrains	Relative lower bound	Relative higher bound	Tolerance
Mass-Flow rate	-0.5%	+0.5%	0.1%
Pressure Ratio	-0.5%	+0.5%	0.1%
Surge Margin	>= initial value	-	0.1%
Target	Relative lower bound	Relative higher bound	Tolerance
Isentropic Efficiency	> initial value	-	0.01%

Table 27 presents list of all the parameters that will take a part into optimization task. Since it was decided to optimize VGV setting, all variable vanes are chosen as variables, within +/- 3° angle deviation. The bounding has been chosen basing on presented in previous chapters studies, which shows limitations of SCM method prediction. All vanes can be varied independently extract maximum potential of the method despite the fact that real HPC is equipped in actuator system where fixed proportionality is being set. Fourth variable is dedicated to RPM adjustment over the design space to cover desired Mass-Flow for new VGV setting.

For the constrains, 3 parameters have been chosen. Mass-Flow rate and Pressure Ratio within +/- 0.5% of variation, and Surge Margin, which cannot be lower than initial value from the starting point. For this purpose each member will be covered with fully calculated speedline with in-house stability criterion for Streamline Curvature Method.

The target of the optimization task is to obtain maximum Isentropic Efficiency for given constrains. Mentioned in the table tolerance has to soften the boundaries to avoid missing of detection of correct, profitable trend during design space sampling.

For the Multi-Fidelity approach to achieve maximum efficiency of the process, it's common to find dominant variables. For presented DoE there were no need of restricting number of used variables. For data aggregation two pairs of the data will be considered – IGV/Stator 1 and Stator 1/Stator 2 consequently, these pairs have been treated as coordinates for spatial data representation.

To evaluate contributions assumed for this thesis, optimization task together with Multi-Fidelity approach was performed for speed range of three conditions - High Speed, Mid Speed and Low Speed therefore, wide operational range has been covered.

5.3 Methodology

5.3.1 The concept

As an outcome of performed studies, literature review, and DoE the following Multi-Fidelity concept has been proposed to utilize considered research (Figure 5.1).

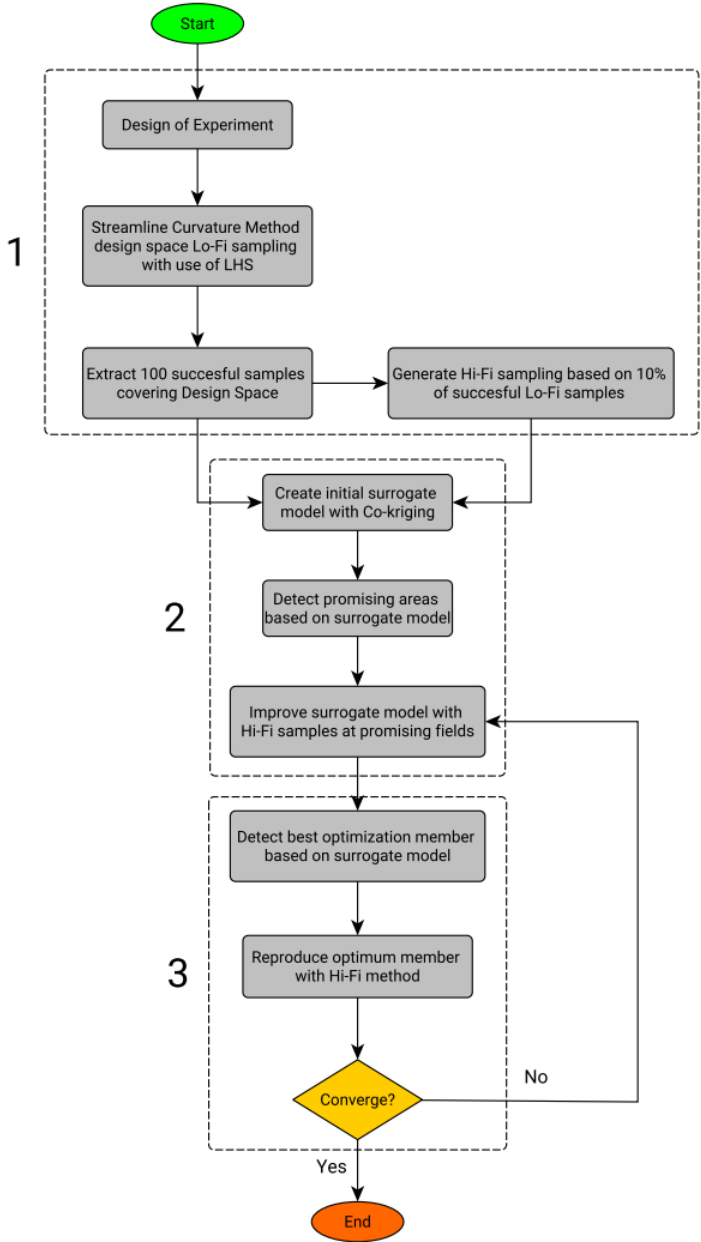


Figure 5.1 Multi-Fidelity concept flowchart

For the purpose of explanation proposed methodology, flowchart has been divided into three phases: Sampling phase (1), Surrogate model creation phase (2), and Best member detection phase (3).

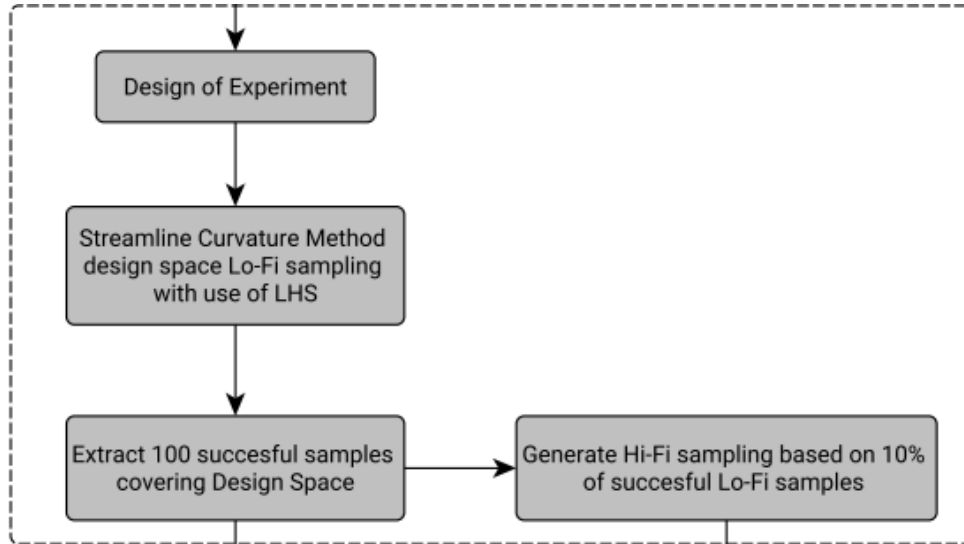


Figure 5.2 Sampling phase of the optimization task

In the phase of Sampling (Figure 5.2) design space is being researched with use of Low-Fidelity, cheap solutions of Streamline Curvature Method. During this process, VGV setting has been varied within bounds set by DoE. Sampling is realized with Latin Hypercube Sampling (LHS) strategy [54, 55] as an efficient sampling plan for initial surrogate building [53]. Sampling was being performed until 100 successful members have been found, therefore the member being valid in terms of set constrains (see Table 27). When Low Fidelity data set was derived, then High Fidelity sampling took place within the area of successful Lo-Fi design space coverage. The sampling ratio has been set to 1:10 for initial surrogate model. This level of data representation is rather low, and it is not recommended for more complex optimization tasks. With increasing number of dimensions, sampling plan towards 1:2 should be the ratio of choice [53].

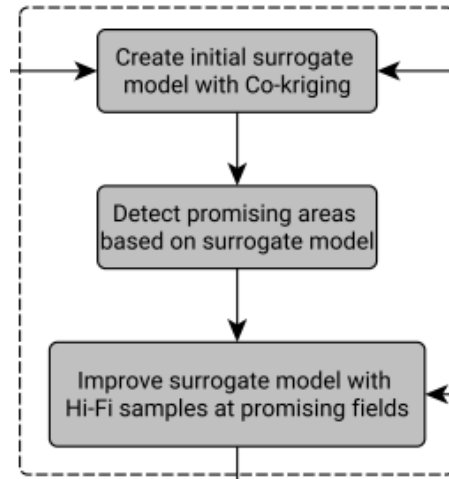


Figure 5.3 Surrogate model definition phase of the optimization task

After the sampling phase, surrogate model has to be build (Figure 5.3) and it is a part of phase 2 of the methodology. Under creation of initial surrogate model, fitting steps required by Co-Kriging method are hid. The details of these steps were presented in the chapter 5.4 but nevertheless to describe the surrogate model building the following activities were performed:

- Creation of spatial data out of Low and High Fidelity dataset
- Creation of prediction grid based on evaluated design space
- Finding fitting model to the semi-variograms of Low and High Fidelity data
- Performing Linear co-regionalization to fit the model to aggregated Multi-Fidelity dataset
- Co-Kriging estimation to the prediction grid

Subsequently estimated design space of promising fields is being improved with further Hi-Fi 3D CFD evaluations – up to 5 evaluations per loop, which are currently based on the initial Lo-Fi samples from the approximated space of improvement. Consequently, expensive samples have been equipped with boundary conditions without additional computations.

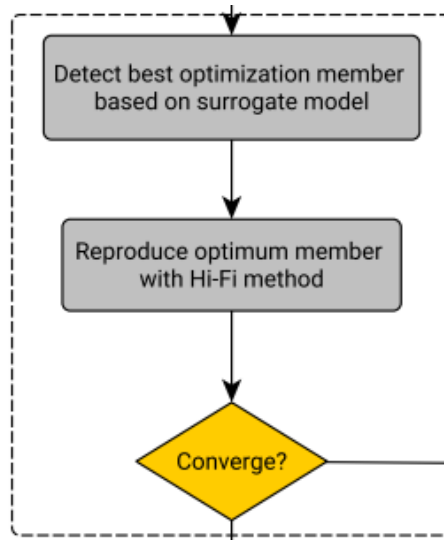


Figure 5.4 Best member detection phase of the optimization task

The last phase in the flowchart has been represented with best member detection (Figure 5.4). The contribution of this step is to extract currently estimated best member, which is correspondingly fitting to all constrains of DoE (Table 27). To validate member of choice, High Fidelity run is being performed. If requirements of DoE are met, then loop stops, if not, the repetition of phase 2 improves the surrogate model for more accurate prediction.

5.3.2 Idea of variogram model

To perform Co-Kriging approximation it is necessary to build a mathematical model of data variability over distance between data points. To make it possible it is required to create discrete function of data representation what in geostatistics is known as variogram.

Variogram is a spatial continuity description of the data. As mentioned, it is a discrete function determined with use of variability between pairs of data points at various distances [56]. Figure 5.5 illustrates variogram together with the nomenclature being in use.

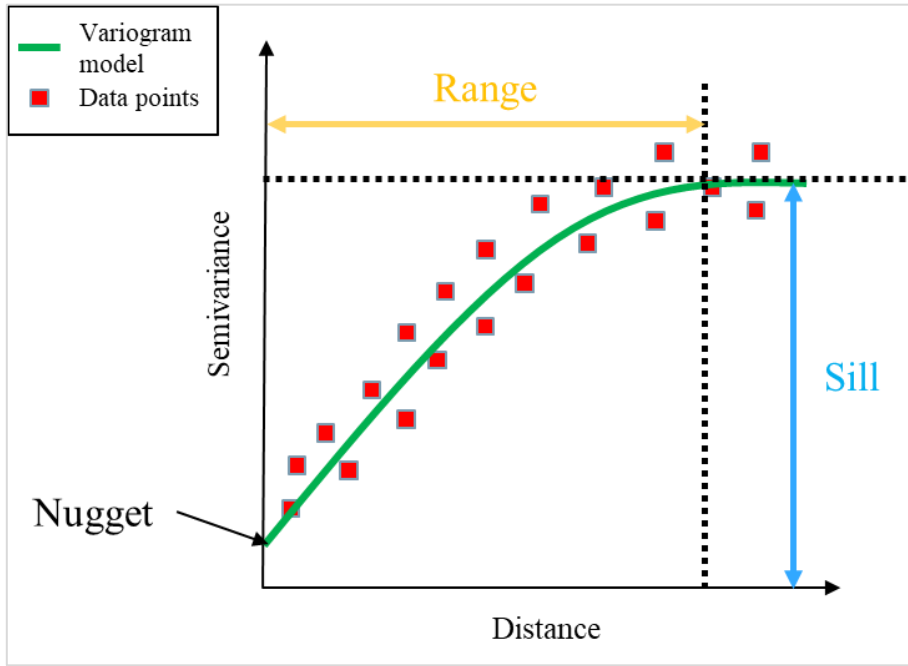


Figure 5.5 Semi-variogram and its parameters

To model the variogram several methods exist [57]. For this thesis, application has been limited due to the character of the data, therefore the following models have found usage:

- Spherical

$$\gamma(h) = c * Sph\left(\frac{h}{a}\right) = \begin{cases} c * \left[1.5\frac{h}{a} - 0.5\left(\frac{h}{a}\right)^3\right], & \text{if } h \leq a \\ c, & \text{if } h \geq a \end{cases} \quad (\text{Eq. 4})$$

- Exponential

$$\gamma(h) = c * Exp\left(\frac{h}{a}\right) = c * \left[1 - \exp\left(-\frac{3h}{a}\right)\right] \quad (\text{Eq. 5})$$

- Gaussian

$$\gamma(h) = c * \left[1 - \exp\left(-\frac{(3h)^2}{a^2}\right)\right] \quad (\text{Eq. 6})$$

, where:

- c – Sill
- h – Distance
- a – Range

5.3.3 Prediction correlation and error

For the evaluation of the predicted data and its quality two measures have been chosen which are commonly exploited in the literature related to Co-Kriging surrogate model creation:

- Coefficient of Determination (R^2)

$$R^2 = \frac{\sum(\hat{y}_i - \bar{y})^2}{\sum(y_i - \bar{y})^2} \quad (\text{Eq. 7})$$

- Root Mean Square Error (RMSE)

$$RMSE = \sqrt{\frac{1}{N} \sum_{i=1}^N (y_i - \hat{y}_i)^2} \quad (\text{Eq. 8})$$

,where

- \hat{y}_i – predicted value of y for observation i
- \bar{y} – mean of y value
- y_i – y value for observation i
- N – number of observations

5.4 Multi-Fidelity prove of concept

The following chapter presents steps for Multi-Fidelity initial surrogate model creation, improving the model and final optimized member evaluation. Beside raw results, semi-variogram models were presented to discuss the difference in the data between fidelities. To visualize the data, plots of the spatial data with predicted parameter have been prepared and showed. At last, statistics of conducted optimizations were collected into a table.

5.4.1 High Speed

As the first considered condition High Speed configuration has been chosen. For the following one, previous studies showed the highest correlation between 3D CFD and SCM method what was an indicator for a successful Multi-Fidelity run.

Figure 5.6 presents all the samples available for initial surrogate model build. As mentioned in the previous chapter, data is represented by 100 Low-Fidelity samples and 10 High Fidelity solutions. Lo-Fi data have been obtained with use of LHS method varying all defined variables and all available solutions are considered as successful in terms of performance point reproduction and fits within tolerance for efficiency and Surge Margin prediction what means that not only improved performance solutions have been found. High Fidelity data is based on Lo-Fi samples distributed in the way of covering Lo-Fi range of variations. When Hi-Fi solutions were found, it has been replacing Lo-Fi reference to avoid overlapping samples.

Because of specificity of the Co-Kriging method, two variables at the time could be evaluated as spatial definition. For that, as mentioned in the concept description, two pairs of variables have been estimated – IGV/Stator 1 and Stator 1/Stator 2 (see Figure 5.6 and Figure 5.7).

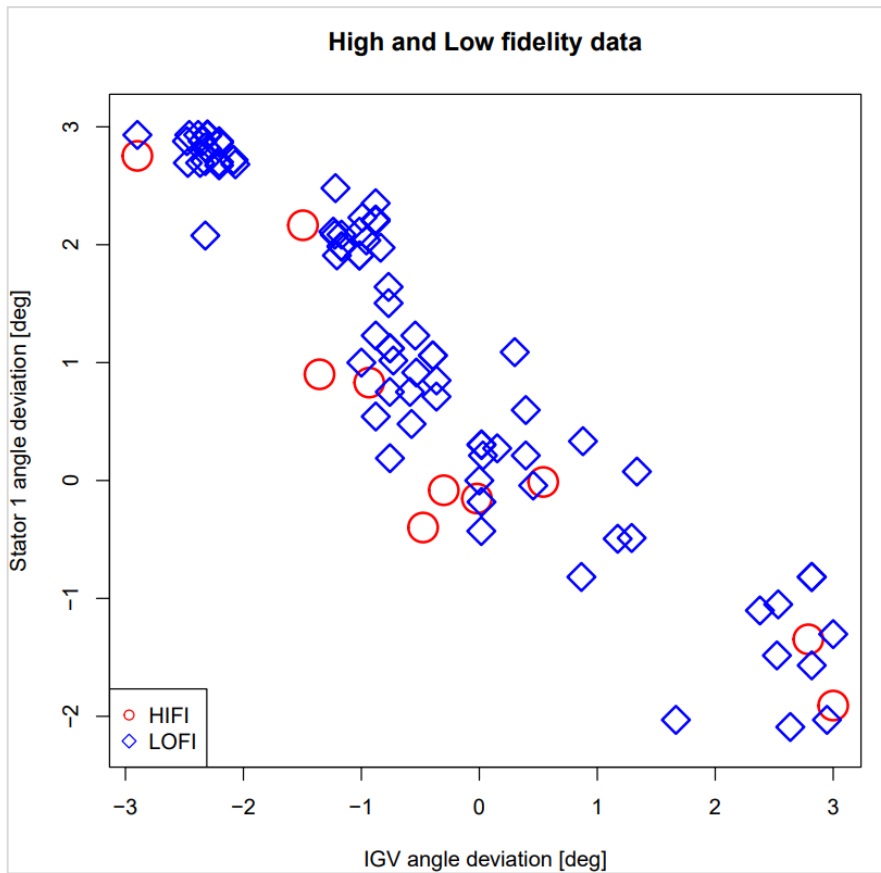


Figure 5.6 Visualisation of spatial distribution of the samples for High Speed IGV/Stator 1 variant

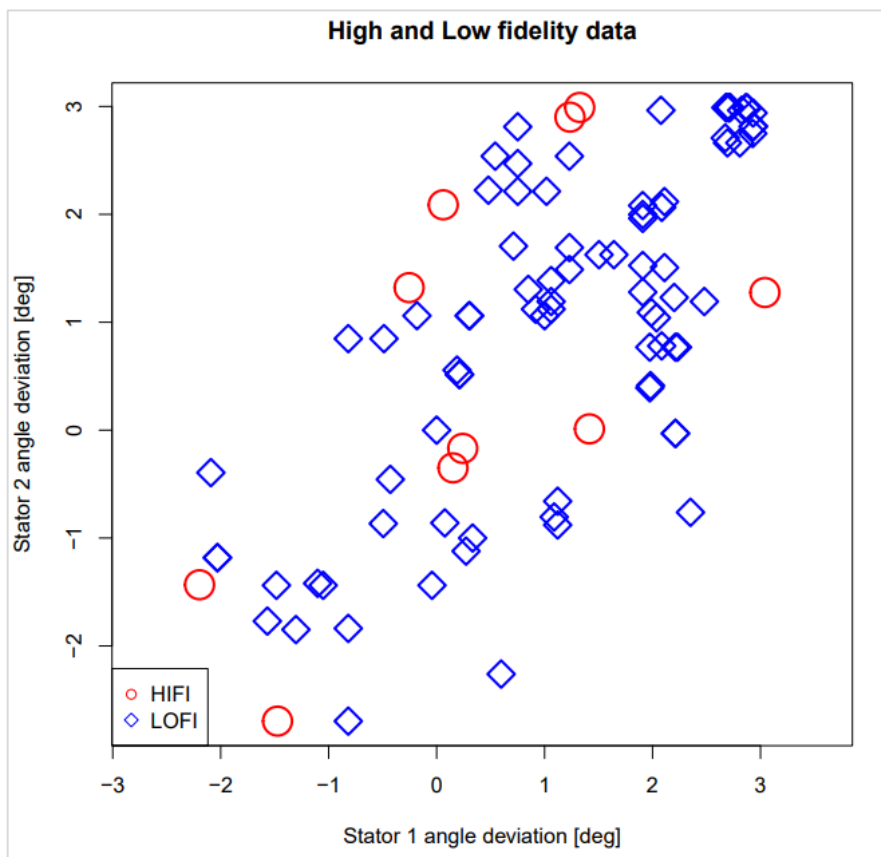


Figure 5.7 Visualisation of spatial distribution of the samples for High Speed Stator 1/Stator 2 variant

While design space sampling is known, the next step was to prepare prediction grids, so the discretization of the field on which prediction has been performed. The procedure of creation the prediction grid, has been simplified to creating a mesh over available data range. The side effect of this approach is the prediction outside the available data, consequently extrapolation took place what is not the desired usage of this method. For the condition of High Speed, prediction grid was created with $0.05[^\circ]$ step. To avoid inconvincible prediction, the final results have been filtered with level of data variation. The visualization of the prediction grid was showed in Figure 5.8.

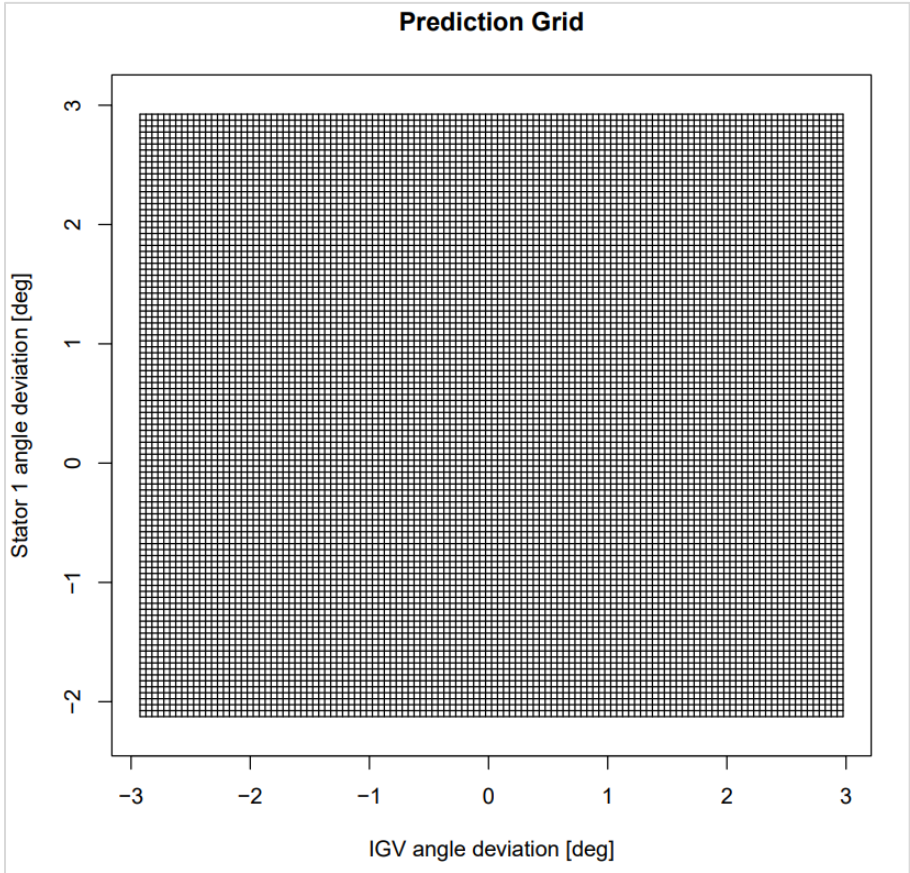


Figure 5.8 Visualisation of prediction grid for High Speed IGV/Stator 1 spatial discretization

The next required step is building the model of semi-variogram. The method of finding best fitting for High and Low fidelity data via regression method was provided with gstat package of R [58]. Co-regionalization, so the fitting two data set semi-variogram models into one, aggregated representation have been performed with use of linear model [59]. Since it wasn't expected to predict exact value of efficiency increase but more to indicate the trend of the performed evaluation, the requirement for the model was allocated in data distribution shape rather than perfectly fitted Nugget and Sill. To present how model

fitting has changed over the data, Figure 5.9 were introduced, where model for High Fidelity, Low Fidelity and aggregated data has been found.

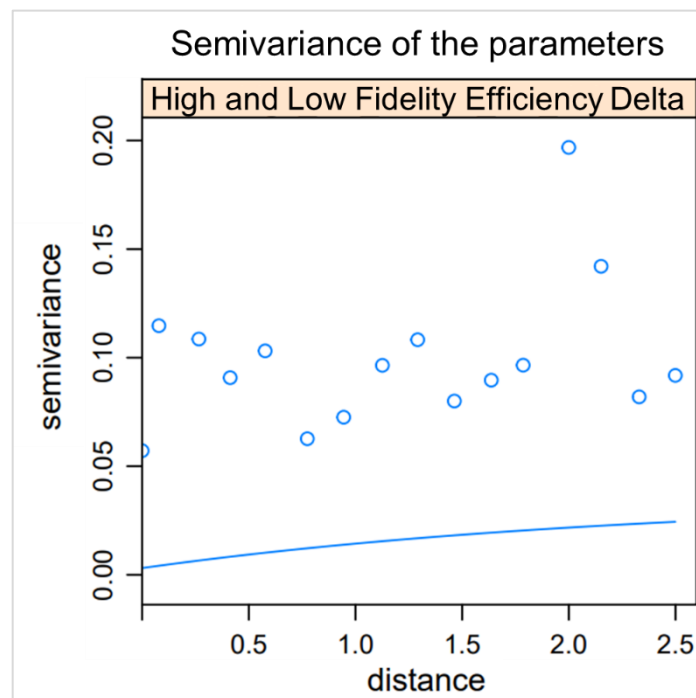


Figure 5.9 Semi-variance model for Multi-Fidelity IGV/Stator 1 efficiency variant

For model creation for High Speed, IGV/Stator 1 spatial estimation , Exponential method was used (Eq. 5). above figure shows not perfectly matched model in terms of Nugget and Sill when compare the aggregated data. Quality miss may be allocated into sampling method, or number of samples itself. Since the aim of this thesis is not considering mathematical development of the Mu-Fi method, no further actions have been taken. From the qualitative point of view, distribution of proposed model covers the data variation, therefore further assessment was continued.

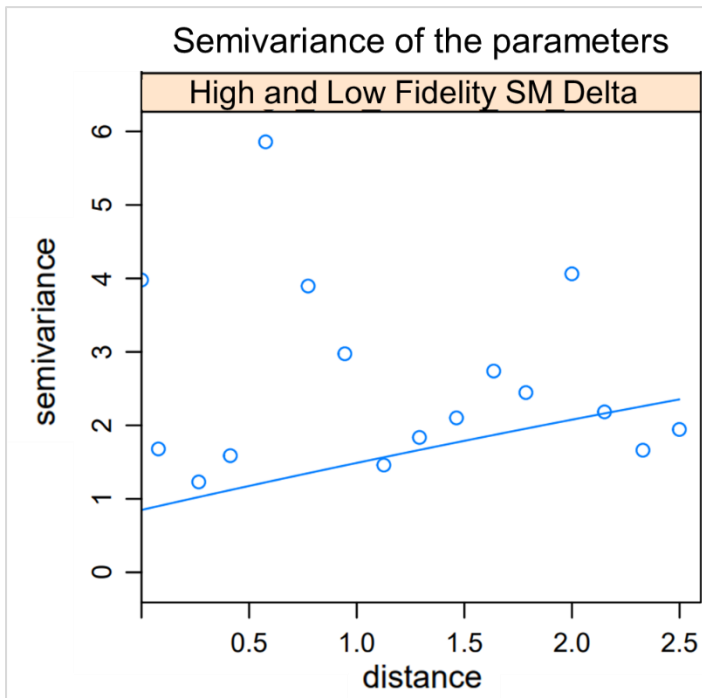


Figure 5.10 Semi-variance model for Multi-Fidelity IGV/Stator 1 Surge Margin variant

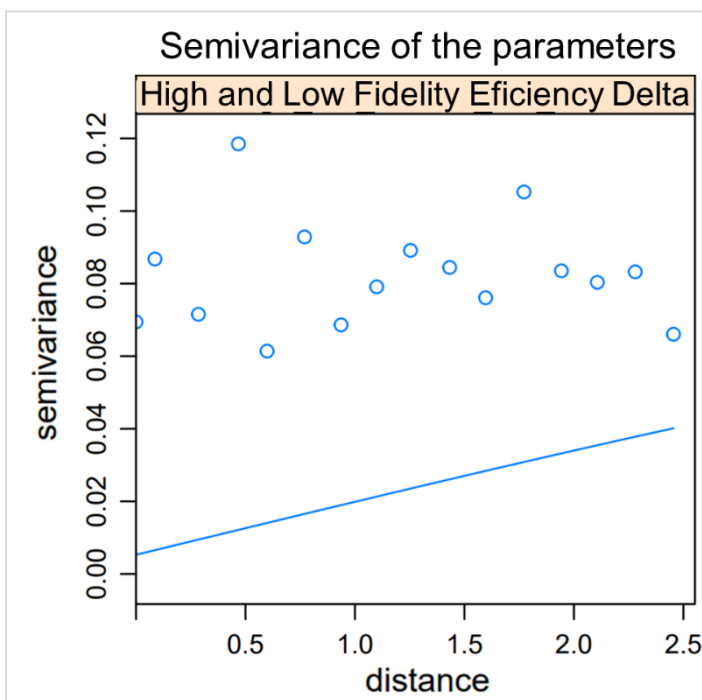


Figure 5.11 Semi-variance model for Multi-Fidelity Stator 1/Stator 2 efficiency variant

For the models of SM prediction and efficiency of Stator 1/Stator 2 variants, also the exponential models were applied (Figure 5.10, Figure 5.11). As soon as model was prepared, it was possible to perform prediction of the chosen parameters. Efficiency prediction has been performed for both spatial frames and Surge Margin inly for IGV/Stator 1 variation to reduce amount of the data since only brief evaluation was required.

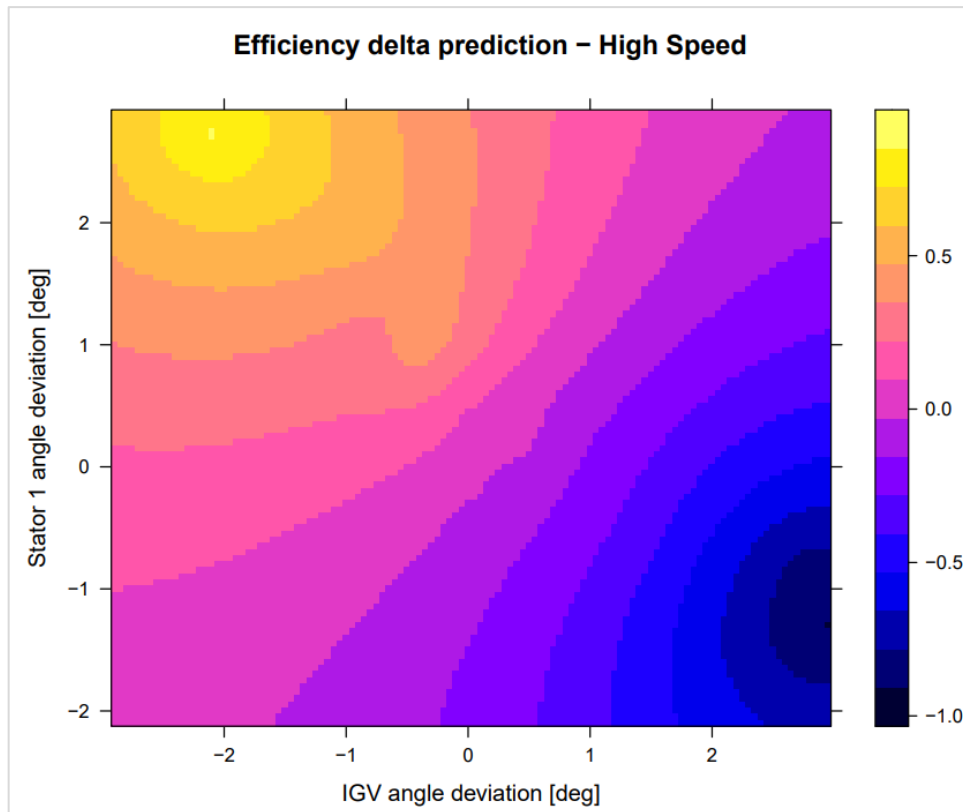


Figure 5.12 Visualisation of Efficiency delta prediction for High Speed IGV/Stator 1 variant

The tendency of the efficiency gain leads to closing IGV and opening Stator 1 (Figure 5.12). The specified promising area is marked with yellowish color, where basing on the initial surrogate model, the highest gain is expected. The correlation of this prediction has achieved $R^2=0.951[-]$, indicating good surrogate model response compared to Hi-Fi data.

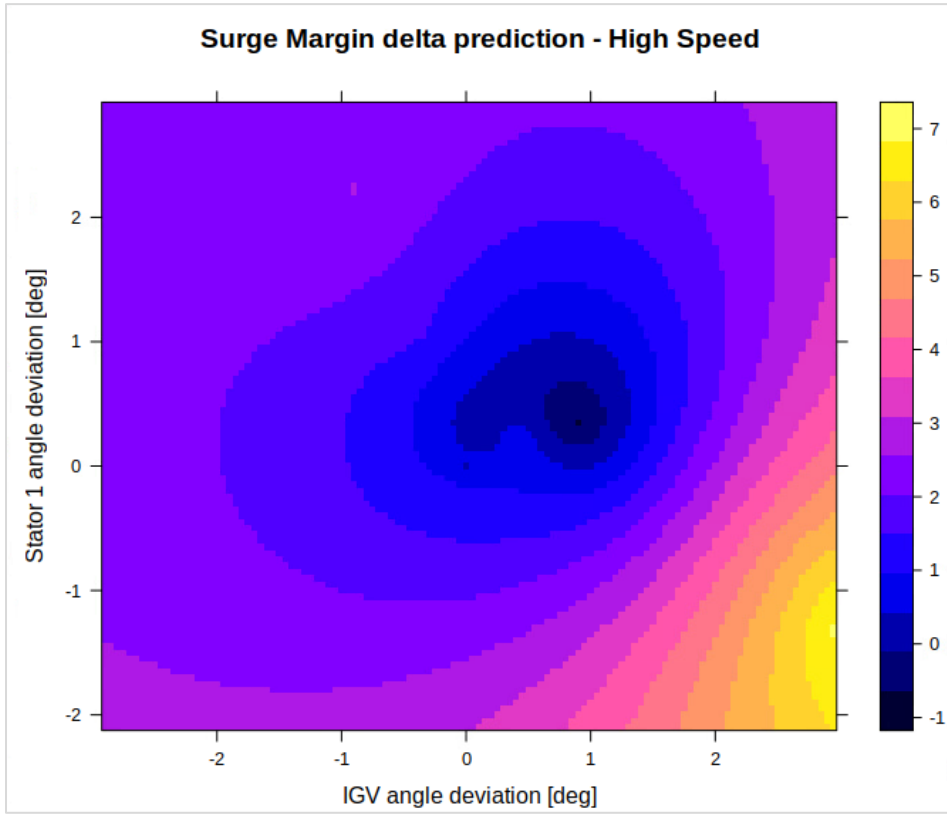


Figure 5.13 Visualisation of Surge Margin delta prediction for High Speed IGV/Stator 1 variant

Interpreting above Surge Margin prediction plot, estimated efficiency gain from Figure 5.12 should not provide stability issue, even slight Surge Margin increase was estimated. The correlation of this prediction has achieved $R^2=0.885[-]$.

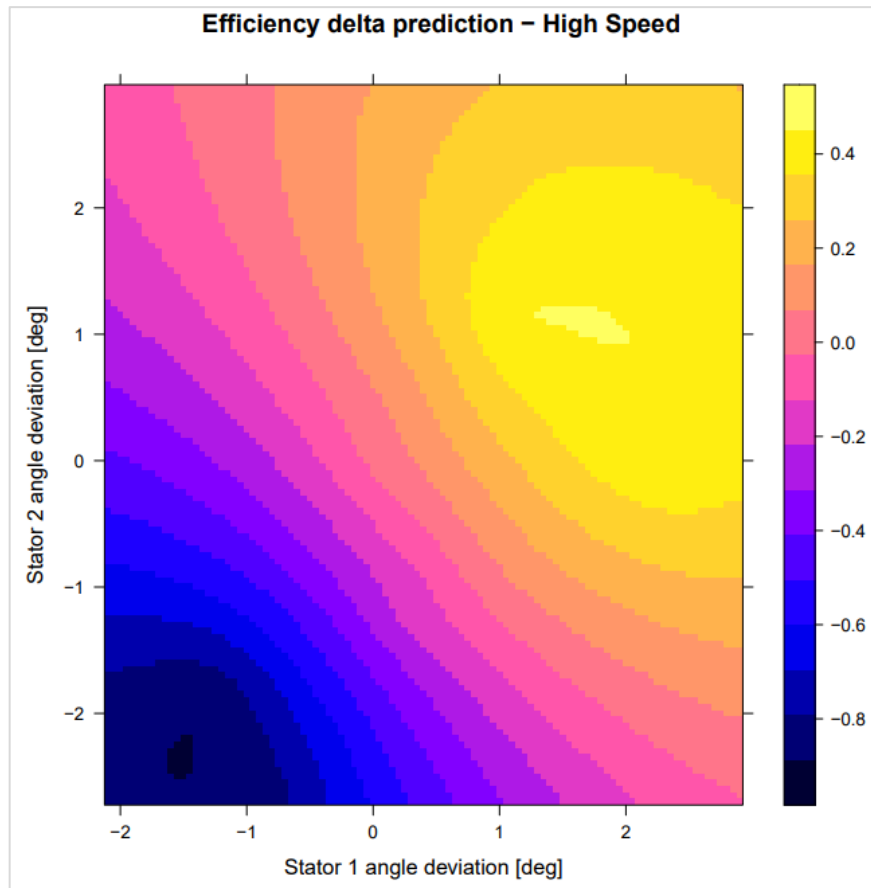


Figure 5.14 Visualisation of Efficiency delta prediction for High Speed Stator 1/Stator 2 variant

Figure 5.14 shows improvement of the efficiency between Stator 1 and Stator 2 in the case of following the opening trend. The correlation of this prediction has achieved $R^2=0.979[-]$.

Basing on the current prediction of the initial surrogate model, efficiency gain is expected in the field of closing the IGV and opening Stator 1 and Stator 2, without sacrificing of the stability of the compressor module. Currently, Coefficient of Determination was satisfactory for all the predictions. Nevertheless the next step is to improve the model with the High Fidelity solutions within promising fields.

For the model improvement, 5 new Hi-Fi solutions have been provided. Positioning in the design space was defined by Lo-Fi successful samples located in the promising areas, given by the initial surrogate model.

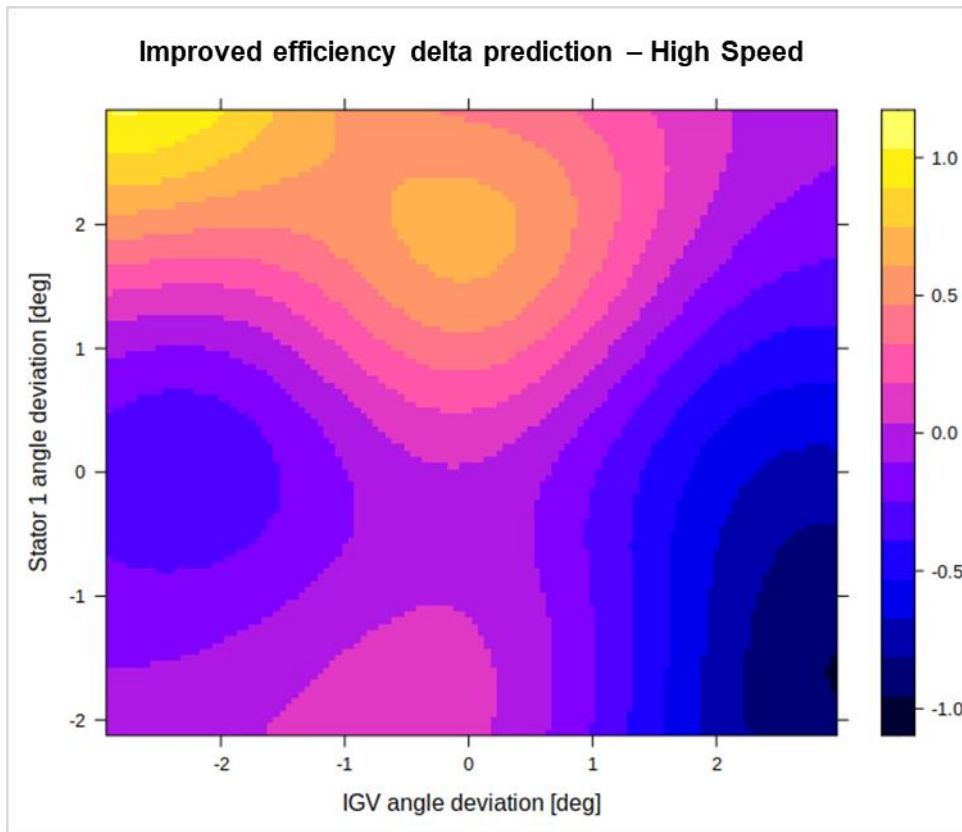


Figure 5.15 Visualisation of improved Efficiency delta prediction for High Speed IGV/Stator 1 variant

After surrogate improvement, Efficiency prediction has strengthened the indication of IGV closure and Stator 1 opening, with the gain of ~1% (Figure 5.15). Comparing to the initial surrogate model, prediction discovers more complex efficiency distribution, where more than one promising spot is present. The correlation of the prediction for improved surrogate model has increased to $R^2=0.978[-]$

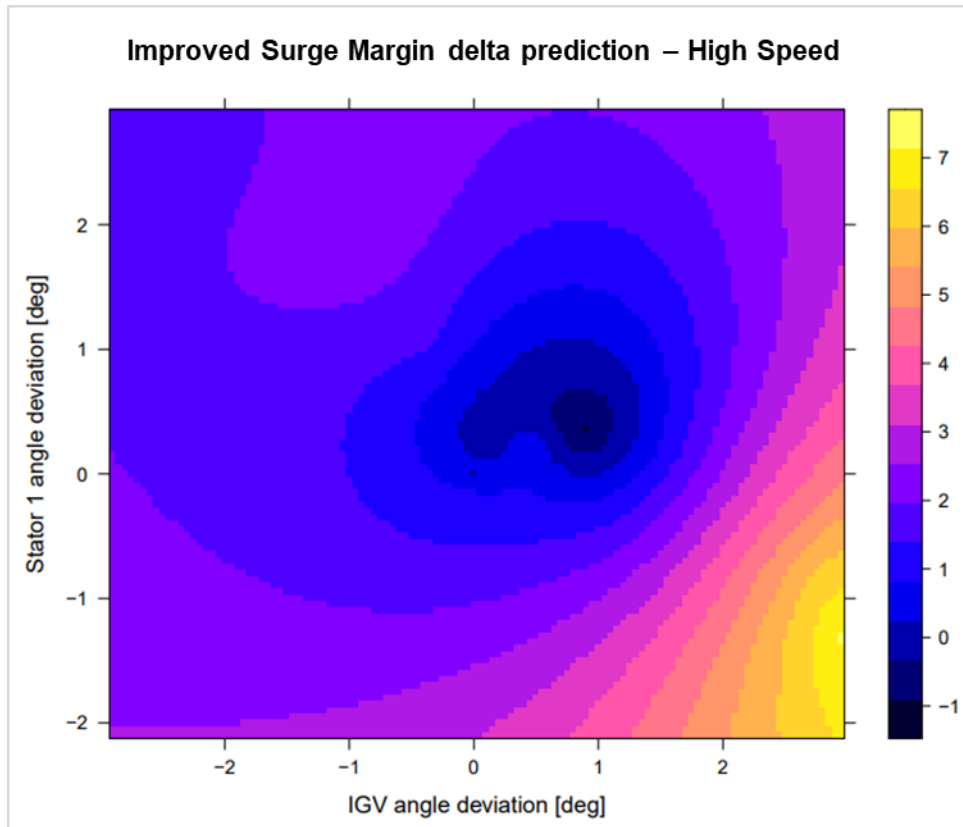


Figure 5.16 Visualisation of improved Surge Margin delta prediction for High Speed IGV/Stator 1 variant

For Surge Margin prediction of improved model, data in Figure 5.16 still presents positive response within the range of Efficiency gain and predicted stability increase $\sim 1\%$ in SM. In compare to initial prediction, no significant change in data distribution was observed. The correlation of the prediction for improved surrogate model has increased to $R^2=0.905[-]$.

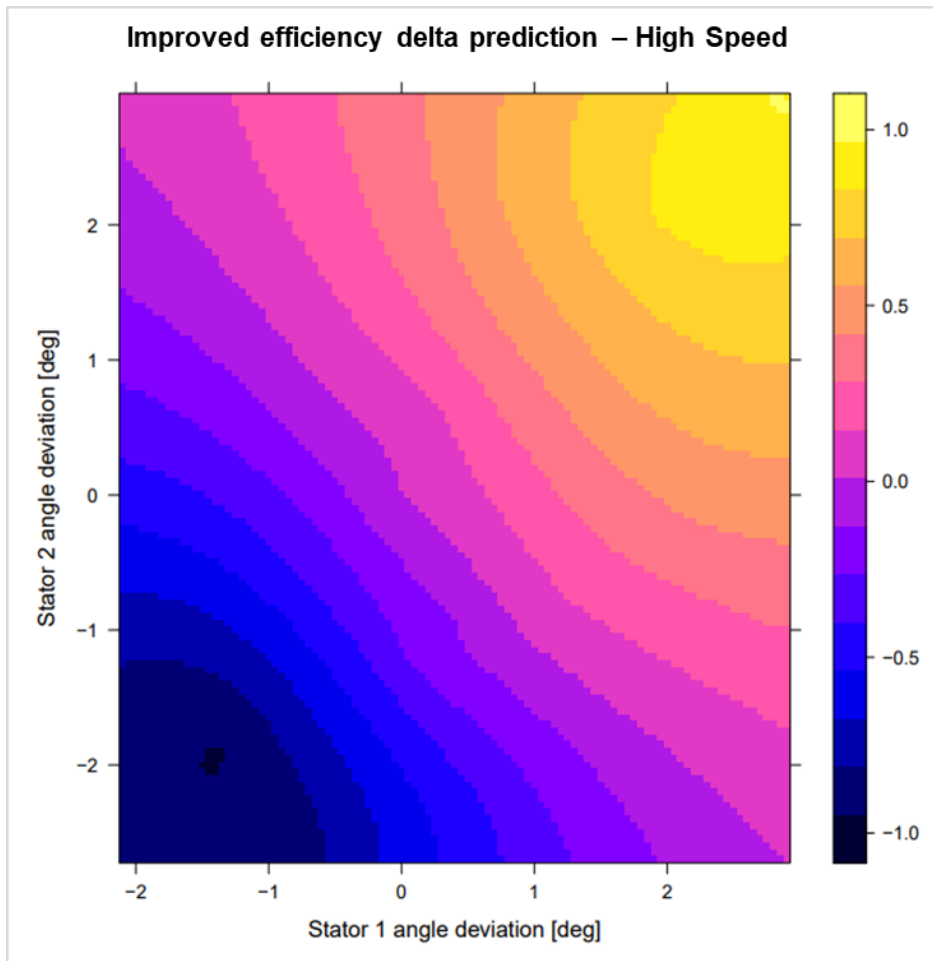


Figure 5.17 Visualisation of improved Efficiency delta prediction for High Speed Stator 1/Stator 2 variant

The efficiency prediction plot of Stator 1/Stator 2 variation presented in Figure 5.17 as the previous one strengthen the trend of following Stator 1 opening by Stator 2. That is showing, that initial guess of the surrogate model was correct in terms of trend over the design space. The correlation of the prediction for improved surrogate model has increased to $R^2 = 0.993[-]$, what indicates high quality of trend estimation done by Co-Kriging model.

To validate the process of Multi-Fidelity approach, it was required to evaluate the prediction of the surrogate model with expensive method and compare with reference “Full model” configuration. For qualitative compare Figure 5.18 shows speedline characteristics for High Speed conditions.

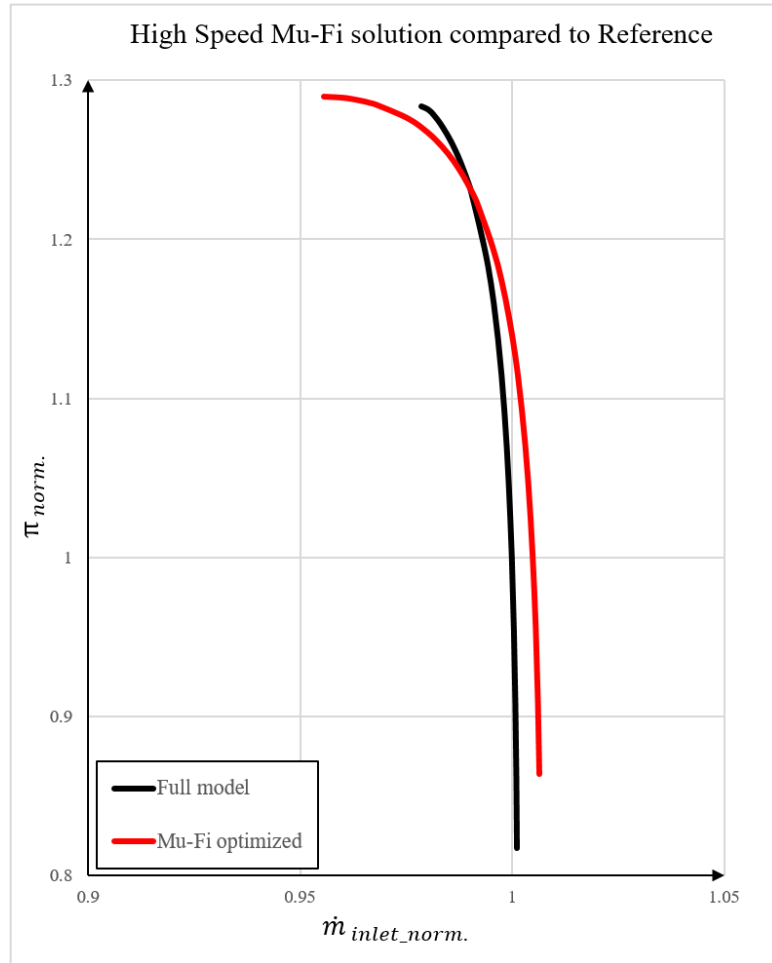


Figure 5.18 Speedlines comparison between reference model and Mu-Fi optimized – High Speed

At the level of Working Line, minor shift of the massflow was observed. The deviation fits within the limits of 1% offset. Optimized member is characterized by flatter character of the Pressure Ratio rise what was observed as stability enhancement.

For quantitative evaluation, parameters of best High Fidelity sample, used for surrogate model creation, raw Multi-Fidelity prediction and validation of Mu-Fi prediction have been compared and presented in the Table 28.

Table 28 Mu-Fi process results compare – High Speed

Case	IGV deviation [°]	S1 deviation [°]	S2 deviation [°]	Efficiency [pp]	Surge Margin [pp]
Best Hi-Fi sample	-2.21	+2.88	+2.99	+1.00	+1.96
Prediction	-2.45	+2.9	+2.9	+1.00	+1.73
Validation	-2.45	+2.9	+2.9	+1.23	+1.24

The final configuration showed increase of the efficiency by 1.23% together with stability increase. In compare to the solutions which were used during the sampling phase, Mu-Fi optimized member revealed the most satisfying performance enhancement. Worth attention is comparison of predicted performance, and how close performance has been achieved with High Fidelity validation. Correlation of the surrogate models was constantly high for all variables what has positive response in the final optimized member.

5.4.2 Mid Speed

The same strategy for sampling scheme was introduced for Mid Speed condition. For this configuration, 3 of 10 High Fidelity samples have failed due to mismatch of performance point adjustment i.e. Mass-Flow and Pressure Ratio were out of 1% allowed deviation. The distribution of the data have been presented in Figure 5.19 and Figure 5.20, where IGV/Stator 1 and Stator 1/Stator 2 variants are samples respectively.

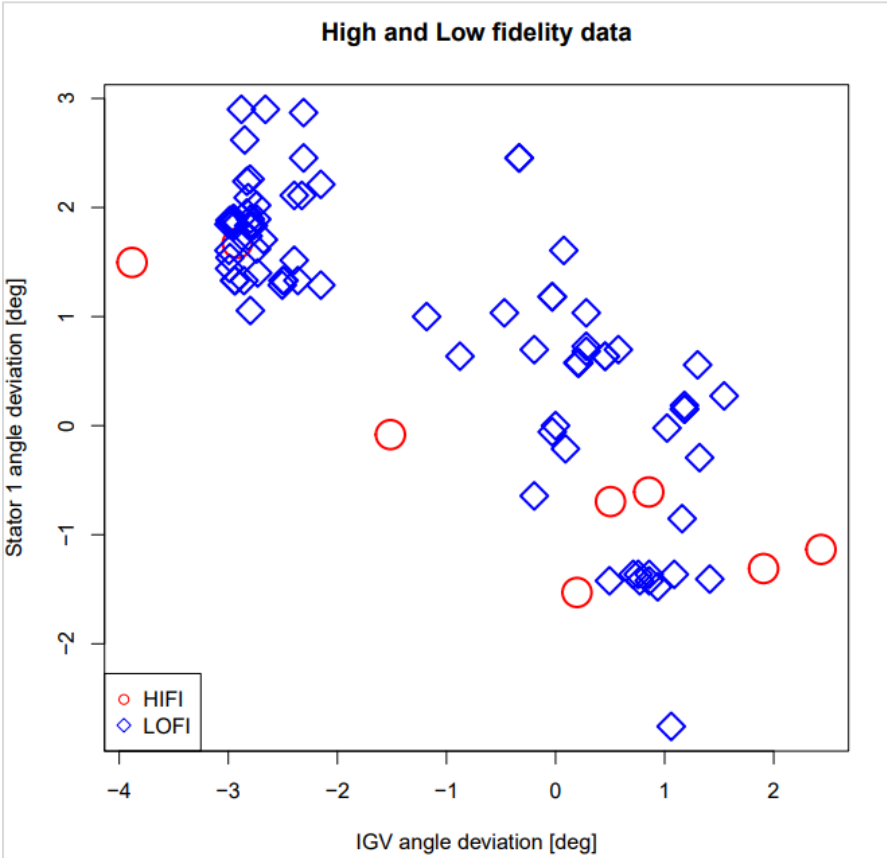


Figure 5.19 Visualisation of spatial distribution of the samples for Mid Speed IGV/Stator 1 variant

Increased density of Lo-Fi samples is a result of Latin Hypercube Sampling approach, where spots with positive response of DoE have been found.

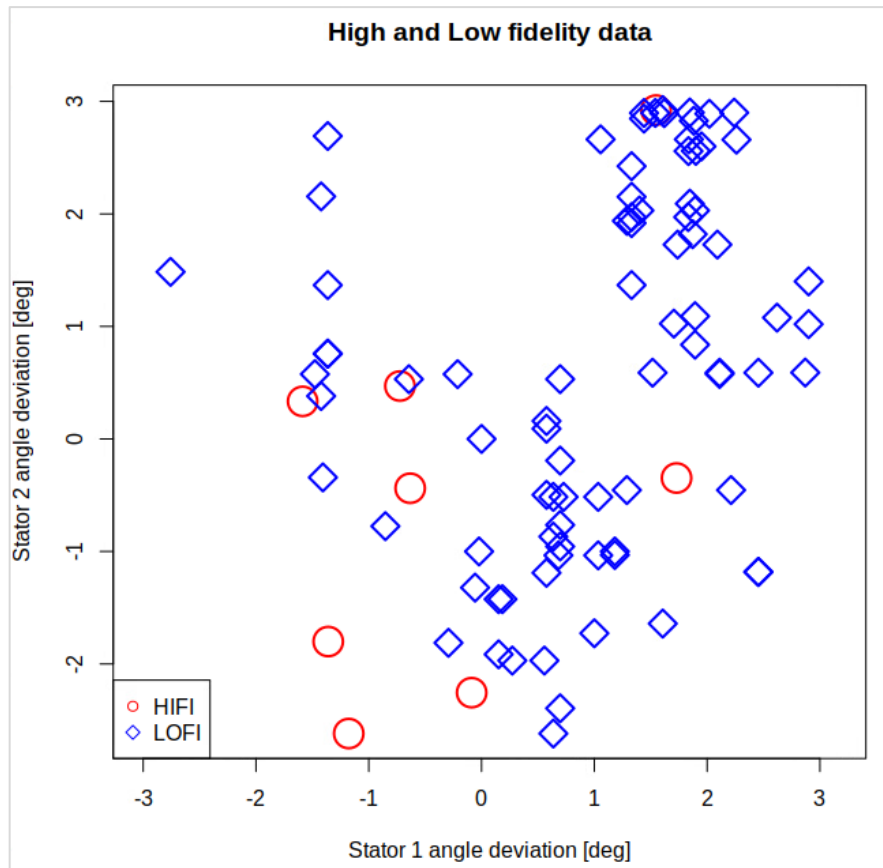


Figure 5.20 Visualisation of spatial distribution of the samples for Mid Speed Stator 1/Stator 2 variant

Prediction grid was prepared in the same manner as for High Speed condition. Box within the limits of successful samples have been set, and mesh with step of $0.05[^\circ]$ have been distributed over design space area. Since no significant information is allocated in the discretization pictures, visualization has been omitted.

In the following figures (Figure 5.21 - Figure 5.23), semi-variograms and models have been presented. For current condition, for efficiency data distribution of both parameters variants, Gaussian (Eq. 6) model has been found as best fit choice. For Mid-Speed variant, and Surge Margin Multi-Fidelity evaluation best fitting has been found using Exponential model.

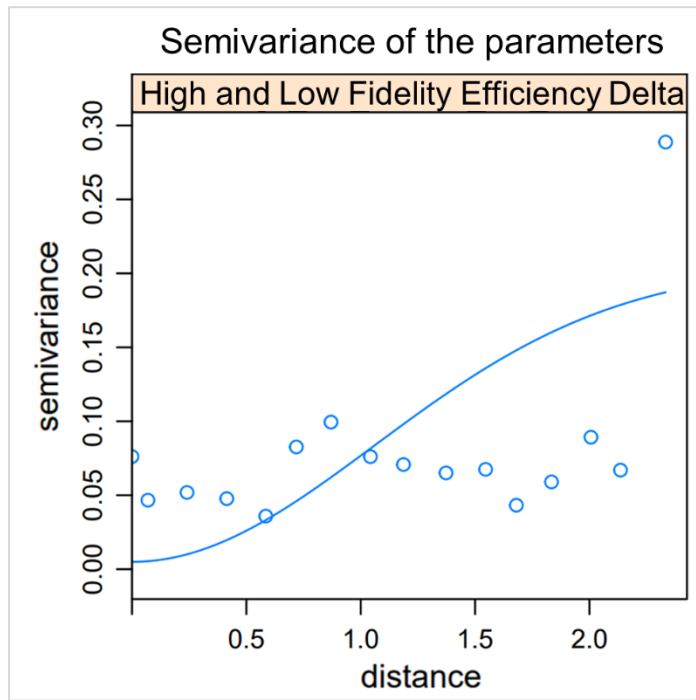


Figure 5.21 Semi-variance model for Multi-Fidelity IGV/Stator 1 efficiency variant

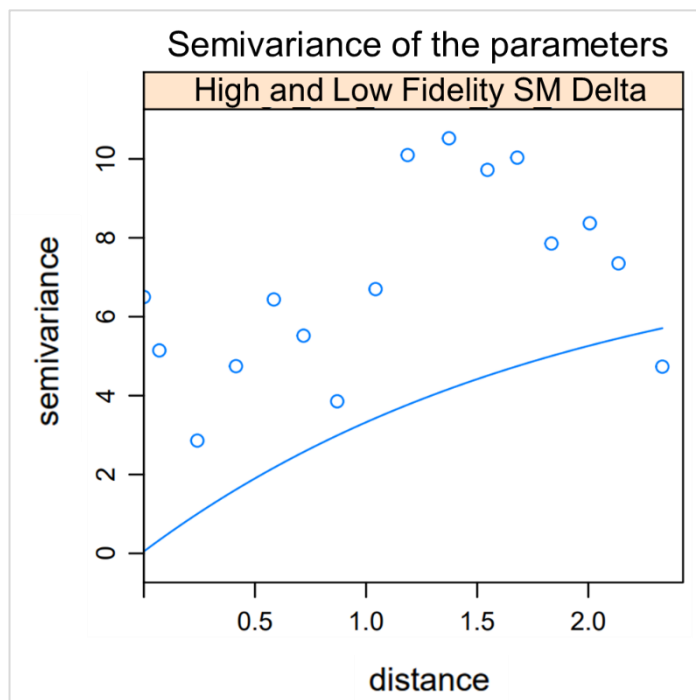


Figure 5.22 Semi-variance model for Multi-Fidelity IGV/Stator 1 Surge Margin variant

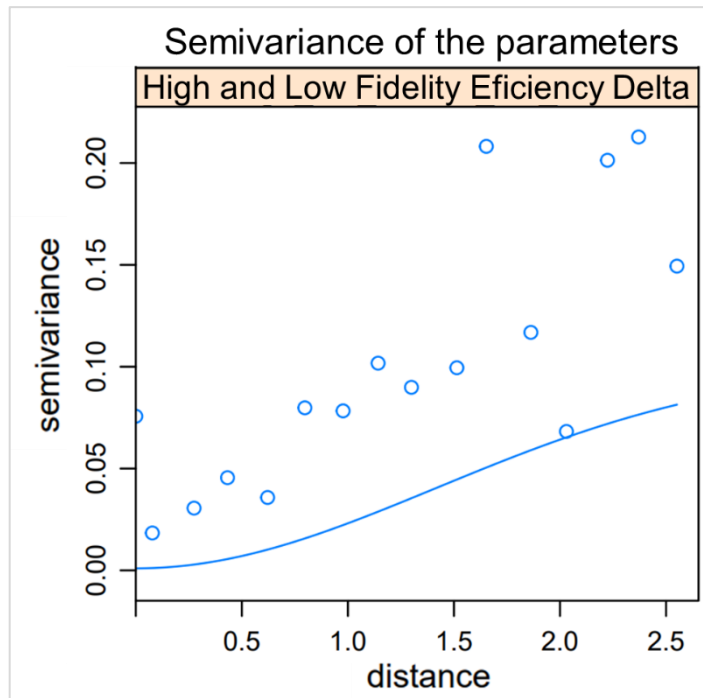


Figure 5.23 Semi-variance model for Multi-Fidelity Stator 1/Stator 2 efficiency variant

According to the procedure, as soon as initial surrogate model was prepared, first prediction have taken place. Sensitivity studies of the model have discovered numerical instabilities for predicting Surge Margin for Mid-Speed conditions (see Figure 4.8 for the details). This fact can influence quality of Surge Margin prediction, by leading to incorrect trends.

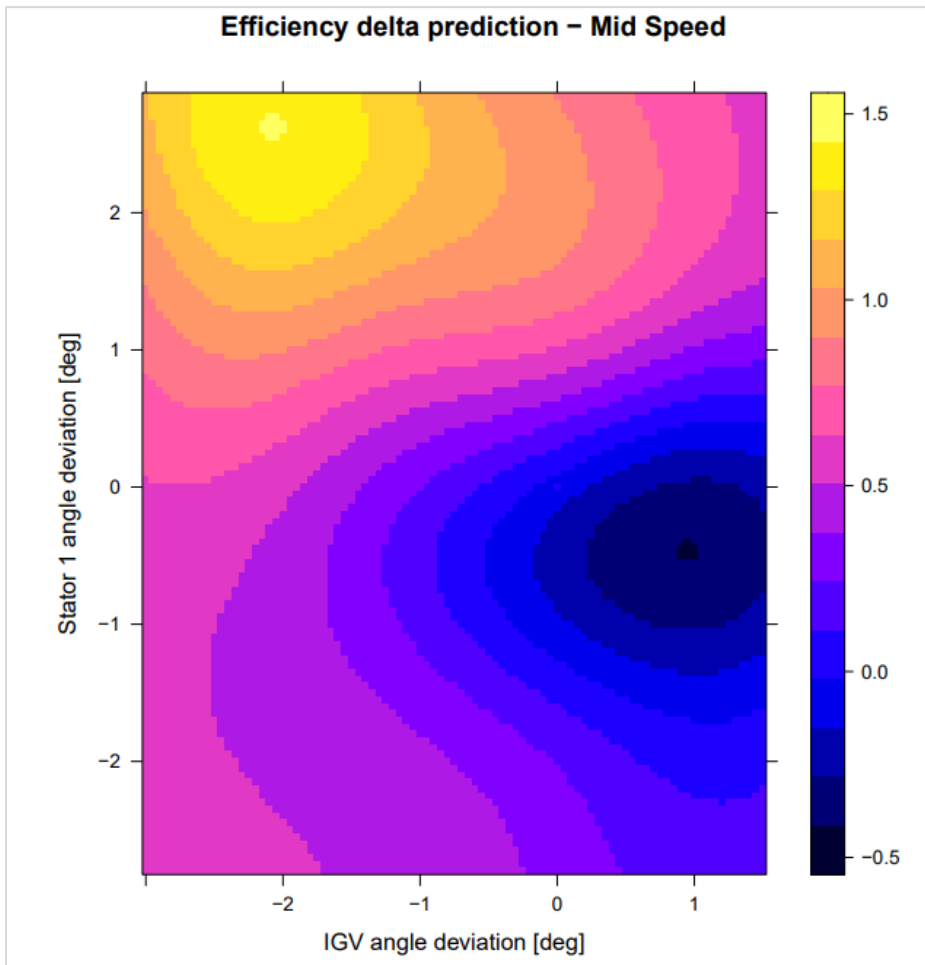


Figure 5.24 Visualisation of Efficiency delta prediction for Mid Speed IGV/Stator 1 variant

Figure above visualizes trend towards closing IGV and opening the Stator 1. The behavior of the compressor component has been similar for High Speed conditions presented in the previous chapter. This indicates potential in the optimization. The correlation for this configuration has been achieved equal to $R^2= 0.889[-]$. Response of the surrogate model become worsen comparing to High Speed conditions according to the coefficient of determination.

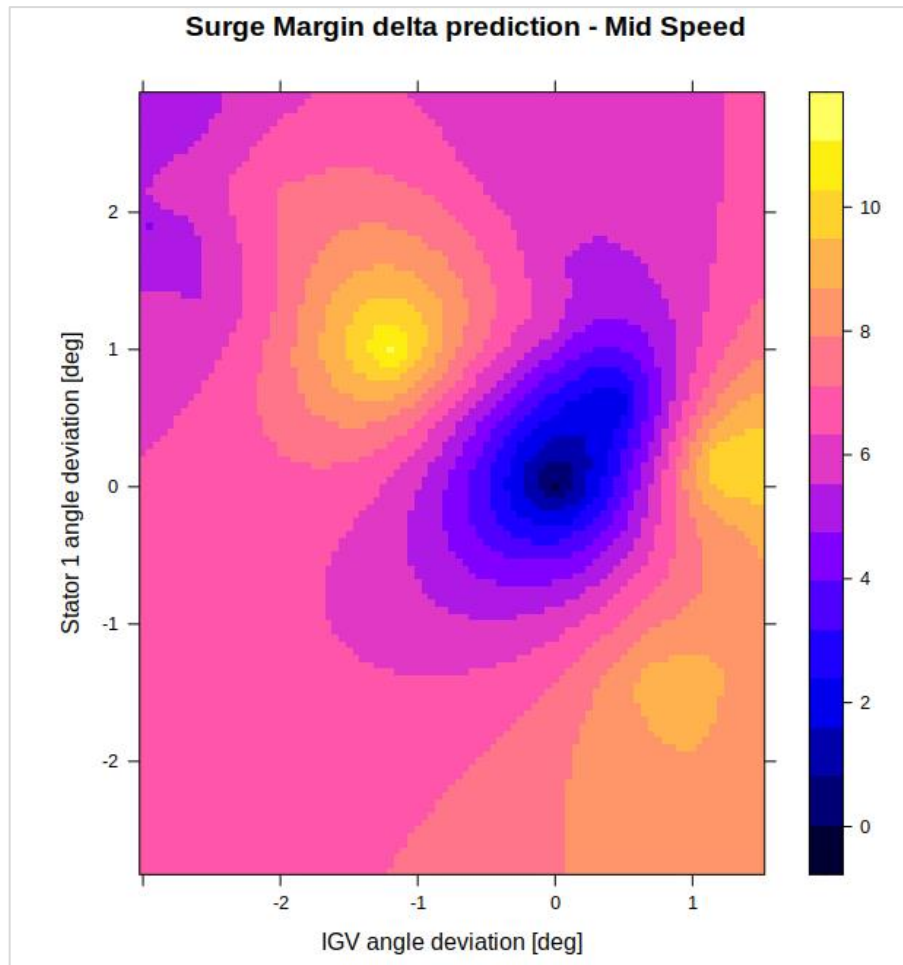


Figure 5.25 Visualisation of Surge Margin delta prediction for Mid Speed IGV/Stator 1 variant

Visualization of Surge Margin delta prediction above shows enhancement nearly all over the design space, together with high gradients. This may indicate discrepancy of the data between fidelities. The correlation of this prediction reached the lowest yet level of coefficient $R^2=0.512[-]$.

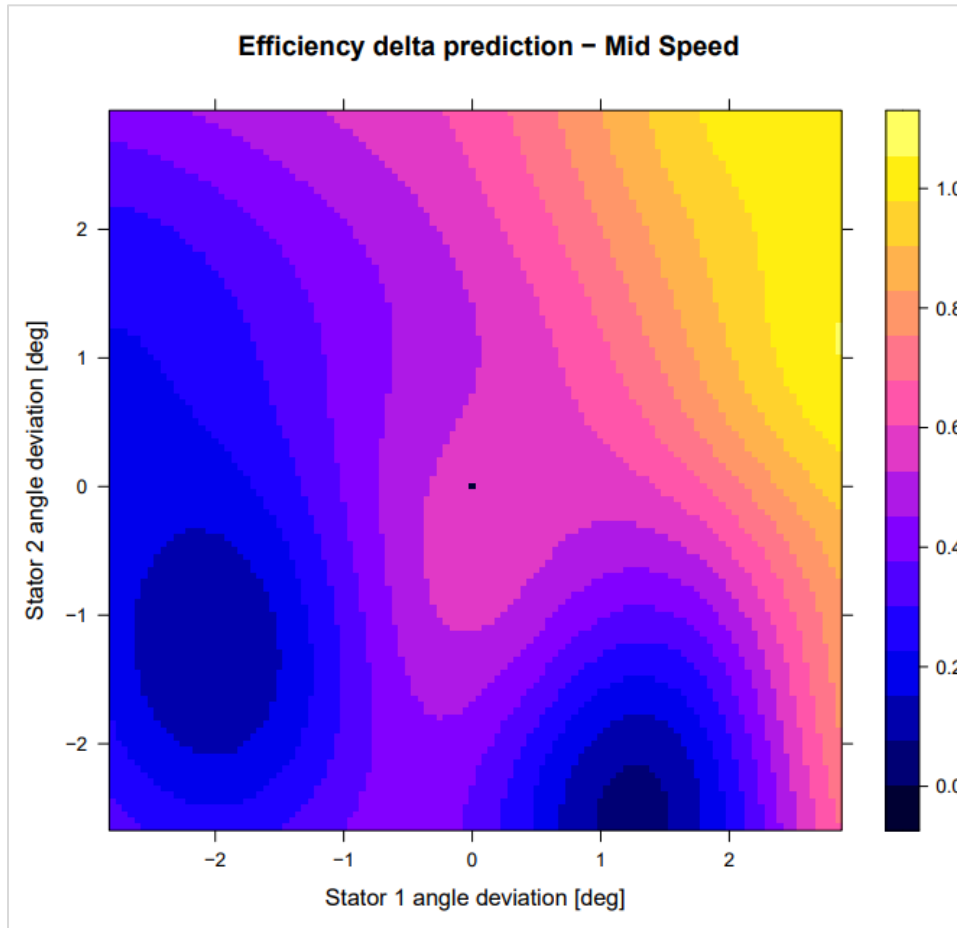


Figure 5.26 Visualisation of Efficiency delta prediction for Mid Speed Stator 1/Stator 2 variant

The efficiency prediction of Stator 1/Stator 2 variant presented in Figure 5.26 shows continued trend from High Speed conditions where gain was observed for following opening of the Stator 2 behind Stator 1. At this stage, the correlation of the prediction was unacceptable, $R^2 = 0.359[-]$ what may indicates poor sampling level.

Despite low levels of the correlation quality, there was a possibility of improving the model, basing on presented predictions. Loop of the improvement have been performed and the results are presented below.

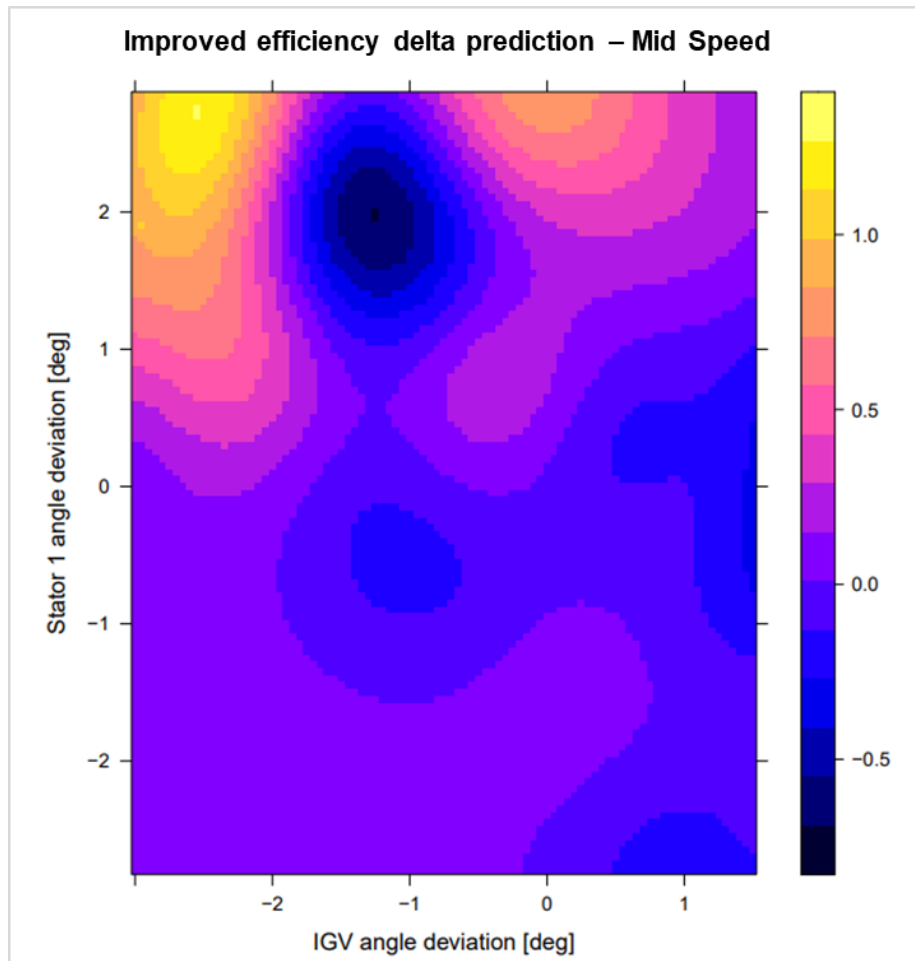


Figure 5.27 Visualisation of improved Efficiency delta prediction for Mid Speed IGV/Stator 1 variant

Efficiency delta prediction, initially well correlated, after improvement sampling of 5 additional expensive solutions, strengthen observed gain for decreasing the angle of IGV and opening Stator 1 (Figure 5.27). The response of High Fidelity model haven't been in line with initial prediction, what caused in decrease of the correlation down to $R^2=0.742[-]$. As confirmation, in compare to the initial estimation, field of negative efficiency delta appeared in the range of $-1[^\circ]$ of IGV closing.

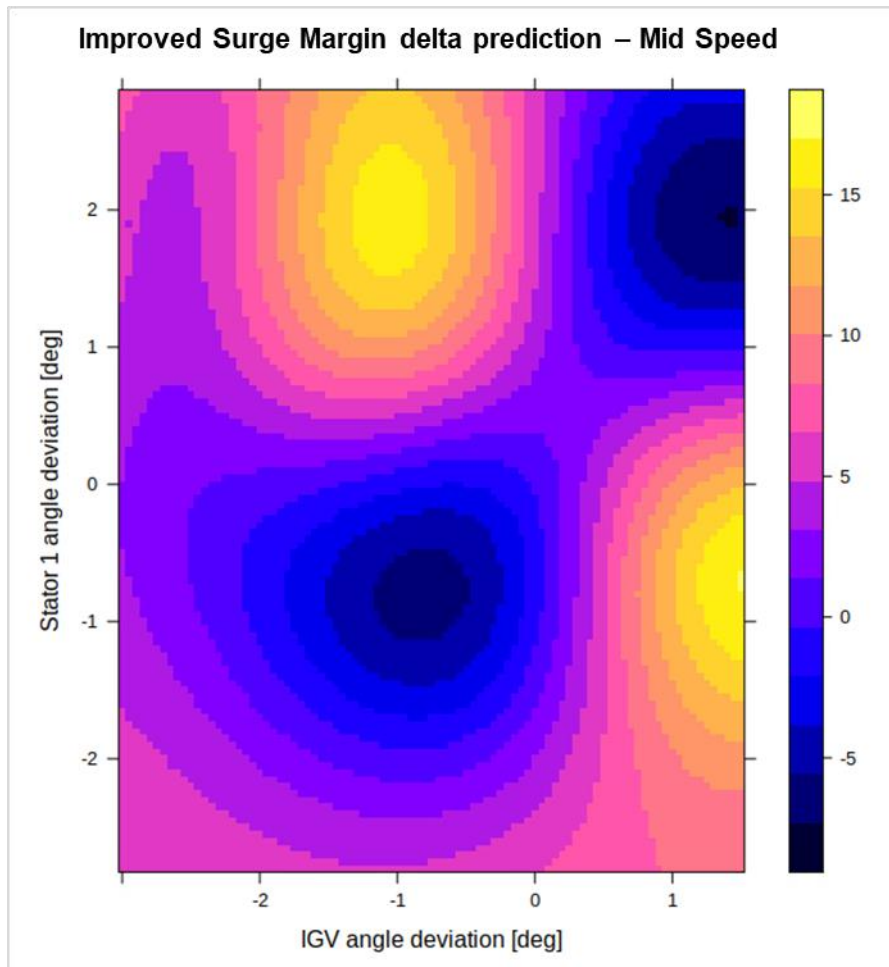


Figure 5.28 Visualisation of improved Surge Margin delta prediction for Mid Speed IGV/Stator 1 variant

Surge Margin correlation of improved prediction increased to $R^2= 0.563[-]$, what still was a low number, but nevertheless from the perspective of efficiency gain, stability level is requested to not go below starting value. Figure 5.28 shows diversity of the stability estimation over the design space, and in compare to initial prediction, data distribution has changed. From two outstanding spots, four are observed showing significant gradients.

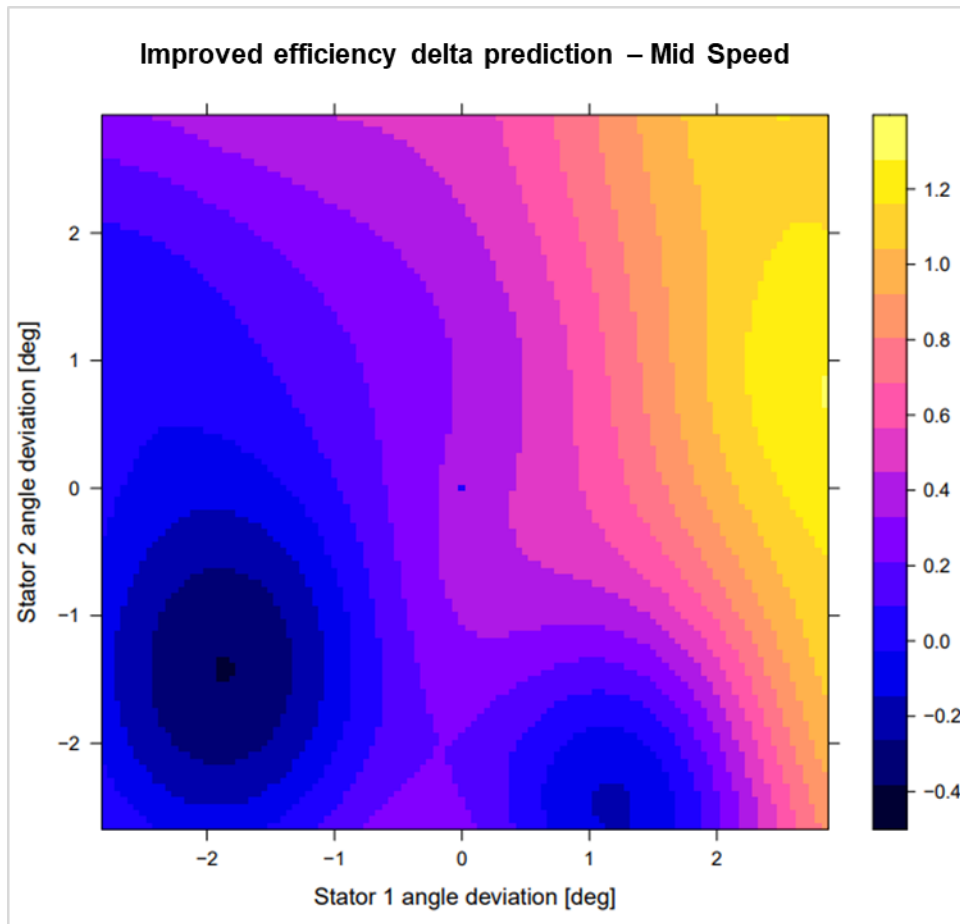


Figure 5.29 Visualisation of improved Efficiency delta prediction for Mid Speed Stator 1/Stator 2 variant

For Stator 1/Stator 2 prediction variant, the tendency stayed the same but the relation between Guide Vanes has changed. Improved estimation intends to less opened Stator 2 in compare to initial surrogate model. Final correlation increased to $R^2= 0.829[-]$.

As a result of Mu-Fi prediction, new VGV setting has been introduced and compared in the qualitative (Figure 5.30) and quantitative (Table 29) manner .

Similarly to High Speed conditions results, new configuration shows minor shift of the Mass Flow, but once more below 1% uncertainty. The curve of new design is not affected by the numerical phenomena observed for the reference case near the Surge Margin.

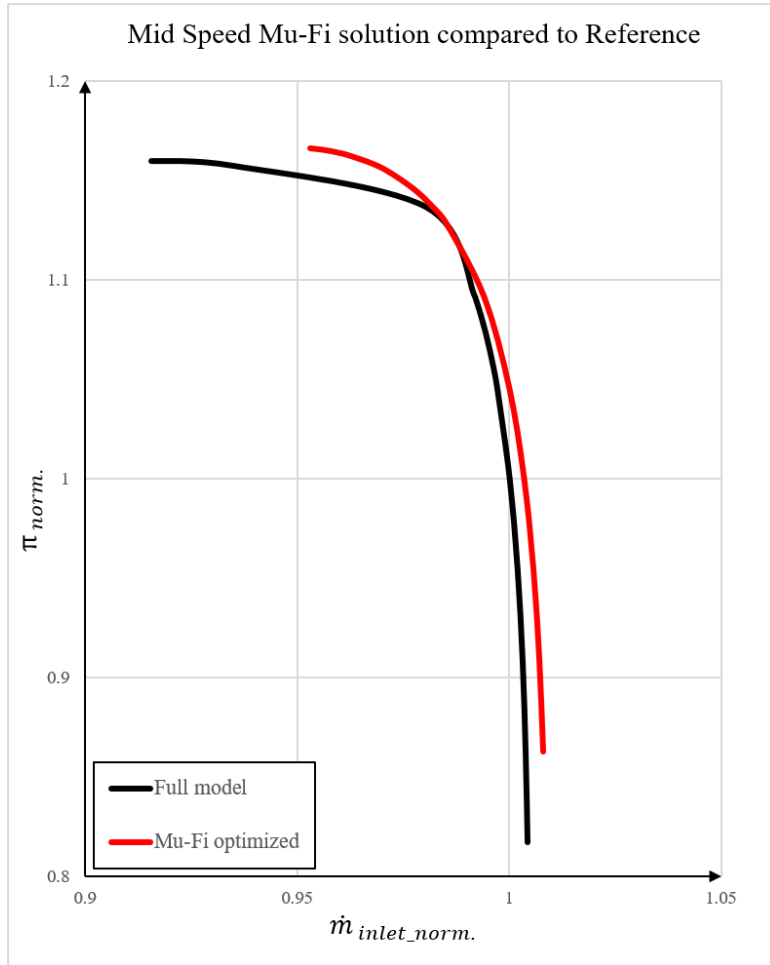


Figure 5.30 Speedlines comparison between reference model and Mu-Fi optimized – Mid Speed

Similarly to the comparison of High Speed conditions, here the table containing three cases with the VGV setting and performance parameters was prepared - Table 29.

Table 29 Mu-Fi process results compare – Mid Speed

Case	IGV deviation [°]	S1 deviation [°]	S2 deviation [°]	Efficiency [pp]	Surge Margin [pp]
Best Hi-Fi sample	-2.88	+2.9	+1.4	+1.45	+6.22
Prediction	-2.55	+2.7	+0.8	+1.27	+5.41
Validation	-2.55	+2.7	+0.8	+1.56	+5.44

Despite lower correlation of the surrogate model, predicted efficiency have revealed to be higher than the Hi-Fi sample with the highest efficiency. This reaction proofs the capability of the method even with lower quality of the surrogate. Comparing to raw prediction, the final results once more is slightly higher in terms of efficiency. By reason of low correlation ($\sim 0.51[-]$) for stability prediction, obtained close result was interpreted

as coincidence, although it proves the agreement in terms of the trends over the design space. As the final result, Mu-Fi concept increased the performance for Mid Speed conditions, providing new VGV setting finding better solution than provided Hi-Fi samples.

5.4.3 Low Speed

As the last configuration used for Multi-Fidelity assessment was Low Speed conditions. Data for this particular case presented the lowest correlation between fidelities what apparently have effect on the quality of the surrogate model. Low rotational speed is also being a deep off-design point that has been chosen as a conditions to test the approach to detect the limits of proposed concept of Multi-Fidelity optimization. Figures below, as for previous examples presents data distribution within the design space initially researched with cheap solutions. As recognizable on the figures Figure 5.31 and Figure 5.32, range of the variables is lower, what indicates highly sensitive conditions and difficulties of the optimizer in finding promising solution.

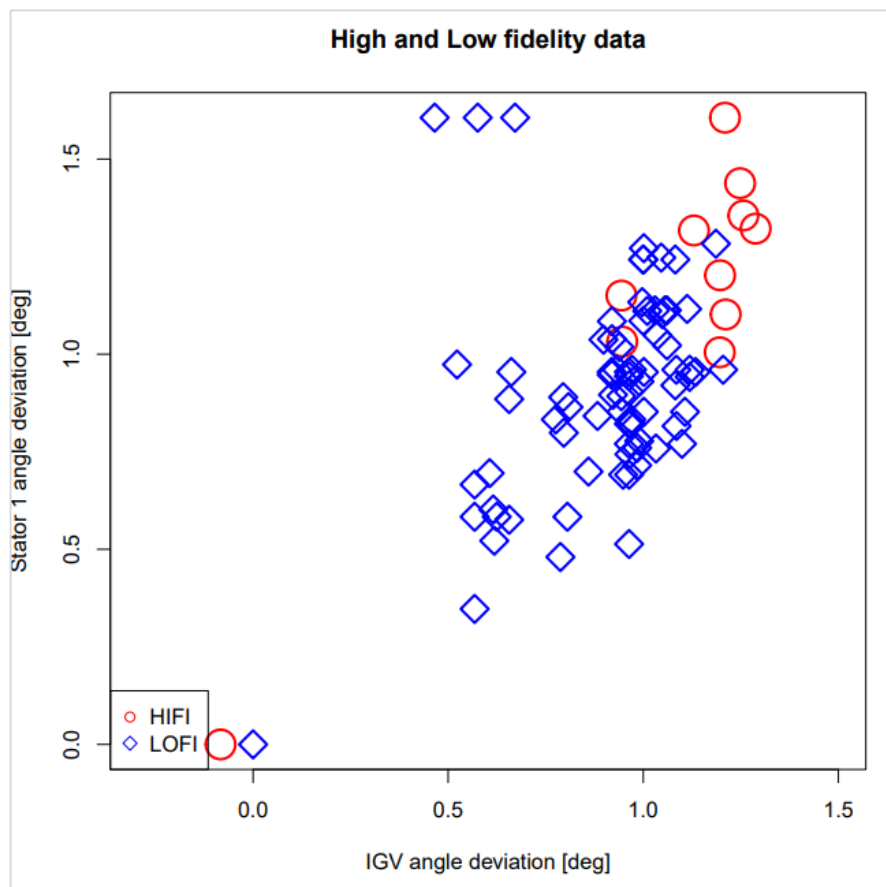


Figure 5.31 Visualisation of spatial distribution of the samples for Low Speed IGV/Stator 1 variant

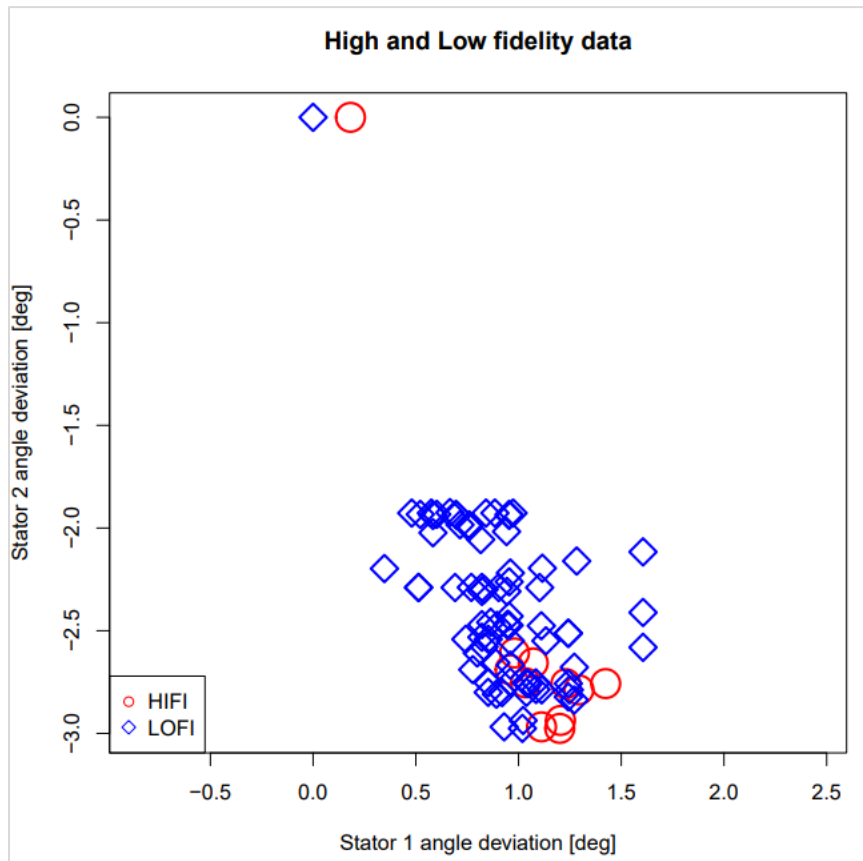


Figure 5.32 Visualisation of spatial distribution of the samples for Low Speed Stator 1 /Stator 2 variant

As a result of low range of variables, the prediction grid has been required to increase the resolution from $0.05[^\circ]$ step to $0.01[^\circ]$ to achieve more detailed vane angle variation with respect to sensitivity of off-design conditions.

In the case of Low speed conditions and IGV/Stator 1 variant of spatial arrangement Gaussian model has been used for semi-variogram representation for both, efficiency and stability. Satisfactory fitting is presented in Figure 5.33 and Figure 5.34. For the semi-variogram of Stator 1/Stator 2 variant model, Exponential method was proposed. Fitting presented in Figure 5.35.

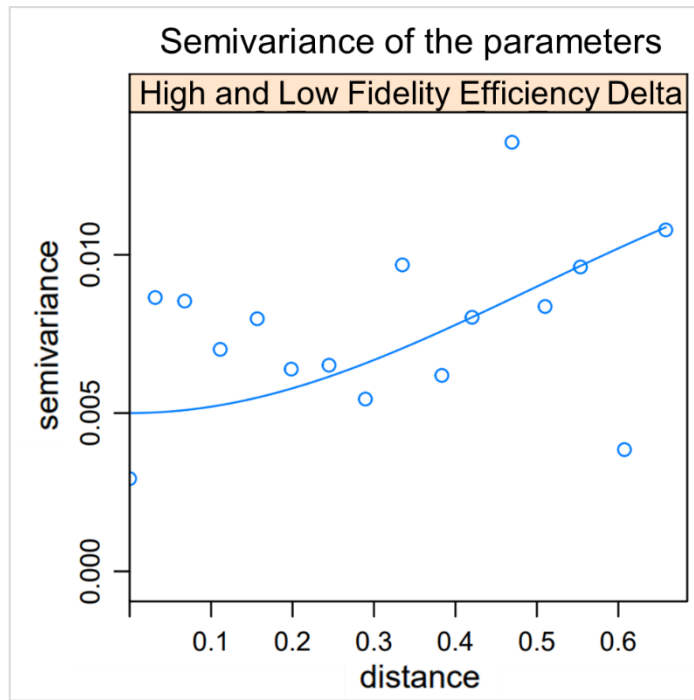


Figure 5.33 Semi-variance model for Multi-Fidelity IGV/Stator 1 efficiency variant

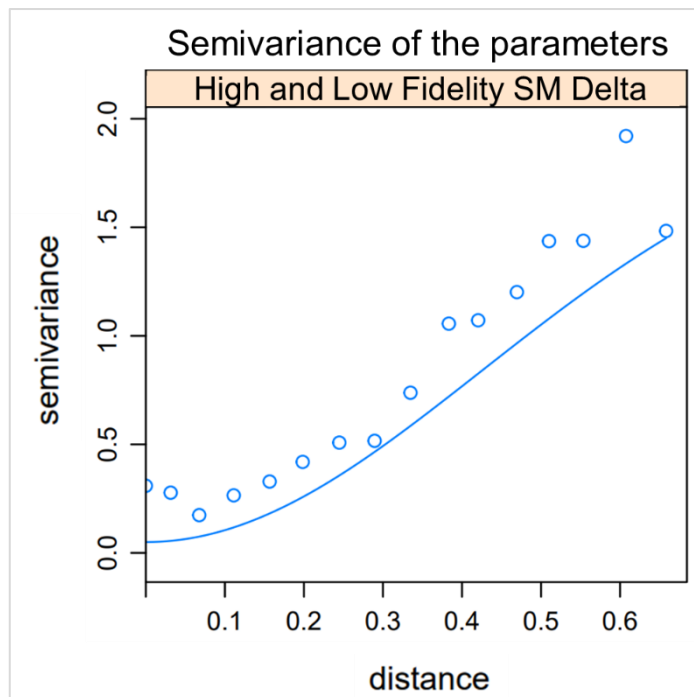


Figure 5.34 Semi-variance model for Multi-Fidelity IGV/Stator 1 Surge Margin variant

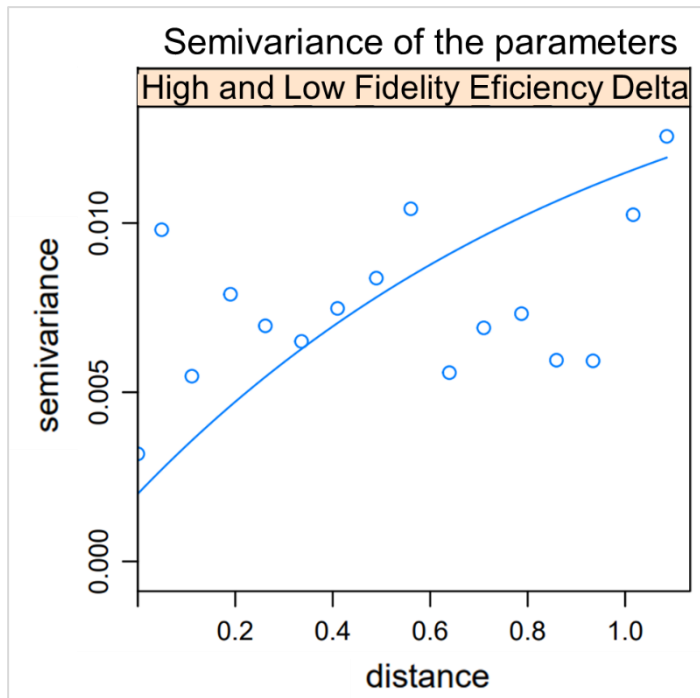


Figure 5.35 Semi-variance models for Multi-Fidelity Stator 1/Stator 2 efficiency variant

Since initial surrogate model is prepared, first loop of the prediction could be performed. As for the previous evaluations, the following figures presents initial predictions plots.

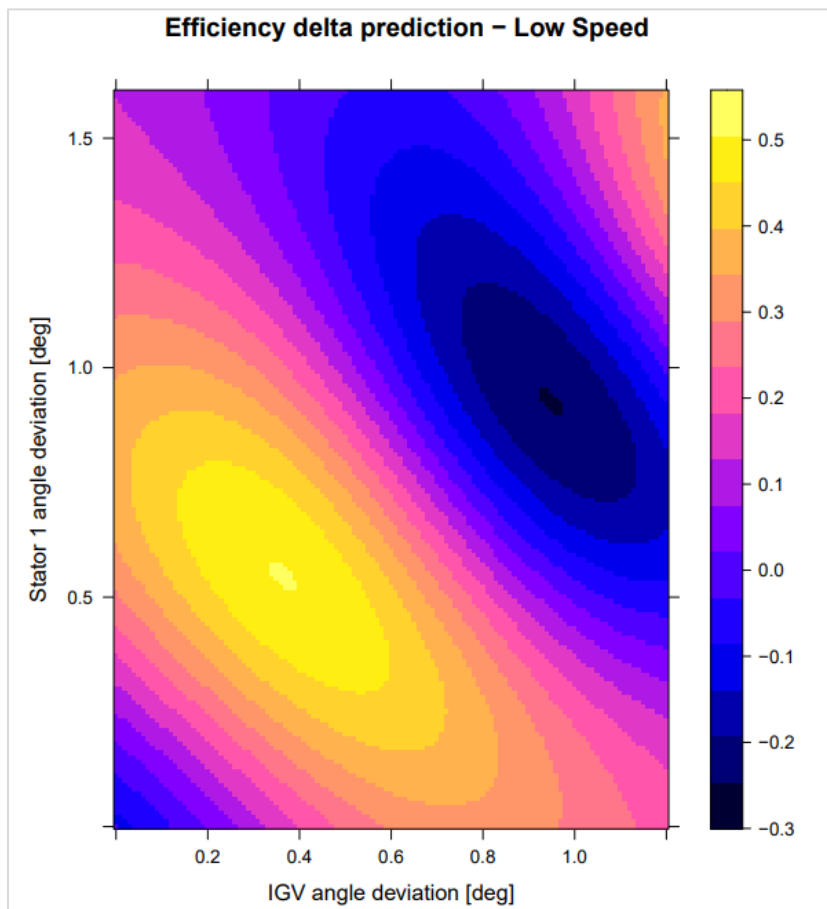


Figure 5.36 Visualisation of Efficiency delta prediction for Low Speed IGV/Stator 1 variant

Figure 5.36 demonstrates efficiency potential in the region of slight opening of the IGV and Stator 1. Therefore in opposite to High and Mid speed, first 2 stages tends come to be unloaded. The correlation for this prediction equals to $R^2=0.752[-]$ what was the worst result for IGV/Stator 1 variant of considered initial surrogate models.

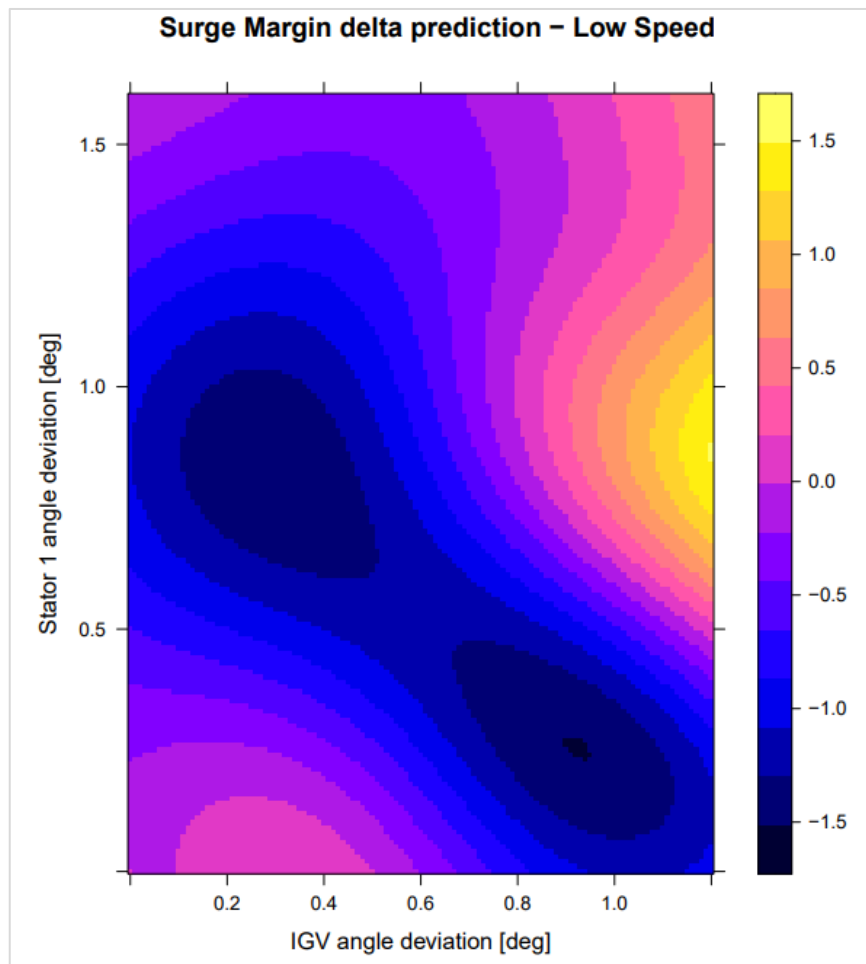


Figure 5.37 Visualisation of Surge Margin delta prediction for Low Speed IGV/Stator 1 variant

Estimated Surge Margin presented in Figure 5.37 indicates lower stability for proposed Vane setting on the initial phase. The correlation for this set is equal to $R^2=0.253[-]$, what shows low correlation of the data and the prediction may not be sufficient for the evaluation.

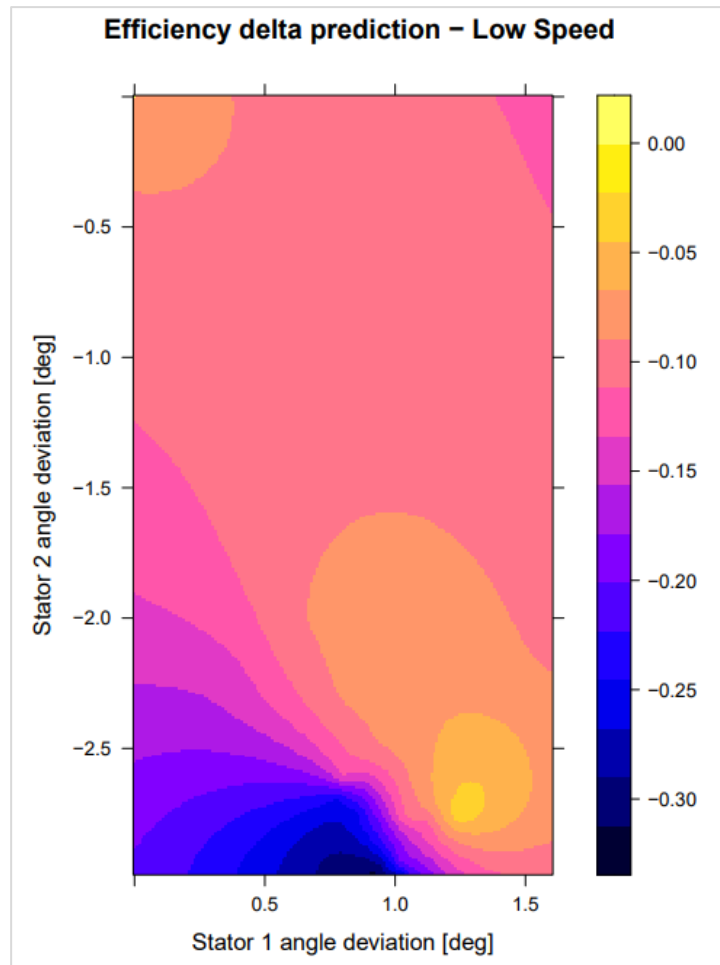


Figure 5.38 Visualisation of Efficiency delta prediction for Low Speed Stator 1/Stator 2 variant

Prediction for Stator 1/Stator 2 variant presented in the figure above shows the tendency of strong closure for Stator 2 to compensate opening of the Stator 1. The correlation of this variant reached $R^2=0.907[-]$ and it was the highest number for the initial surrogate model along Low Speed configuration.

Initial levels of the correlation were promising in predicting compressor performance despite Surge Margin where $R^2=0.253[-]$ being an unacceptable level for prediction providing. The following Figures shows the impact of improving the model with additional 5 expensive samples computed within promising fields according to the concept.

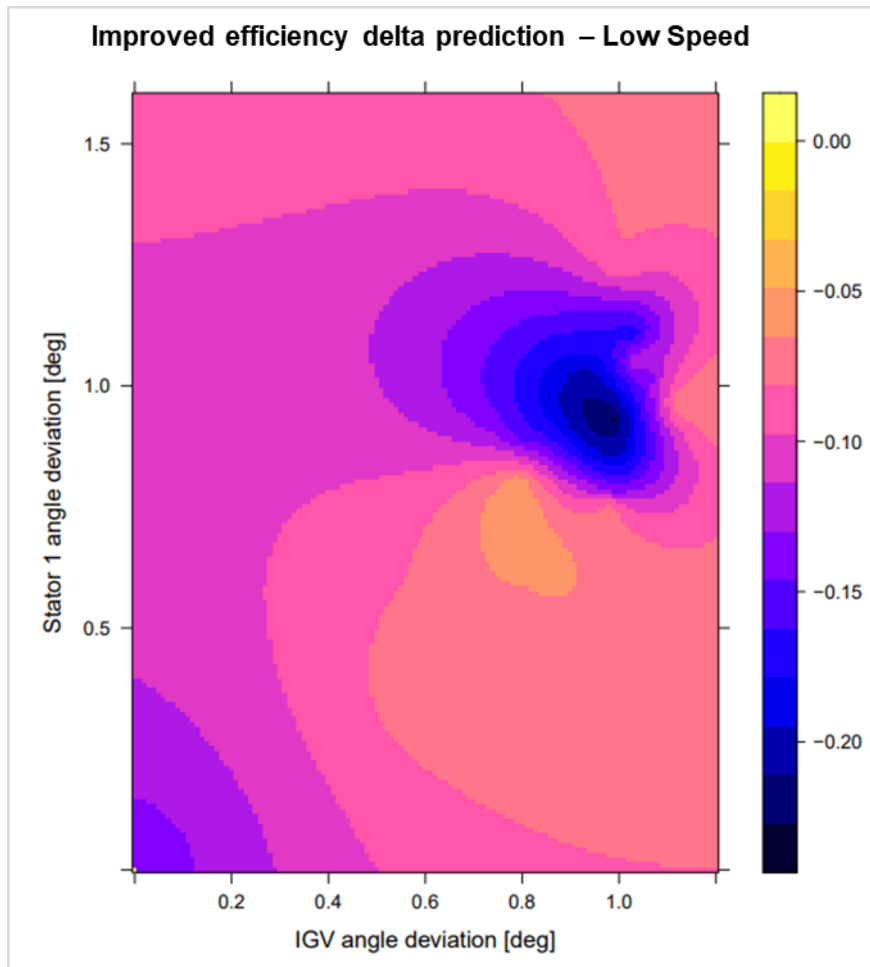


Figure 5.39 Visualisation of improved Efficiency delta prediction for Low Speed IGV/Stator 1 variant

After model improvement, data distribution has completely changed, discarding previously observed spots. Current prediction shows neutral/slightly negative impact on efficiency for the most of the design space. Correlation for efficiency delta prediction of IGV/Stator 1 variant (Figure 5.39) increased to $R^2=0.766[-]$, and results shows low possibility for efficiency gain throughout design space.

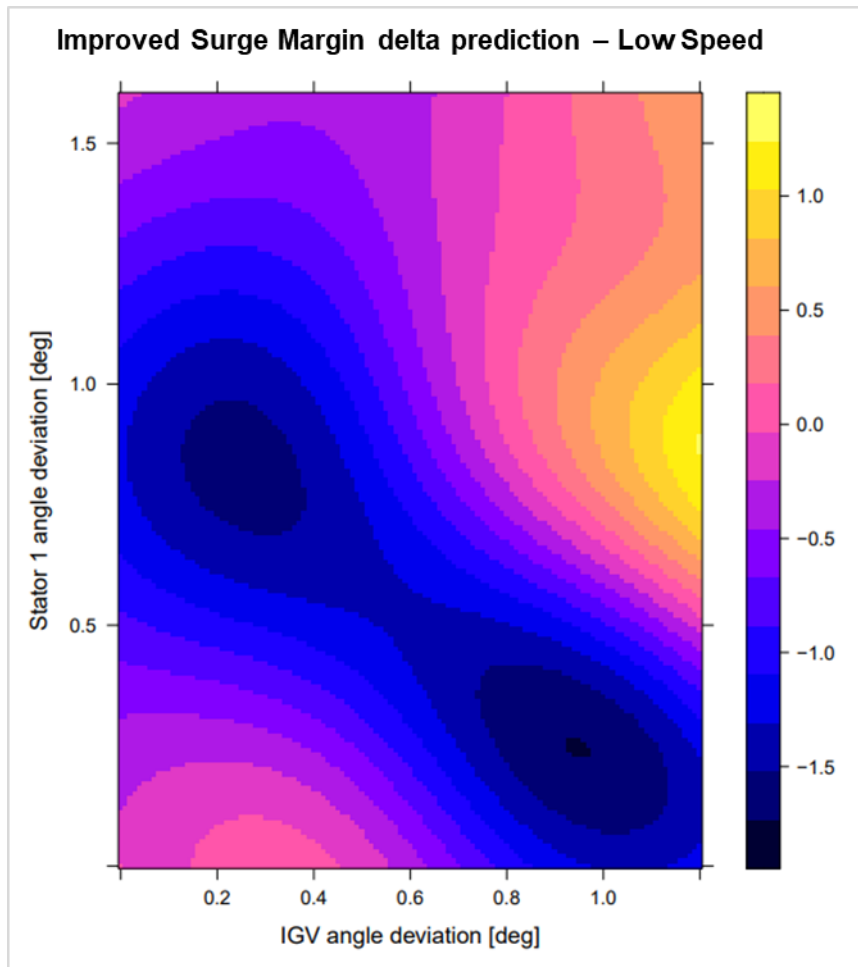


Figure 5.40 Visualisation of improved Surge Margin delta prediction for Low Speed IGV/Stator 1 variant

Similarly low correlation enhancement is observed for Surge Margin prediction, $R^2=0.267[-]$. Concerning data distribution, minor change is observed (Figure 5.40).

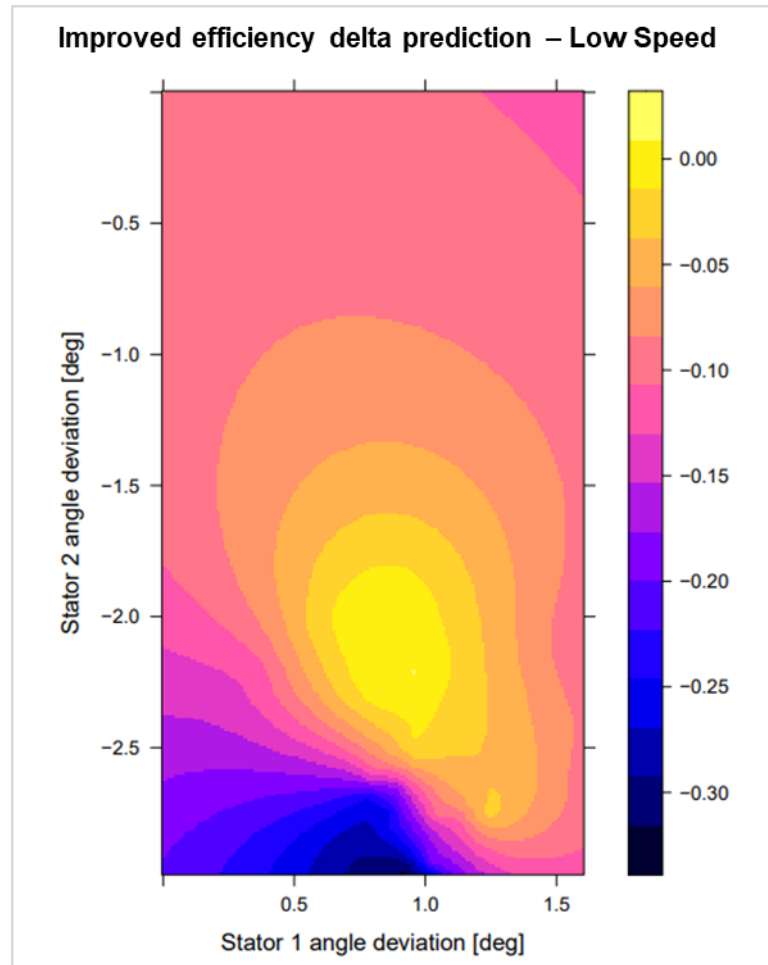


Figure 5.41 Visualisation of improved Efficiency delta prediction for Low Speed Stator 1/Stator 2 variant

Observable change takes place for Stator 1/Stator 2 variant efficiency prediction. The field off neutral/positive performance impact has increased but stayed within the same range of VGV angles change(Figure 5.41). The correlation increased to $R^2=0.936[-]$.

Basing on the Multi Fidelity predictions with use of improved surrogate model, new VGV setting was found. High Fidelity validation run, confirmed correct adjustment of the performance point fitting within 1% allowed deviation. Comparison of the speedlines is presented in the Figure 5.42 for qualitative evaluation purpose.

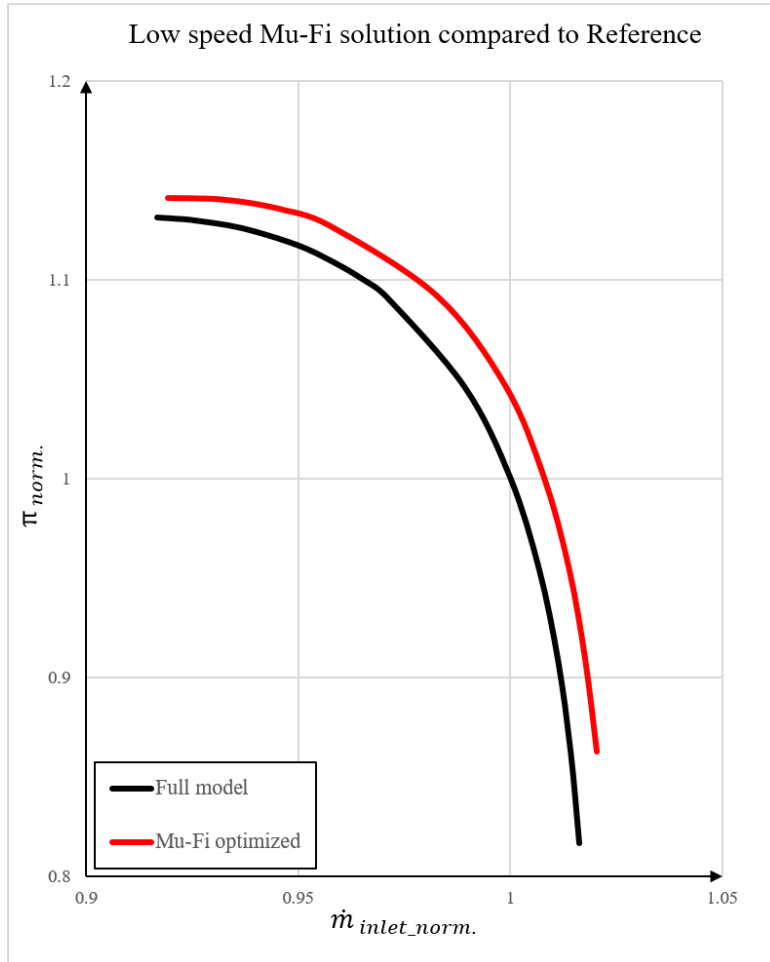


Figure 5.42 Speedlines comparison between reference model and Mu-Fi optimized – Low Speed

Analyzing the shape of the characteristics it shows very similar Pressure Ratio response under throttling in compare to the reference compressor representation. No numerical issues have been observed.

Table below presents comparison of the Variable Guide Vanes settings to determine prediction quality in compare to pure estimation and the best Hi-Fi sample used for surrogate model improvement.

Table 30 Mu-Fi process results compare – Low Speed

Case	IGV deviation [°]	S1 deviation [°]	S2 deviation [°]	Efficiency [pp]	Surge Margin [pp]
Best Hi-Fi sample	+1.12	+0.96	-2.21	+0.09	+0.233
Prediction	+1.2	+0.96	-2.22	+0.01	+1.17
Validation	+1.2	+0.96	-2.22	+0.1	+1.1

The correlation for Low Speed conditions had the lowest value throughout all considered cases. Even though validation member showed performance increase in compare to the reference case. Absolute values differs in compare to the predicted one, but trend was correct and predicted member has higher efficiency and stability than samples utilized for model improvement.

5.4.4 Summary and statistics

To summarize performance of the concept process tests, Multi Fidelity quantities have been collected into a table below.

Table 31 Summary table of performed optimization processes

Conditions	Initial model R ² [-]			Initial model RMSE[-]			Failed Lo-Fi runs	Failed Hi-Fi runs	Efficiency change [pp]	SM change [pp]
	IGV/S1 Eff.	IGV/S1 SM	S1/S2 Eff.	IGV/S1 Eff.	IGV/S1 SM	S1/S2 Eff.				
High Speed	0.951	0.885	0.979	0.232	1.368	0.152	546	0	+1.23	+1.24
Mid Speed	0.888	0.512	0.359	0.236	3.290	0.500	459	3	+1.56	+5.44
Low Speed	0.752	0.253	0.907	0.210	0.779	0.049	196	1	+0.1	+1.1

Proposed concept of Multi Fidelity process was performed for all three conditions, representing different operational condition from close to design down to off-design conditions. Experiment had to determine capability of the method beyond optimal operational range.

Coefficient of determination R² has showed decreasing correlation of the surrogate prediction in line with lowering rotational speed. This also confirms increase of discrepancy of SCM method for off-design conditions. Despite Stator 1/Stator 2 variant of efficiency prediction for Mid Speed, initial model revealed good level of efficiency estimation. Surge Margin surrogate model quality decreases with rotational speed, and the data suggests to providing more expensing samples for surrogate model building.

Analyzing Root Mean Square Error, for IGV/Stator 1 efficiency prediction variant, magnitude stays on similar low level. Similarly for Stator 1/Stator 2 efficiency prediction variant, with exception for Mid Speed, where lower R² was observed. Presented error estimations from the initial model were relatively low, what provides good initial design space evaluation for further surrogate improvement.

In terms of the statistics for sampling, table shows number of the failed sampling trials during Latin Hypercube Sampling, and means how many samples have failed until 100 succeeded cases have been delivered. Failed term is standing behind all the cases which resulted in numerical problems and performance point misalignment. The reducing number towards lower speed doesn't mean better performance of the sampling strategy, it means, for lower speed, design space wide seek was unavailable to due numerical stability, and narrow range of variables could be researched.

For all tested cases, performance improvement has been found based on the Multi-Fidelity prediction, which indicated VGV setting with higher efficiency gain than any available Hi-Fi sample used for surrogate model had. The approach proved to be applicable for all considered rotational speeds, showing capability of performance improvement even for off-design, Low-Speed condition. Results of the performed works revealed potential for further development and increasing number of variable parameters to extend method application.

6 Final conclusions

6.1 Summary

A methodology for Multi Fidelity optimization for wide operational range of axial compressors has been developed, integrating High Fidelity 3D CFD solutions of Reynolds Average Navier Stokes together with Streamline Curvature Method with use of Co-Kriging method for surrogate model definition. The concept has been tested with demonstrator being a specific Design of Experiment, with 4 variable parameters where number of samples was defined in advance to provide equal initial conditions for surrogate model building in the reasoning of weakness emphasizing. All the work was done for three conditions of rotational speed: High, Mid and Low Speed. Usage of different operational conditions had fundamental impact on the results of the concept validation, confirming potential of proposed methodology. Validation was designed to create initial surrogate model out of 100 Low Fidelity samples and 10 High Fidelity samples. For the initial model, deficit in the High Fidelity samples has been revealed. Improvement of the surrogate model didn't bring increase of R^2 coefficient for all the variants of spatial definition, but final outcome delivered satisfactory model response. Despite variate correlation of the data versus surrogate model, for all rotational speed it was possible to enhance axial compressor performance for each of evaluated condition.

The sensitivity studies performed before establishing the concept were aimed on definition of available solutions for lowering the fidelity. Experiments within 3D CFD method showed minor improvement in terms of expense of simulations delivering results with increased discrepancy. No significant benefits were possible to achieve using Low Fidelity RANS simulations in the usage of Multi-Fidelity.

Usage of Streamline Curvature Method revealed significance of quality dependence of adjustment of the compressor representation for particular conditions. Especially for efficiency trend prediction, tool was capable of researching the design space being an ideal candidate for Low Fidelity method for Multi-Fidelity approach.

6.2 Conclusions

1. The developed methodology is capable of improvement of the axial compressor efficiency and stability for extended operational range with application of Multi-fidelity approach providing major computational cost reduction.
2. Proposed concept, utilizes 3D CFD Reynolds Average Navier Stokes simulations for High Fidelity sampling and Streamline Curvature Method for Low Fidelity sampling. Mentioned methods were capable of delivering results being accessible for Co-Kriging surrogate model creation to predict performance estimation for presented Design of Experiment.
3. The accuracy of the final prediction indicates opportunities for estimation of more complex, multi-dimensional optimization problems, enabling design constraints located in off-design conditions of axial compressor performance. Completed experiment was covered with the optimization of Variable Guide Vanes setting, where 3 pairs of variables were defined – IGV/Stator 1 for efficiency and Surge Margin estimation and Stator 1/Stator 2 for only efficiency prediction.
4. Studies performed on different fidelities of the 3D CFD model have revealed limitations and best practice for choosing level of accuracy model representation. The level of representation has major impact especially on estimating stability limit of axial compressor. Resigning from secondary flow volumes may introduce overestimation and misleads the mechanism behind the stall phenomenon. For efficiency estimation, only main gas path model – “Pure model” - showed positive trends within this aspect. The lowest impact on general performance estimation has been exposed by reducing mesh resolution with keeping initial boundary layer discretization. The observations have been achieved for all mentioned rotational speeds – High, Mid and Low Speed.
5. Analyzing efficiency and Surge Margin distribution over the design space for considered cases, anisotropy of the parameters can be observed. Despite this behavior, Mu-Fi approach has been capable to detect multiple promising fields, what provides to select actual best solution. It is a major advantage over gradient optimization methods which tend to stuck on local maximum.

6.3 Recommendations for development

As the concept has been confirmed to be able to predict performance improved member during the optimization demonstration, future work and recommendations are provided:

1. Performing an optimization task based on more variables of interest. Presented in this thesis demonstration of the capability of the method, has to avoid expanding the studies for defining dominant parameters at complex design task. Currently when methodology is established and shows potential results for wide operational range, complex, multi-dimensional optimization problem is to be conducted.
2. Developing a aggregation method of the predicted data. When more complex optimization task will be handled, there is a necessity to develop a method for evaluation of multidimensional predictions. In the thesis, 3 pairs of variables were used allowing to simply pick best solutions which fulfilled Surge Margin constrain. For more complex problem, more mathematically sophisticated method will be essential.
3. Developing of the semi-variogram model fitting method. Throughout this thesis, type of the model for semi-variogram adaption has been defined in advance by the user, and then parameters were adjusted with fitting model with data regression. For future work, especially with increased number of the variables, automatized process of model selection could be an advantageous.
4. Adopting ratio between High and Low Fidelity samples. For presented Design of Experiment it was assumed to keep High to Low ratio at ratio level of 1:10 for the initial model and ~1:7 for the improved surrogate model. Works have shown that depending on the conditions, model quality may vary, so there is a need for developing best practices on sampling ratios.

7 Bibliography

- [1] EASA. (2022). European Aviation Environmental Report. EASA. <https://www.easa.europa.eu/en/domains/environment>.
- [2] *GTF Engine.* (N/A). Pratt&Whitney. <https://www.prattwhitney.com/en/products/commercial-engines/gtf>.
- [3] *Future products.* (N/A). Rolls-Royce. <https://www.rolls-royce.com/products-and-services/civil-aerospace/future-products.aspx#section-overview>.
- [4] *Water-enhanced turbofan.* (N/A). MTU Aero Engines. <https://www.mtu.de/technologies/clean-air-engine/water-enhanced-turbofan/>.
- [5] N. A. Cumpsty, "Compressor Aerodynamics," *Longman Scientific and Technical*, England, 1989.
- [6] Veres, J. . "Axial and Centrifugal Compressor Mean Line Flow Analysis Method," AIAA 2009-1641. *47th AIAA Aerospace Sciences Meeting including The New Horizons Forum and Aerospace Exposition*. January 2009.
- [7] Koliass I, Alexiou A, Aretakis N, Mathioudakis K. Axial Compressor Mean-Line Analysis: Choking Modelling and Fully-Coupled Integration in Engine Performance Simulations. *International Journal of Turbomachinery, Propulsion and Power*. 2021; 6(1):4. <https://doi.org/10.3390/ijtpp6010004>.
- [8] Wu, C., & Wolfenstein, L. (1949). Application of Radial-Equilibrium Condition to Axial-Flow Compressor and Turbine Design.
- [9] Holloway, P.R., Koch, C.C., Knight, G., & Shaffer, S.L. (1982). Energy efficient engine. High pressure compressor detail design report.
- [10] Jörger, A. T. Incorporation of High-Fidelity Flow Field Information into Preliminary Design of Multi-Stage Axial Compressors. PhD's thesis, Massachusetts Institute of Technology.
- [11] Denton JD, Dawes WN. Computational fluid dynamics for turbomachinery design. *Proceedings of the Institution of Mechanical Engineers, Part C: Journal of Mechanical Engineering Science*. 1998;213(2):107-124. doi:10.1243/0954406991522211.
- [12] Cengel, Y.A. and Cimbala, J.M. (2014). Fluid Mechanics. Fundamentals and Applications. 3rd Edition. *McGraw-Hill*, New York.
- [13] Belamri, T, Galpin, P, Braune, A, & Cornelius, C. CFD Analysis of a 15 Stage Axial Compressor: Part I — Methods. *Proceedings of the ASME Turbo Expo 2005: Power for Land, Sea, and Air. Volume 6: Turbo Expo 2005, Parts A and B*. Reno, Nevada, USA. June 6–9, 2005. pp. 1001-1008. ASME. <https://doi.org/10.1115/GT2005-68261>.

- [14] Cornelius, C., Biesinger, T., Galpin, P., and Braune, A. (November 28, 2013). Experimental and Computational Analysis of a Multistage Axial Compressor Including Stall Prediction by Steady and Transient CFD Methods. *ASME. J. Turbomach.* June 2014; 136(6): 061013. <https://doi.org/10.1115/1.4025583>.
- [15] Erler, E., Vo, H. D., and Yu, H. (December 22, 2015). "Desensitization of Axial Compressor Performance and Stability to Tip Clearance Size." *ASME. J. Turbomach.* March 2016; 138(3): 031006. <https://doi.org/10.1115/1.4031865>.
- [16] Möller, D., and Schiffer, H. (January 18, 2021). On the Mechanism of Spike Stall Inception and Near Stall Nonsynchronous Vibration in an Axial Compressor. *ASME. J. Eng. Gas Turbines Power.* February 2021; 143(2): 021007. <https://doi.org/10.1115/1.4049450>.
- [17] Li, J., Du, J., Li, Z., and Lin, F. (May 10, 2018). Stability Enhancement With Self-Recirculating Injection in Axial Flow Compressor. *ASME. J. Turbomach.* July 2018; 140(7): 071001. <https://doi.org/10.1115/1.4039806>.
- [18] Romera, D., and Corral, R. (November 16, 2020). Efficient Passage-Spectral Method For Unsteady Flows Under Stall Conditions. *ASME. J. Turbomach.* December 2020; 142(12): 121007. <https://doi.org/10.1115/1.4047934>.
- [19] Denton, J. D. (September 26, 2017). Multall—An Open Source, Computational Fluid Dynamics Based, Turbomachinery Design System. *ASME. J. Turbomach.* December 2017; 139(12): 121001. <https://doi.org/10.1115/1.4037819>.
- [20] Joly, M, Verstraete, T, & Paniagua, G. Full Design of a Highly Loaded Fan by Multi-Objective Optimization of Through-Flow and High-Fidelity Aero-Mechanical Performances. *Proceedings of the ASME Turbo Expo 2012: Turbine Technical Conference and Exposition*. Volume 8: Turbomachinery, Parts A, B, and C. Copenhagen, Denmark. June 11–15, 2012. pp. 2293-2301. ASME. <https://doi.org/10.1115/GT2012-69686>.
- [21] Stürzebecher, T, Goinis, G, Voss, C, Sahota, H, Groth, P, & Hammer, S. Automated Aerodynamic Optimization of an Aggressive S-Shaped Intermediate Compressor Duct. *Proceedings of the ASME Turbo Expo 2018: Turbomachinery Technical Conference and Exposition*. Volume 2D: Turbomachinery. Oslo, Norway. June 11–15, 2018. V02DT46A002. ASME. <https://doi.org/10.1115/GT2018-75184>.
- [22] Siller, U., Voß, C., Nicke, E. Automated Multidisciplinary Optimization of a Transonic Axial Compressor, AIAA 2009-863. *47th AIAA Aerospace Sciences Meeting including The New Horizons Forum and Aerospace Exposition*. January 2009. <https://doi.org/10.2514/6.2009-863>.
- [23] Ratz J, Leichtfuß S, Beck M, Schiffer H-P, Fröhlig F. Surge Margin Optimization of Centrifugal Compressors Using a New Objective Function Based on Local Flow Parameters. *International Journal of Turbomachinery, Propulsion and Power*. 2019; 4(4):42. <https://doi.org/10.3390/ijtp4040042>.
- [24] Day, I. J. (October 13, 2015). Stall, Surge, and 75 Years of Research. *ASME. J. Turbomach.* January 2016; 138(1): 011001. <https://doi.org/10.1115/1.4031473>.

- [25] Dodds, J., and Vahdati, M. (May 1, 2015). Rotating Stall Observations in a High Speed Compressor—Part II: Numerical Study. *ASME. J. Turbomach.* May 2015; 137(5): 051003. <https://doi.org/10.1115/1.4028558>.
- [26] Righi, M., Pachidis, V., Könözy, L., Pawsey, L. (2018). Three-Dimensional Through-flow Modelling of Axial Flow Compressor Rotating Stall and Surge. *Aerospace Science and Technology.* 78. 10.1016/j.ast.2018.04.021.
- [27] Guan, Di & Sun, Dakun & Xu, Ruize & Bishop, Daniel & Sun, Xiaofeng & Ni, S., Du, J., Zhao, D. (2021). Experimental investigation on axial compressor stall phenomena using aeroacoustics measurements via empirical mode and proper orthogonal decomposition methods. *Aerospace Science and Technology.* 112. 106655. 10.1016/j.ast.2021.106655.
- [28] Zeng, H., Zheng, X., and Vahdati, M. (January 4, 2022). A Method of Stall and Surge Prediction in Axial Compressors Based on Three-Dimensional Body-Force Model. *ASME. J. Eng. Gas Turbines Power.* March 2022; 144(3): 031021. <https://doi.org/10.1115/1.4053103>.
- [29] Koch, C. C. (October 1, 1981). Stalling Pressure Rise Capability of Axial Flow Compressor Stages. *ASME. J. Eng. Power.* October 1981; 103(4): 645–656. <https://doi.org/10.1115/1.3230787>.
- [30] Peherstorfer, B., Willcox, K., Gunzburger, M., Survey of multifidelity methods in uncertainty propagation, inference, and optimization, *Siam Rev.* 60 (3) (2018) 550–591, doi:10.1137/16M1082469.
- [31] Shahpar, S., Brooks, C., Forrester, A., Keane, A. (2011). Multi-fidelity Design Optimisation of a Transonic Compressor Rotor. *9th European Conference on Turbomachinery: Fluid Dynamics and Thermodynamics, ETC 2011 - Conference Proceedings.* 2.
- [32] Forrester, A., Sobester, A., Keane, A. (2007). Multi-fidelity optimization via surrogate modelling. *Proc. R. Soc. A.* 463. 3251-3269. 10.1098/rspa.2007.1900.
- [33] Bonfiglio, L., Perdikaris, P., Brizzolara, S., Karniadakis, G. (2017). A multi-fidelity framework for investigating the performance of super-cavitating hydrofoils under uncertain flow conditions. 10.2514/6.2017-1328.
- [34] Bonfiglio, L., Perdikaris, P., Brizzolara, S., Karniadakis, G. (2017). Multi-fidelity optimization of super-cavitating hydrofoils. *Computer Methods in Applied Mechanics and Engineering.* 332. 10.1016/j.cma.2017.12.009.
- [35] Bonfiglio, L., Royset, J., Karniadakis, G. (2018). Multi-Disciplinary Risk-Adaptive Design of Super-Cavitating Hydrofoil. 10.2514/6.2018-1177.
- [36] Joly, M., Verstraete, T., Paniagua, G. (2014). Integrated multifidelity, multidisciplinary evolutionary design optimization of counterrotating compressors. *Integrated Computer Aided Engineering.* 21. 10.3233/ICA-140463.

- [37] Schemmann, C, Geller, M, & Kluck, N. A Multi-Fidelity Sampling Method for Efficient Design and Optimization of Centrifugal Compressor Impellers. *Proceedings of the ASME Turbo Expo 2018: Turbomachinery Technical Conference and Exposition*. Volume 2D: Turbomachinery. Oslo, Norway. June 11–15, 2018. V02DT46A001. ASME. <https://doi.org/10.1115/GT2018-75160>.
- [38] Zhang, H, Li, Y, Chen, Z, Su, X, & Yuan, X. Multifidelity Based Optimization of Shaped Film Cooling Hole and Experimental Validation. *Proceedings of the ASME Turbo Expo 2019: Turbomachinery Technical Conference and Exposition*. Volume 2D: Turbomachinery. Phoenix, Arizona, USA. June 17–21, 2019. V02DT46A001. ASME. <https://doi.org/10.1115/GT2019-90088>.
- [39] Schnoes, M., Schmitz, A., Goinis, G., Voß, C., Nicke, E. (2019). Strategies for Multi-Fidelity Optimization of Multi-Stage Compressors with Throughflow and 3D CFD.
- [40] Holmes, DG. Mixing Planes Revisited: A Steady Mixing Plane Approach Designed to Combine High Levels of Conservation and Robustness. *Proceedings of the ASME Turbo Expo 2008: Power for Land, Sea, and Air*. Volume 6: Turbomachinery, Parts A, B, and C. Berlin, Germany. June 9–13, 2008. pp. 2649-2658. ASME. <https://doi.org/10.1115/GT2008-51296>.
- [41] Wilcox D.C. Turbulence Modeling for CFD. *DCW Industries, Inc.*, 1993.
- [42] Menter F.R., Kuntz M., Langry R. Ten Years of Industrial Experience with the SST Turbulence Model. *Turbulence, Heat and Mass Transfer 4*, ed: Hanjalic K., Nagano Y., Tummers M. Neell House, Inc., 2003;625-632.
- [43] Muchowski, R., Gubernat, S. M. (2021). Influence of Axial Compressor Model Simplification and Mesh Density on Surge Margin Evaluation. *Advances in Science and Technology Research Journal*, 15(3), 243-253. <https://doi.org/10.12913/22998624/140541>.
- [44] Khalid, S. A., Khalsa, A. S., Waitz, I. A., Tan, C. S., Greitzer, E. M., Cumpsty, N. A., Adamczyk, J. J., and Marble, F. E. (July 1, 1999). Endwall Blockage in Axial Compressors. *ASME. J. Turbomach.* July 1999; 121(3): 499–509. <https://doi.org/10.1115/1.2841344>.
- [45] Tulik, W. (2021). *Sensitivity verification of an axial compressor CFD model*. Master's thesis, Politechnika Rzeszowska.
- [46] Wu, C. H. (1951). *A general through-flow theory of fluid flow with subsonic or supersonic velocity in turbomachines of arbitrary hub and casing shapes*. Report, NASA Technical Reports Server.
- [47] Casey, M., and Robinson, C. (April 7, 2010). A New Streamline Curvature Throughflow Method for Radial Turbomachinery. *ASME. J. Turbomach.* July 2010; 132(3): 031021. <https://doi.org/10.1115/1.3151601>.
- [48] Co-Kriging. (N/A). *Geospatial Data Science in R*. <https://zia207.github.io/geospatial-r-github.io/cokriging.html>.

- [49] Armstrong, M. (1998). The Theory of Kriging. In: Basic Linear Geostatistics. *Springer*, Berlin, Heidelberg. https://doi.org/10.1007/978-3-642-58727-6_7.
- [50] Ihaka, R., Gentleman, R. (1996) R: A Language for Data Analysis and Graphics, *Journal of Computational and Graphical Statistics*, 5:3, 299-314, DOI: 10.1080/10618600.1996.10474713.
- [51] Bivand, R. (2004). Using the R statistical data analysis language on GRASS 5.0 GIS data base files. *Computers and Geosciences*. 26. 10.1016/S0098-3004(00)00057-1.
- [52] Pebesma, E.J. (2004) Multivariable Geostatistics in S: The GSTAT Package. *Computers and Geosciences*, 30, 683-691. <https://doi.org/10.1016/j.cageo.2004.03.012>
- [53] Forrester, A., Keane, A. (2009). Recent advances in surrogate-based optimization. *Progress in Aerospace Sciences*. 45. 50-79. 10.1016/j.paerosci.2008.11.001.
- [54] Morris, M.D. (1991). Factorial sampling plans for preliminary computational experiments. *Technometrics* 33, 2 (May 1991), 161–174. <https://doi.org/10.2307/1269043>.
- [55] Helton, J.C. & Davis, F.J.. (2002). Latin hypercube sampling and the propagation of uncertainty in analyses of complex systems. *Reliability Engineering & System Safety*. 81. 23-69. 10.1016/S0951-8320(03)00058-9.
- [56] Isaaks, E.H., & Srivastava, R.M. (1989). An Introduction to Applied Geostatistics. *Oxford University Press*, New York. 413 pages. 163-170.
- [57] Deutsch, C.V. and Journel, A.G., (1997). GSLIB Geostatistical Software Library and User's Guide, *Oxford University Press*, New York, second edition. 369 pages. 24-25.
- [58] Rossiter, D.G. (2007). *Note : Co-kriging with the gstat package of the R environment for statistical computing*.
- [59] Pebesma, E. (N/A). *Fit a Linear Model of Coregionalization to a Multivariable Sample Variogram*. <https://search.r-project.org/CRAN/refmans/gstat/html/fit.lmc.html>
- [60] Pre-Processing & Meshing Solutions. (N/A). Numeca. <https://www.numeca.de/en/products-meshing-solutions/>
- [61] Burberi, C., Michelassi, V., Scotti Del Greco, A., Lorusso, S., Tapinassi, L., Marconcini, M., Pacciani, R. (2020). Validation of Steady and Unsteady CFD Strategies in the Design of Axial Compressors for Gas Turbine Engines. *Aerospace Science and Technology*. 107. 106307. 10.1016/j.ast.2020.106307.